

Large-scale and local morphological impact along the northern side of DELTA 21

Zhaoyi Li



Large-scale and local morphological impact along the northern side of DELTA 21

By

Zhaoyi Li

Student number: 4831713

to obtain the degree of Master of Science
at the Delft University of Technology,
to be defended publicly on Monday November 16th, 2020 at 8:30 AM.

Thesis committee: Prof. dr. ir. S.G.J. (Stefan) Aarninkhof Delft University of Technology

Ir. M. (Martijn) Onderwater Delft University of Technology

Dr. ing. M.Z. (Mark) Voorendt Delft University of Technology

An electronic version of this thesis will be available at <http://repository.tudelft.nl/>.



Acknowledgements

This document represents the MSc thesis needed to fulfill my academic requirements for completing the Master of Science in Hydraulic Engineering (Costal Engineering specialization) at the TU Delft.

First of all, I want to express great thanks to the graduation committee for the time they invested in me. My daily supervisor Martijn Onderwater gives me valuable feedback and fruitful discussions during our meetings. Thanks for your patient guidance and always being so responsive to my emails during the entire project. Furthermore, many thanks to Stefan Aarninkhof and Mark Voorendt for the intensive and enthusiastic meetings we always had. Your constructive suggestion on report construction are very appreciated.

Second, thanks to Huub Lavooij and Leen Berke from DELTA 21 project for letting me be a part of the project and give me all the freedom in terms of decision-making about my thesis. Also, many thanks to Jan van Overeem for your guidance in the first stage of the project. Your help in forming my graduation committee and thesis proposal laid the foundation of subsequent work.

Furthermore, I would not forget the help and support from the fellow students. Thanks Jelmer and Mayra for your technical support with Delft3D. Without your help, establishment of the Delft3D model in this study could not go so successfully. Chu Chen and Jiechen Zheng, I'm grateful for your help in plotting and advises about thesis writing.

Also, I want to thank my family and friends in the final part of my acknowledgement. Great thanks to my parents for your unconditional trust and support through my whole life. To my friend Xinrui: I'm so glad to have you during two years Master study in Delft. Thanks for your accompany, encourage and the happiness we shared together.

Zhaoyi Li

Delft, November 2020

Summary

The world is now facing looming threat of sea level rise and increasing needs for clean, renewable energy due to climate change. The the DELTA 21 project is a proposed large scale spatial plan located at Dutch coast with three ambitions: flood safety, energy storage and nature restoration. The DELTA 21 project is located west of the Haringvliet and adjacent to the Maasvlakte 2 and comprises a tidal lake (Getijmeer) and a storage basin (Valmeer) with a size of 20 km². The coastal zone has a crucial significance for humankind. With large population density, extensive infrastructure and property development, development of the coastline need to be well studied before the implementation of interventions.

This report investigates the long-term morphological changes caused by the DELTA 21 project at the northern side, including the large scale morphological development caused by tidal currents and at local scale the coastline deformation induced by tidal and wave motion. The necessity of the layout design improvement of DELTA 21 is analyzed by comparing different results in case of the improved layout and the original layout.

The UNIBEST-LT model, UNIBEST-CL model and depth-averaged (2DH) Delft3D model is used to make estimation of long-term morphological development after the construction of the DELTA 21 project. The local scale sedimentation and erosion happens along the sandy beach of Valmeer are analyzed by 10 years' long-term simulation of UNIBEST-CL model. Tidal induced large scale morphological changes is study by 20 years morphodynamic simulation in Delft3D.

On local scale, the model results indicate that shoreline retreat will happen around the head of Valmeer and large amount of sediment is lost in that section in case of both original layout and improved layout. And the improvement in the layout of DELTA 21 project has remarkable influence on coastline evolution and sediment balance. With a regular shape of the coastline, the morphological process happens along the sandy beach is more predictable. Maximum shoreline retreat and sediment loss is reduced dramatically after the improvement.

On large scale, a scour hole near the most western location of the Valmeer and a large submerged sand bar at the northern side of Valmeer are developed after 20 years. In case of original layout, the scour hole gives a larger maximum depth. The large scale deposition at the northern side of Valmeer is migrating towards northeast direction, which may cause large amount of sediment in the area around Maasvlakte 2 in the future.

Therefore, this long term morphological impact of the DELTA 21 project on both large scale and local scale is estimated based on numerical simulations. It can be concluded that the improved layout of DELTA 21 gives better performance on both large scale and local scale.

Table of contents

Acknowledgements.....	i
Summary.....	ii
Table of contents.....	iii
1 Introduction.....	1
1.1 Background information.....	1
1.2 Problem statement.....	3
1.3 Objective and research questions.....	5
1.4 Methodology.....	6
2 Theoretical background.....	9
2.1 Introduction.....	9
2.2 Sediment transport.....	9
2.2.1 General introduction.....	9
2.2.2 Bijker formula.....	11
2.2.3 Van Rijn formula.....	12
2.3 Residual current and sediment transport.....	14
2.4 Coastline deformation.....	14
3 Study area.....	17
3.1 Geology background.....	17
3.2 Maasvlakte 2.....	18
3.3 Hydrodynamic forcing.....	20
3.3.1 Tide.....	20
3.3.2 Wave.....	20
4 Local-scale model setup.....	22
4.1 Introduction.....	22
4.2 Setup of UNIBEST LT-model.....	22
4.2.1 Wave and tide.....	23
4.2.2 Depth profile.....	24
4.2.3 Closure depth and active height.....	25
4.2.4 Sediment transport parameters.....	26
4.3 Setup of UNIBEST CL-model.....	27
4.3.1 Definition of the coastline.....	27
4.3.2 Definition of the global climate.....	28
5 Local-scale model results analysis.....	30
5.1 Introduction.....	30
5.2 Theoretical analysis.....	30
5.2.1 Sediment transport curve.....	30
5.2.2 Result for the original layout.....	33

5.2.3 Sandy hook development.....	35
5.2.4 Result for the improved layout	37
5.3 UNIBEST CL-model results	38
5.3.2 Result of improved layout.....	41
5.3.3 Assessment of layout improvement.....	43
5.4 Conclusion	46
6 Large-scale model setup	47
6.1 Introduction	47
6.2 Grid and bed schematization.....	47
6.3 Boundary conditions	49
6.4 Model setup.....	50
6.5 Morphological scale factor.....	50
7 Large-scale model results analysis.....	56
7.1 Introduction.....	56
7.2 Flow patterns.....	56
7.2.1 Flow pattern during over tidal cycles	56
7.2.2 Residual currents	62
7.3 Long-term simulation for Maasvlakte 2.....	63
7.3.1 Bed level change.....	63
7.4 Long-term simulation for the original layout of DELTA 21.....	66
7.4.1 Bed level change.....	66
7.4.2 Residual currents and Sediment Transport	70
7.5 Long-term simulation for the improved layout of DELTA 21	73
7.5.1 Bed level change.....	73
7.5.2 Residual currents and Sediment Transport	76
7.6 Conclusions.....	78
8 Conclusions and Discussions.....	80
8.1 Discussions.....	80
8.2 Conclusions.....	81
8.3 Recommendations.....	83
Reference	85
List of figure	88
List of table	91
A Wave climate in UNIBEST-LT	92
B Geological borehole research.....	96
C Additional simulation results	99

1

Introduction

1.1 Background information

The coastal zone has a crucial significance for humankind. It is extensively used for fishing, tourism, transportation, industry, housing, mineral and fossil mining (Bosboom and Stive, 2015). Moreover, with the exploration of renewable energy, it becomes the significant sites for power plants.

The morphology of the coast is dynamic and determined by both natural influence and human interference. At the Dutch coast, the increasing rate of sea level rise lead to a large need of sediment. Increased sea level disturbs the equilibrium beach profile and the sand from beach section is eroded to restore profile at foreshore. Over several decades, large scale human activities, like closures in the Wadden Sea, closures in the Delta area and construction of the Maasvlakte 2, has a marked impact on the Dutch coastal system. With large population density, extensive infrastructure and property development, development of the coastline need to be well studied before the implementation of interventions (Bosboom and Stive, 2015).

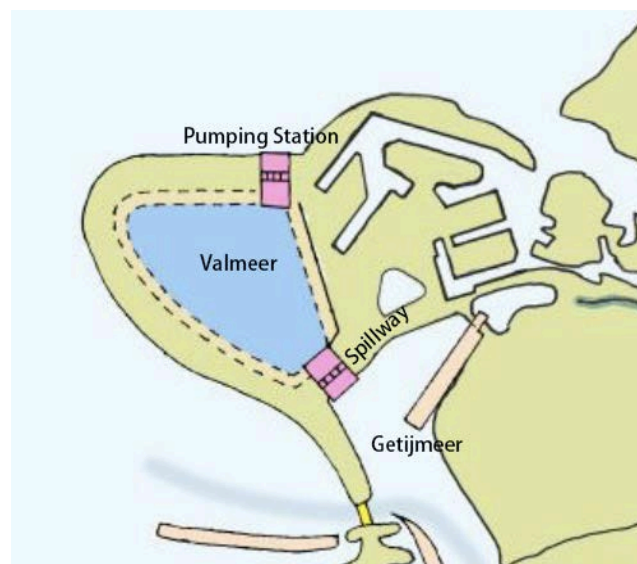
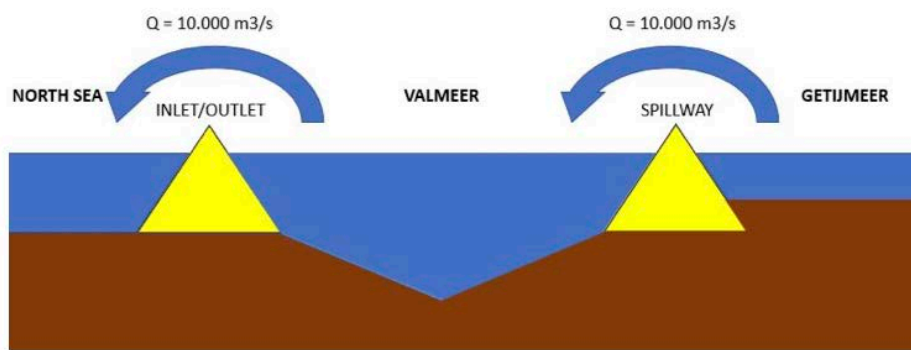


Figure 1 : Layout version 2019 of DELTA 21 project (Berke and Lavooij, 2019)

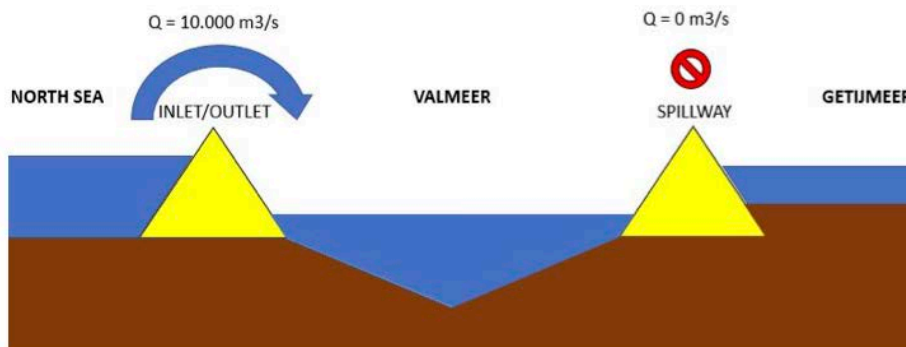
This research deals with the DELTA 21 project, a proposed large scale spatial plan located at Dutch coast. With three ambitions: flood safety, energy storage and nature restoration, the DELTA 21 project is

triggered by the the looming threat of sea level rise and increasing needs for clean, renewable energy due to climate change. The DELTA 21 project is located west of the Haringvliet and adjacent to the Maasvlakte 2, shown in Figure 1. The Delta 21 project comprises a tidal lake (Getijmeer) and a storage basin (Valmeer) with a size of 20 km².

To guarantee the flood safety and energy demand, there will be basically two working conditions for the DELTA 21 project, depending on the appearance of storm on the sea side or extreme discharge from the river. With a pumping station and a deep energy storage lake (Valmeer), during flooding condition, the tidal power plant will be shut down and work as barrier. River discharge will flow into the Valmeer through spillway and be pumped out into the North Sea through the pumping system, as shown in Figure 2(b). Both of the pumping station and the spillway has a capacity of 10,000 m³/s. In this way, the Haringvlietdam can be reopened, allowing salty water to reach the upstream of Haringvliet.



(a) Flood protection function during severe storm conditions



(b) Energy generation function during daily working condition

Figure 2: Conceptual drawing of DELTA 21 project (Ruiz, 2020)

For the daily working condition, the tidal power plant is turned on, the sea water is exchanged twice a day in Getijmeer through the tidal power plant and energy is generated through turbines. In the very deep Valmeer, there will also be daily exchange of the sea water through the pump for energy storage purpose, which is so called “Pumped Hydro Storage”(PHS). At the pumping station, the turbines can be converted into pumps in seconds. With a very low water level in the Valmeer, water will flow into the Valmeer during the day and generate energy through turbines. During night, the water will be pumped back up from the lower basin for repeatedly use with less energy consumption. Also, it helps to store energy from wind farm and floating solar energy power plant in the Valmeer. The water level in the energy storage lake can rise or fall by maximum of 17.5 m.

Under severe storm conditions, the tidal power plant will be shut down and work as tidal barrier, the river discharge will flow into the Valmeer through the spillway and will be pumped out into the North Sea through the pumping system. With the DELTA 21 project taken the duty for flood defence, the Haringlietdam will be reopened after the DELTA 21 project put into service.

Later in 2020, the layout of DELTA 21 was further improved considering its negative effect in the aspects of morphology, economics and ecology. In the original version of 2019, the Valmeer had a bulge shape towards the offshore and the pumping station is located at the northern boundary. The new layout has a streamline boundary ensures a smooth flow around the Valmeer, as shown in Figure 3. By offering more space for the Hinderplaat, shallow sandbank in the Voordelta and the Natura 2000 area is better protect against erosion. Also the entrance of the Valmeer is moved to the southwest boundary. In this way, the wave load at the inlet of pumping station can be reduced. With same structure components and operating principle the improved design of DELTA 21 project has exactly same function as the original design.

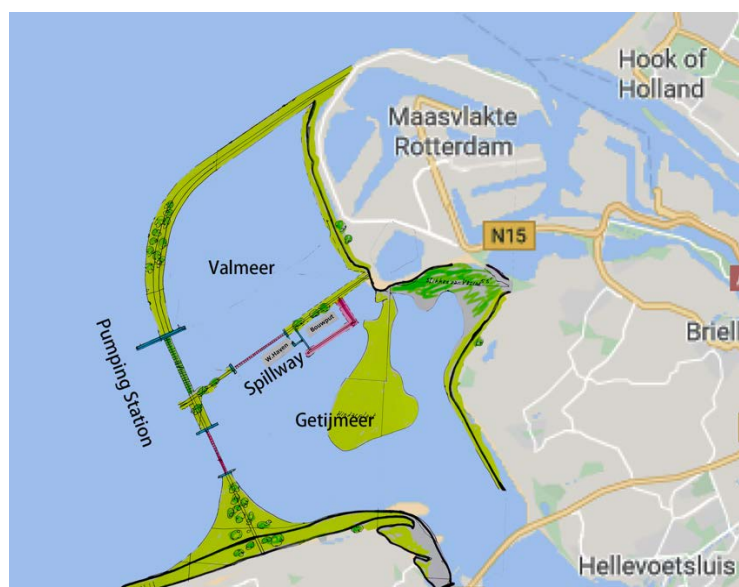


Figure 3: Improved layout of DELTA 21 project (delta21.nl)

1.2 Problem statement

The original layout designed in 2019, will result in several morphological problem in large scale and local scale. The Valmeer will be connected to the Maasvlakte 2 and extend further seaward. With a relative large spatial size, the DELTA 21 project will significantly change the shape of the coastline. The seaward bulge shape of the Valmeer will cause contraction of the tidal flow, similarly as the Maasvlakte 2 did. Also, the dune structure will expose to a more intense wave and current in deep water.

With transformation of the flow pattern at the Haringvliet estuary and the morphology of the coastline, the DELTA 21 project will influence the hydraulic processes and in consequence the morphological processes. Considering the safety, economic and social matters, there are several topics about morphological changes due to the DELTA 21 project need to be clarified.

- 1) In a larger scale, due to the concentration of tidal currents, morphological changes will happen along the coast. With a bulge shape, the Valmeer will significantly change the tide current at the head of the Valmeer and lead to a series of change in flow pattern and sediment transport pattern along the Dutch coast. Consequently, this may lead to generation of large scour hole and sediment accretion, which may bring negative effect to structure stability, navigation and operation of the Port of Rotterdam. The shipping channel of the Port of Rotterdam is of great importance to the operation of the largest port in Europe. If there is aggradation in the shipping channel after the construction of DELTA 21, then extra dredging work is needed.
- 2) At a local scale, due to the bulge shape at the northwest side and the angle at the transition part, there will be certain erosion and sedimentation pattern along the beaches of the Valmeer and Maasvlakte 2 caused by wave and current motion. Large amount of erosion along the seawall of DELTA 21 project will in the first place pose a threat to the structure stability.
- 3) Sedimentation along the sea defense will threaten the stability of Maasvlakte 2. For the northern sea defense of the Maasvlakte 2, it consists of a cobble shore with a reef of concrete cubes on the foreshore, which has relative large roughness to reduce run-up height. Sediment transport that passes the transition zone between the soft defense and hard defense may cause deposition on the profile of hard defense. Sedimentation on the rock surface may lead to a relative smoother surface which may cause serious overtopping. As a result, it will threaten the stability of the hard defense and other facility on the inner side.



Figure 4: Maasvlakte 2 with hard sea defense design and built (Loman, 2012)

- 4) The location of the Getijmeer is used to be the old Haringvilet estuary, and the new tidal power plant cut through the Haringvilet ebb-tidal delta. The morphological development used to be forced by several hydraulic processes, like tide, river discharge and waves. With the reopen of the Haringvilet dam and altering of tidal current, the morphology near the in-out let of the Getijmeer will be remarkably altered.
- 5) Sedimentation or erosion of sand and silt within the Getijmeer due to tidal currents. With the construction of the tidal power plant, new tidal lake Getijmeer is formed, which covers part of the old Haringvilet estuary. Inside the Getijmeer, asymmetry tidal current can lead to net sediment transport, with flood dominant tide indicate an net import and ebb dominant tide indicate a net export. Also, the silt transport will be effected by the HW-slack and LW-slack duration of the

horizontal tide. In this way, the ebb channel and tide flat in the Getijmeer will react to the changes of the boundary and in-out let of the tidal basin, which will lead to a series of morphological changes.

As for the improved layout, similar morphological effects remain while it is relieved on some issues. The development of the ebb-tidal delta and silt transport at southern will be similar with the original condition. At the northern side of the project, large scale erosion and deposition due to tidal concentration maybe reduced due to a gentler radian of the Valmeer outline. Also considering the smoother connection with Maasvlakte 2, erosion and sedimentation along the sea defense due to wave motion can be weakened, which can result in a more stable structure and less maintenance work.



Figure 5: Northern side of the DELTA 21 project

This research focus on the morphological problems at northern side of the DELTA 21 project, which includes topic 1 and 2. The research objective and thesis outline is developed based on these three topics.

1.3 Objective and research questions

Based on the previous discussed problems, this study is aimed to analysis the long-term morphological changes caused by the DELTA 21 project at the northern side. The analysis deals with both the original project layout and the improved project layout. By analyzing the negative effect of the morphological changes caused by the original layout, the necessity of the layout design adjustment can be explained.

The large scale scour and deposition caused by the tidal flow concentration due to the DELTA 21 project is assessed by comparing the morphological development with the DELTA21 project with a situation without this project. In a large scale and deep water condition, the influences of wave on bed level change is quite limited. This means that no wave related process need to be included in the analysis at a large scale (Elias et al, 2006). The result of the long term simulation for the cases with and without the DELTA 21 will be compared.

Locally erosion and sedimentation along the sea defense of Valmeer and Maasvlakte 2 will then be analyzed qualitatively and quantitatively.

- Qualitatively, the long-term development of the shoreline position will be simulated. The position of sand gain and loss will be spotted and extreme condition of unstoppable morphological development will be predicted.
- Quantitatively sediment input or output in different section of the sea defense will be calculated.

For this study, the general research question is formed as follow:

Focusing at northern side of DELTA 21 project, what is the necessity of improving the original project layout from a morphological aspect, and what will be the morphological changes which are caused by the DELTA 21 project ?

Several sub-questions are proposed to find an answer for the general research question:

- What are the characteristics of the water motion and which mechanism should be included in the large scale and local scale morphology analysis, respectively?
- How will the layout of the Valmeer effect the morphological change at a local scale in case of the original layout?
- How will the layout of the Valmeer effect the morphological change at a local scale with the improved layout?
- How will the DELTA 21 influence the coastal morphological evolution at a large scale on the northern side of Valmeer?
- How will the DELTA 21 influence the coastal morphological evolution at a large scale around Maasvlakte 2?

1.4 Methodology

To answer the previously proposed research questions, this research will carry out a modelling study with numerical model in UNIBEST (LT and CL module) and Delft3D. The research has been divided into four stages.

Stage 1: Literature review

The literature review for this research will focus on mainly two aspects: theoretical backgrounds and information about the study area. The theoretical background that explains the mechanisms behind the morphological evolution is given in Chapter 2. The information of the study area includes basic geological and hydraulic parameters, the history interventions and relative consequence in long-term morphological development. The study area is introduced in Chapter 3.

Stage 2: Local-scale morphological modeling

The morphological development along the sea defense at a local scale due to wave motion will be analyzed based on UNIBEST-CL modelling. The UNIBEST-CL model contains LT model and CL model. Process of local-scale model setup is demonstrated in Chapter 4

With proper depth profile, sediment data, wave climate and long shore current information, the UNIBEST LT model gives a $S-\varphi$ curve, which shows the relation between sediment transport volume and the coast line orientation. The coastline evolution can then be predicted and the sand loss of different sections is calculated. These $S-\varphi$ curves will be used for both the analysis of the original layout condition and improved layout condition.

The UNIBEST-CL model then gives a schematization result of the coastline evolution. The input parameter in the UNIBEST-CL model will include the initial coastline, type of coastline, structures along the coastline, sources of sediment and losses of sediment (sinks). With the result of UNIBEST-CL model, the altering of the coastline position can be intuitively analyzed. In this study, UNIBEST-CL models are prepared for the initial layout and improved layout, respectively.

Stage 3: Large-scale morphological modelling

The Delft3D model will be used for the long-term morphodynamic simulation of the large-scale morphological development in case of the original layout and improved layout. In Chapter 6, the setup of morphodynamic Delft3D model is introduced.

The model used in this study is developed based on the salinity Delft3D model of the Maasvlakte 2 designed in previous study (PUMA, 2008) by a fellow student in DELTA 21 project group (IJntema, 2020). He expands the area of the model grids and covered the Nature 2000 area. The Maasvlakte 2 morphology model is constructed, calibrated and validated by him. IJntema also built up the model of DELTA 21 in case of improved layout, which will also be used in this study. In this study, the model of DELTA 21 in case of original layout is developed.

In Delft3D, curvilinear staggered grids are applied. Different parameters, like depth and velocity components, are defined on the numerical grid (Deltares, 2014a). For a long-term large scale morphodynamic simulation, the hydraulic boundary conditions, including tide and water level, is applied into the model. With the bathymetry and hydraulic boundary set, sediment transport calculated by solving the non-linear shallow water equation on the applied grid (Deltares, 2014a).

The model is then be calibrated and validated before running for the long term simulations. I'll run two simulation to find the effect of the DELTA 21 project on the large scale morphological development:

Condition 1: Simulation of Maasvlakte 2 model and uniform sediment (without the DELTA 21 project)

Condition 2: Simulation of DELTA 21 model in case of original layout and uniform sediment

Condition 3: Simulation of DELTA 21 model in case of improved layout and uniform sediment

Stage 4: Investigation of model results

Results of the simulations will be analyzed and discussed in Stage 4. The analysis will be composed of mainly two parts: local scale morphological development based on UNIBEST model results in Chapter 5 and large scale morphological development based on Delft3D model results in Chapter 7.

Based on the $S-\varphi$ curves given by the UNIBEST-LT model and schematization result given by the UNIBEST-CL model, the coastline evolution of both original layout condition and improved layout condition will be analyzed and compared. Also, the sand loss in different sections along the beach will be

quantitatively calculated. In this way, an assessment on the necessity and effectiveness of the layout improvement is provided.

At a large scale, by comparing the simulation result with and without DELTA21 project as well as comparing the original and improved layout, its impact on the seabed level evolution will be concluded.

2

Theoretical background

2.1 Introduction

This chapter introduces the theoretical background of the sediment transport and morphological development. The concept and computational formula for sediment transport in coastal zone is treated in Section 2.2. Two formula that often used for sediment transport, Bijker (1968) and Van Rijn (1993) are introduced. In Section 2.3, the relation between long-shore sediment transport and coastline deformation is given.

2.2 Sediment transport

2.2.1 General introduction

The total load of sediment transport in coastal zone is consists of two parts of transport, the bed-load transport and the suspended transport . Over decades, several different formulas are developed to estimate the sediment transport in coastal environment due to wave and currents. These formulas applied different approaches and focus on different aspects of this problem. They are developed based on two main approach, which are the energetics approach developed by Bagnold (1963) and a probabilistic approach introduced by Einstein (1972). The Bijker (1968) and Van Rijn (1993) deal with the total sediment transport, and are constructed similarly based on Einstein approach. The Ribberink (1998) formula deals with a quasi-steady model of sediment transport and only considered the bed load transport. The Bailard (1981) formula deals with the total load and is an energetics formulation for sediment transport due to waves. The Dibajnia and Watanabe (1992) total load formula is calculated based on the instantaneous velocity due to wave and current interaction. In the Section, the mostly used Bijker and Van Rijn formula is introduced. Both formula can be applied for only current induced

The bed load is the sediment transport caused by jumping and rolling of sediment particles in a thin layer above the bottom, as shown in Figure 6 (Van Rijn, 1993). When the bed shear stress or bed shear stress exceeded a crucial value, bed load transport happens. With a further increased current velocity, the particles moving in the bottom layer will be suspended in the water column. The bed load transport

caused by a regular wave is considered to be zero due to the symmetrical oscillatory velocity. For irregular waves in reality, the velocity under wave crest is larger than that under the wave trough, which caused net transport (Jenniskens, 2001).

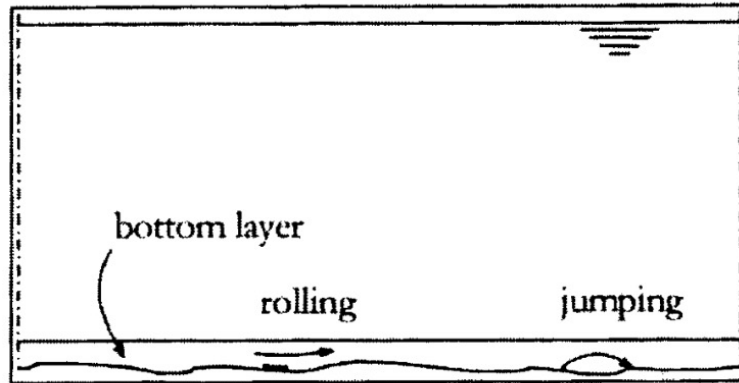


Figure 6: Bed load transport (Van Rijn, 1993)

With large current velocity and strong wave motion, sediment is brought into suspension and sediment concentration over the water depth, as given in Equation (1).

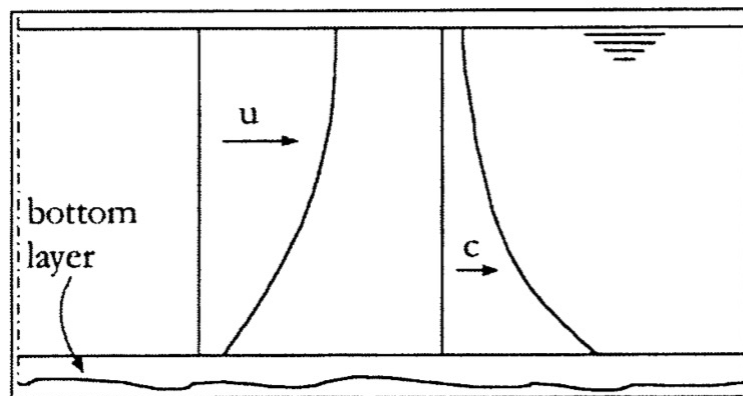


Figure 7: Suspended transport (Van Rijn, 1993)

$$S_x = \int_{\delta_h}^h \bar{c}(z) * \bar{u}(z) dz \quad (1)$$

where

- S_x :suspended sediment transport
- δ_h :thickness of the bottom transport
- $\bar{c}(z)$: time averaged concentration
- $\bar{u}(z)$: time averaged velocity in current direction

The average concentration of sediment is varied along the depth of water column and can be calculated as Equation (2). Different sediment diffusion coefficient distribution applies for Bijker and Van Rijn formula.

$$w * \bar{c}(z) + \varepsilon_x(z) \frac{d\bar{c}(z)}{dz} = 0 \quad (2)$$

where

- w : fall velocity of sediment particles
- z : elevation above the bed level
- $\bar{c}(z)$: time averaged concentration at level z
- $\varepsilon_x(z)$: sediment diffusion coefficient distribution

The logarithmic distribution of velocity over the depth can be described by using the fluid diffusion coefficient, as given in Equation (3). The velocity profile is further adjusted for the condition considering the influence of wave motion.

$$u(z) = \frac{u_*}{\kappa} \ln\left(\frac{z}{z_0}\right) \quad (3)$$

where

- $u(z)$: velocity at level z
- z : elevation above the bed level
- u_* : shear stress velocity
- κ : Von Karman coefficient (0.4)
- z_0 : elevation at which the velocity is zero

2.2.2 Bijker formula

The Bijker transport formula is derived from the formula Einstein developed for currents only condition (Bijker, 1968). For the bed load transport formula, Bijker adapted the Kalinke and Frijlink formula as given in Equation (4). The bottom layer thickness is set to be the bottom roughness height. The influence of the wave motion is included by changing the bottom shear stress. The suspended transport is calculated by integrating the product of velocity and sediment concentration over water depth as previous introduced. A parabolic sediment diffusion distribution is applied which is start at the height of bottom

roughness. The concentration over the remaining depth is decided by the reference concentration at a height equal to the thickness of bottom layer. Therefor the suspended transport is related to the bed load transport. With the influence of wave motion, increased shear stress induced larger reference concentration will also results in larger sediment concentration over the entire water depth (Camenen and Larroude 2003).

$$q_{sb} = C_b d \sqrt{\frac{\mu_c \tau_c}{\rho}} \exp\left(-0.27 \frac{(\rho_s - \rho)}{\mu_c \tau_{cw}}\right) \quad (4)$$

$$q_{ss} = 1.83 q_{sb} (I_1 \ln \left[\frac{33h}{\delta_c} \right] + I_2) \quad (5)$$

where

- q_{sb} :sediment fluxes of bed load
- q_{ss} :sediment fluxes of suspended load
- C_b :breaking wave parameter
- μ_c : ripple parameter
- τ_c : shear stress due to current only
- τ_{cw} : shear stress due to wave-current interaction
- ρ_s : sediment density
- ρ : water density
- I_1, I_2 : Einstein integrals (suspended load)
- $\delta_c = 100d/h$: dimensionless thickness of the bed load layer

2.2.3 Van Rijn formula

In Van Rijn formula, more parameters is applied to represent the process of sediment transport. The critical bed shear stress is calculated according to Shields parameter. The influence of wave motion is included in bed shear stress , velocity distribution, concentration distribution and others. The bed load transport formula is given as Equation (6). For the current only condition, the logarithmic velocity profile is applied. Considering the effect of both current and waves, the velocity in the wave related near bed mixing layer is described differently and becomes time-dependent.

$$q_{sb} = 0.25dD_*^{-0.3} \left(\frac{\tau_{cf}}{\rho} \right)^{0.5} \left(\frac{\tau_{cw} - \tau_{cr}}{\tau_{cr}} \right)^{1.5} \quad (6)$$

$$\tau_{cf} = \mu_c \alpha_{cw} \tau_c$$

where

- q_{sb} :sediment fluxes of bed load
- q_{ss} :sediment fluxes of suspended load
- D_* : dimensionless sediment diameter
- τ_{cf} : total shear stress due to current only
- τ_{cr} :critical shear stress for sediment transport
- α_{cw} :coefficient due to the presence of waves
- μ_c :shape factor

For suspended load, the the diffusion distribution is assumed to be a combination of parabolic distribution and constant distribution. The concentration distribution is then calculated according to Equation (7). The sediment diffusion coefficient distribution for the influence of current and waves is decided separately and the combined distribution is obtained according to Equation (8) (Camenen and Larroude, 2003).

$$q_{ss} = \int_a^h \overline{u(z)} c(z) dz \quad (7)$$

$$\frac{dc}{dz} = - \frac{(1-c)^5 c W_s}{\varepsilon_{scw}} \quad (8)$$

$$\varepsilon_{scw} = \sqrt{\varepsilon_{sc}^2 + \varepsilon_{sw}^2}$$

where

- $c(z)$:mean volume concentration (time average) at height z
- ε_{scw} : sediment diffusion coefficient for currents and waves
- ε_{sc} :sediment diffusion coefficient for currents only

- ε_{sw} : sediment diffusion coefficient for waves only

2.3 Residual current and sediment transport

Tidal currents are unique among the processes responsible for sediment transport and deposition because of their regularity, with the speed and direction varying with the frequency of the governing astronomical period (Dalrymple and Choi, 1978). For an ideal tide current transport case, the ebb current and flood current for a tidal cycle has same duration and velocity but opposing direction. However in the shallow water area of the coast zone, the crest of the tidal wave travels faster than the trough because the latter experiences greater frictional retardation. As a result, the duration of flood tide is shorter but velocity is larger. So the tidal signal becomes asymmetric. The residual current caused by the asymmetric tide can be calculated as Equation 9 (Imasato, 1983).

$$U_c(x, y) = \frac{1}{T} \int_0^T U(x, y, t) dt \quad (9)$$

Different components of sediment transport react differently to the asymmetric tidal signal. For the suspended sediment transport, the threshold velocity for fine-grained material is low. So it can continue to move for some time. Therefore it is likely to be influenced by the weak residual currents.

While for the sand-sized bed-load transport is more affected by the bed shear stress, since this effect the sediment concentration in the bottom layer described in Section 2.2. The calculated bed-load sediment transport is related to a power function of current speed. Therefore the residual sediment transport direction of the bed-load is usually decided by comparing the maximum velocity during ebb tide and flood tide. The sandy non-cohesive material is mainly transported through bed-load transport, so it tends to be transported in the direction with higher peak speed.

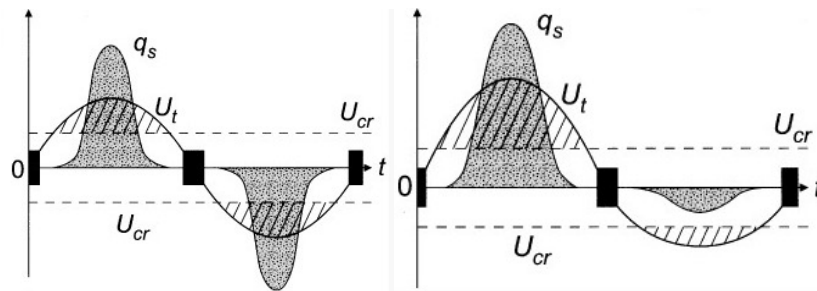


Figure 8: Bedload transport by symmetric tidal current (left) and asymmetric tidal current (right)
(Dalrymple and Choi, 1978)

2.4 Coastline deformation

The change of coastline position is often governed by the long-shore sediment transport. The years averaged sediment transport change under different wave conditions with variations of magnitude and direction determines the coastline deformation (Bosboom and Stive, 2015). For a stable coastline section, the input sediment transport S_{in} equals output sediment transport S_{out} . When S_{in} is larger than S_{out} , some material needs to be eroded from this section and result in shoreline retreat as shown in Figure 9,

which can be given as $\partial S/\partial x > 0$. For the condition of $\partial S/\partial x < 0$, S_{in} is greater than S_{out} , some sediment is deposited in this section and shoreline moves towards seaward.

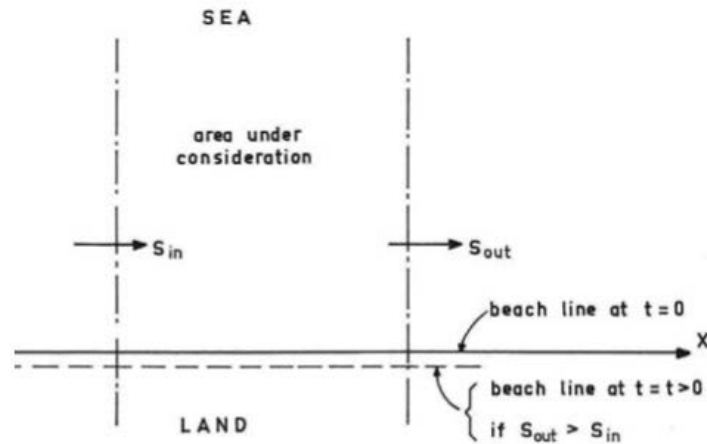


Figure 9: Longshore sediment transport and coastline deformation (Bosboom and Stive, 2015)

In the region where sediment transport is wave dominated, the coastline deformation can be solve by the single line theory. The content of the single line theory assumption is that, the cross-shore profile does not change in time, as shown in Figure 10. Considering shoreline movement in unit width, the sediment entering the coastline section equals to the sediment volume needed for the shoreline moving forward with ΔY . This gives the continues equation as Equation (9).

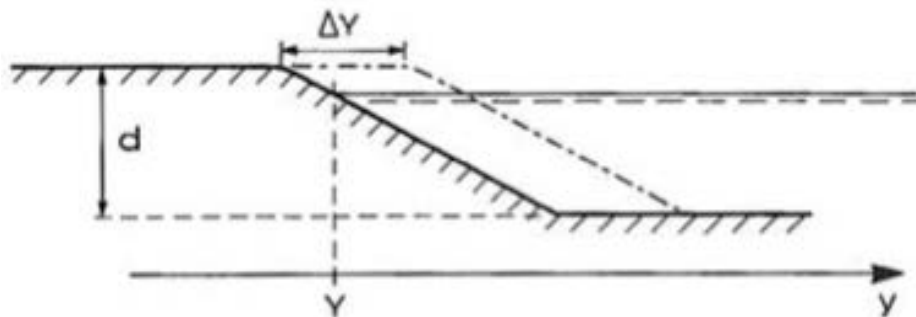


Figure 10: Costal change in a cross-shore view (Bosboom and Stive, 2015)

$$\frac{\partial Y}{\partial t} + \frac{1}{d} \frac{\partial S_x}{\partial x} = 0 \quad (9)$$

where

- Y : shoreline position
- S_x : long-shore sediment transport rate

From the continues equation, a parabolic partial differential equation for coastline position Y , given as Equation (10). This equation is really numerically solved in the coastline development model, such as UNIBEST-CL model (Bosboom and Stive, 2015) .

$$\frac{\partial Y}{\partial t} + \frac{1}{d} \frac{\partial S_x}{\partial \varphi} \frac{\partial^2 \varphi}{\partial x^2} = 0 \quad (10)$$

3

Study area

3.1 Geology background

The DELTA21 project is located at the Southwest Dutch Delta and west of the Haringvliet. The delta area is separated from the Holland coast by the Maasgeul navigation channel. The delta area consists of a series of five estuaries, from north to south Brielse Maas, Haringvliet, Grevelingen, Eastern Scheldt and Western Scheldt (Hijma, 2015). Nowadays, only the Eastern Scheldt and Western Scheldt are still tidal basins after various human interventions at these contiguous ebb-tidal deltas. Going from south to north, the depth of the Voordelta decreases, the channels become smaller and the surface area of intertidal shoals increases (Terwindt, 1973). The slopes of the ebb-tidal deltas have gradient less than 1:1000 to 1:100 and the seaward slopes are ranging from 1:1000 to steeper than 1:100. The ebb-tidal deltas segmented by the ebb- and flood channels have intertidal and supratidal sand bars on top. The coast of Holland (north of the Maasgeul) has a continuous shoreface which extends 120 km to the north. The shoreface of the coast of Holland has a relatively steep surfzone, which can be steeper than 1:100, and consists shore-parallel breaker bars. The lower shoreface of the coast of Holland has small gradients between 1:100 to 1:1000.

The sea bed at the shoreface is predominantly sandy, with some clay deposits, and an admixture of gravel and mollusc shells (Hijma, 2015). To get a look into the bed composition, the data of subsurface research from the DINOLOket at several location is analyzed. The information about the bed composition, grain size distribution (D_{n50} and D_{n90}) and the sand layer sickness is listed in Table 1. The locations that the subsurface taken place is given in Figure 11. Locations of the geological borehole research are in or around the DELTA21 project and Maasvlakte 2. The bed composition is almost all sandy of different categories. According to the borehole log profile, the sandy layer thickness can reach up to 20 m. The grain size distributions show that at the considered locations, the D_{n50} of the bed material is likely to be larger than 0.20 mm. At the near shore location BS031020, the material is finer and D_{n50} is smaller than 0.20 mm. Detailed borehole log profiles and grain size distributions at the considered locations are given in Appendix B.

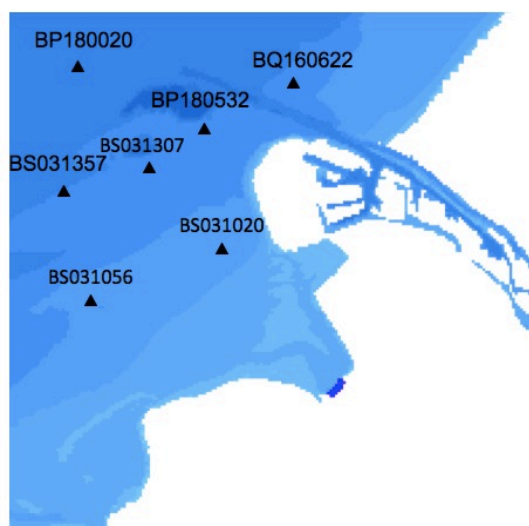


Figure 11: Geological borehole research identification and location from DINoloket (dinoloket.nl)

Table 1: Geological borehole research information form DINoloket

	Bed composition	Sand layer thickness (m)	Dn50 (mm)	Dn90 (mm)
BS031056	Sand(coarse)	4	0.32	0.48
BS031020	Sand(fine),Sand(medium)	10	0.17	1.10
BS031357	Sand(coarse),Sand(medium)	20	0.37	0.71
BS031307	Sand(coarse),Sand(medium)	20	0.27	0.38
BP180532	Sand(coarse),Sand(medium)	20	0.23	0.36
BQ160622	Sand(medium)	3	0.21	0.50
BP180020	Sand(coarse)	4	0.21	0.38

3.2 Maasvlakte 2

Maasvlakte 2 is an enlargement of Rotterdam harbour with 20 km². Half of this area is used for harbour related activities like container terminals, distribution of goods and chemical industry. The other half is used for dikes, roads and harbour basins. The protection of Maasvlakte 2 consist of a hard- and soft-flood defence (see Figure 12). The hard flood defence is 3.5 km long and consists of a cobble beach with a cube reef in front. The soft flood defence is built as a 7.5 km long sandy beach with single dune. Between the hard and soft protection a transition zone is present. Transition zones are often vulnerable and unpredictable components of a coastal defence system.

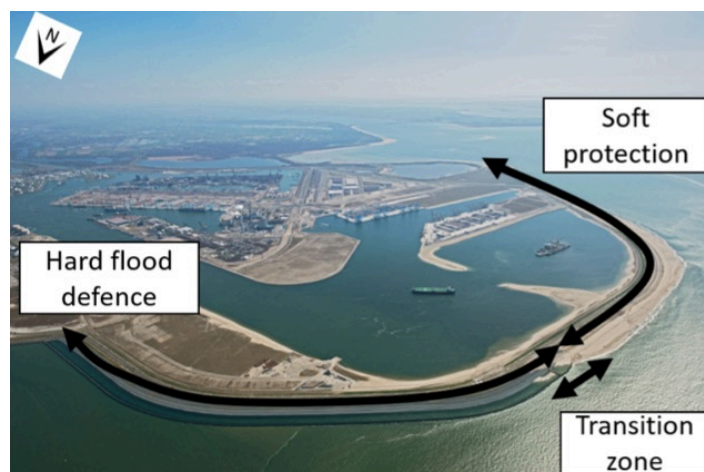


Figure 12: Sea defence of Maasvlakte 2 (Mann, 2019)

To construct the land reclamation an amount of about 290 million cubic meters of marine sand was needed for the outer contour. Later on another 75 million cubic meters were needed for the construction of new quays inside the harbour basin.

Most of the sand is extracted from the area south of the Euro/Maas channel, as shown in Figure 13.



Figure 13: Sand extraction area of Maasvlakte 2 (Stolk and Dijkshoorn, 2009)

Prediction of future morphological evolution has been done for the Maasvlakte 2. For the construction of Maasvlakte 2, in the context of the EIA study, a study was performed on the effect of Maasvlakte 2 using the morphodynamic Delft3D model. The simulation result indicates the occurrence of a large scour hole due to contraction of the tidal current at the head of Maasvlakte 2. The calculations in the modelling is based on uniform (non-graded) soil material. This means that the result is considered as upper limit (Roelvink and Aarninkhof, 2005) with respect to the scour depth. A sensitivity study was then be done for the Maasvlakte 2 to study the armouring effect of graded bed material. When applying the graded sediment, the model results shows a significant decrease in the depth of the scour hole (Elias et al, 2006).

The sand loss as a result of wave-driven transport at the sandy coast is modeled by both Delft3D and Unibest-CL (PUMA, 2008). Based on the model results, the the required maintenance volume was predicted.

3.3 Hydrodynamic forcing

3.3.1 Tide

The paper of Van der Werf (2017b) showed the hydrodynamic characters in the study area, including tide, wind and wave conditions. Along the Dutch coast, the mean tidal range decreased from south to north, and from 3.8 m to 1.4 m. Around the location of the Maasvlakte 2, the mean tidal range is approximaely 1.75 m. The tidal signal retrieved from Delft Dashboard at station Xtide Tidal Station Haringvliet 10 which is outside of the Haringvliet outer delta is given in Figure 14. The alongshore-directed tidal current is deflected by the Coriolis force, which gives a onshore bended flood current and a offshore bended ebb current.

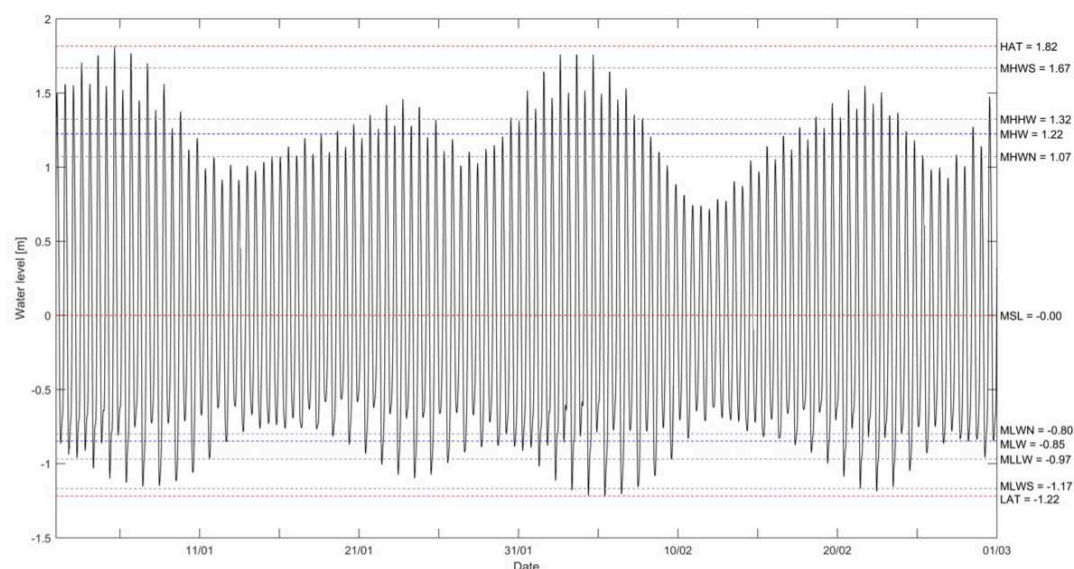
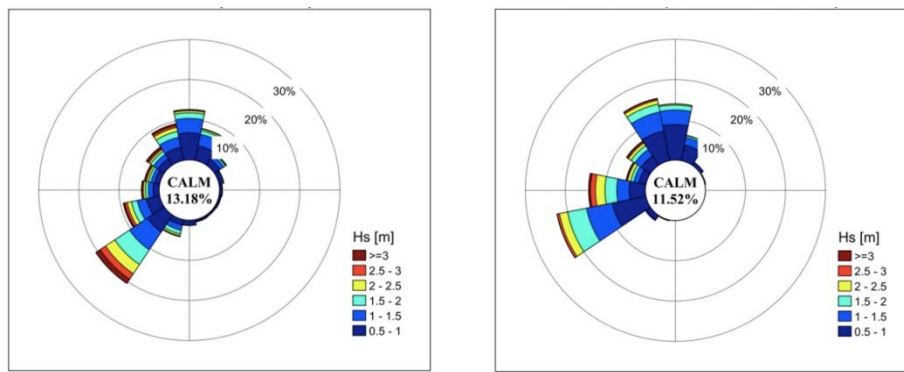


Figure 14: Tidal signal retrieved from Delft Dashboard measuring station: Xtide Tidal Station Haringvliet 10 (Colina, 2018)

3.3.2 Wave

The direction of incoming wave measured at Europlatform is mainly distributed from southwest to north as shown in Figure 15(a) (Mann, 2019). The wave from southwest carries that has largerst energy flux, has great chance of significant wave height reach up to 1.5 m. To get the onshore wave climate, the offshore wave needs to be transformed to near-shore with program SWAN. At the location near Maasvlakte, this transformation has done by former student Olthoff (2019) and the result is given in Figure 15(b). The nearshore wave is further more concentrated in the direction from southwest to north. The wave energy flux is dramatically reduce due to wave breaking. Still wave coming from west carries most energy.



(a) Wave rose from Europlatform

(b) Nearshore wave rose (800m offshore)

Figure 15: Waves roses from 2013-2018 obtained from the Europlatform and a point 800m offshore from the sand layer area (Mann, 2019)

4

Local-scale model setup

4.1 Introduction

This chapter deals with the model setup in UNIBEST based on the methodology introduced in Section 1.4. The parameters setting of UNIBEST-LT model are shown in Section 4.1. The construction of UNIBEST-CL model for the original layout and improved layout are introduced in Section 4.2, including the construction of the basic coastline model and simulation period deformation.

4.2 Setup of UNIBEST LT-model

The UNIBEST LT-model gives the long-shore sediment transport caused by the tidal and wave induced long-shore currents. Along the coastline of Delta21, UNIBEST LT-model calculates the sediment transport at Various locations. As a result, the distribution of long-shore transports along the profile is known along the entire northern part of the Delta21 area. The coastline orientation in relation to the direction of incoming wave determines influences the longshore sediment transport rate. The curve in which this relationship is given, is called a $S-\varphi$ curve. These $S-\varphi$ curves are the basis for theoretical analysis and also input file in CL-model. Within the UNIBEST LT-model for the DELTA 21 coastline, the grain size and depth profile along the sea defense is set to be constant. This means that the sediment transports along the Delta21 coastline are determined by the coastline orientation and wave climate.

The coastline orientation along the northern part of the Delta21 area (Valmeer) differs from 250°N to 360°N and cannot be covered in only a single $S-\varphi$ curve. For that reason, the sea defenses of Valmeer can be cut into several sections. The original layout has three segments, and the applied coast orientation for these sections are 250°N, 305°N and 360°N, respectively. For the improved layout with a simple shape, it has two sections. The applied coast orientation are 250°N and 305°N, as shown in Figure 16.

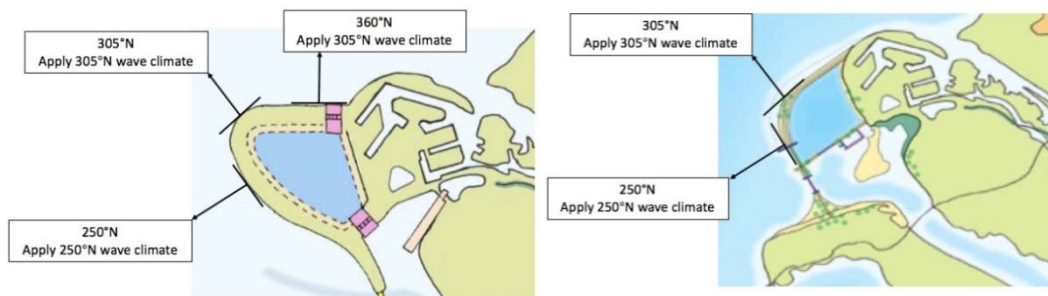


Figure 16: The coastal orientation and wave climate aoupled with original layout (left) and improved layout (right)

4.2.1 Wave and tide

As input for the UNIBEST LT-model wave climates are applied which were also applied for the design of the soft sea defense of Maasvlakte 2 (source: PUMA). There are two wave climates are applied in the LT-model, which are the wave climates at the toe of the Maasvlakte 2 soft defense. These wave climates are applicable for a coastline orientation of 250°N (southwest) and 305°N (northwest). The wave climates is visualized in the wave-rose diagram in Figure 17. The wave climate applied at the southwest coastline has 39 reduced wave conditions and predominantly comes southwest and northwest direction. The wave conditions applied at the northwest coast covers the direction from southwest to northeast. Wave climate applied on the northwest coast carries more energy with larger occurrence probability of high wave significant height. In especial for the wave from northwest, there is a noticeable proportion of wave condition with wave height larger than 3m. In the model of the original layout, the northwest wave climate is also applied for coast section of 360°N. The combination of wave climate and coast orientation is shown in Figure 16. The detail of the wave current and tidal current applied in the model is introduced in Appendix A.

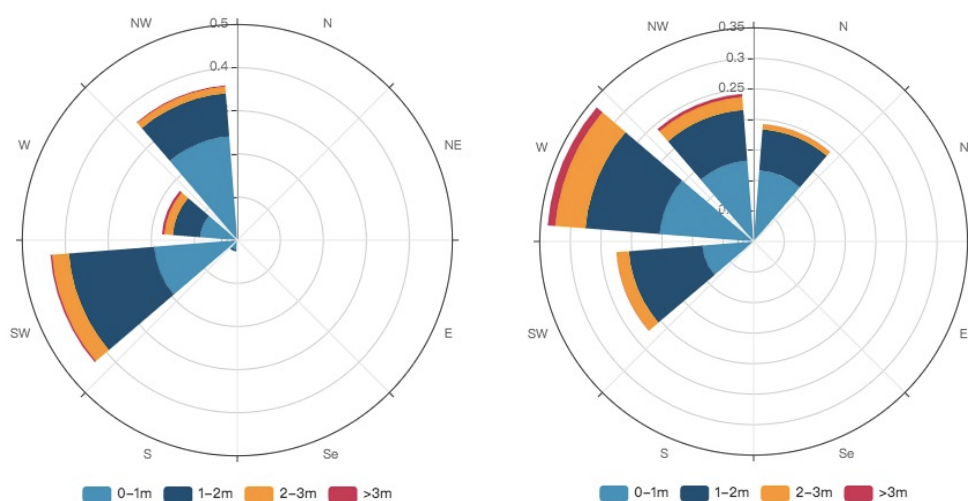


Figure 17: Wave-rose for wave climates applied at southwest coast (left) and northwest coast (right)

Conclusively, the wave climates as applied in the UNIBEST LT-model are listed in Table 1.

Table 2: The coast orientation and wave climate applied in LT-model

	Coast orientation	Applied wave climate
1	250°N	Northwest
2	305°N	Southwest
3	360°N	Southwest

4.2.2 Depth profile

For a UNIBEST LT-model, the cross-shore profile should be specified along the coastline. The cross-shore profile is defined by the table of x-location and water depth. The x value specified the location with the axis positive towards onshore direction. Since the specific dune structure in DELTA 21 project is still in a design stage, the cross-shore profile in the Maasvlakte 2 model is applied and set to be constant along the sea defense, as listed in Table 2.

Then, the spatial grid is specified on the cross-shore profile. To reduce the amount of calculation, the grid length is reduced from 50m to 5m towards the onshore direction. This results in a higher grid density in the area where high a spatially varying sediment transports are expected.

Table 3: Cross-shore depth profile in LT-model

	x(m)	Depth(m)
1	-1037	17.5
2	-887	17.5
3	-717	9
4	-588	7.5
5	-408	5
6	-292	3
7	-227	1.5
8	-120	-1
9	-70	-3
10	-70	-3
11	-52	-12
12	-37	-12
13	-28	-9
14	-11	-9
15	0	-5.5

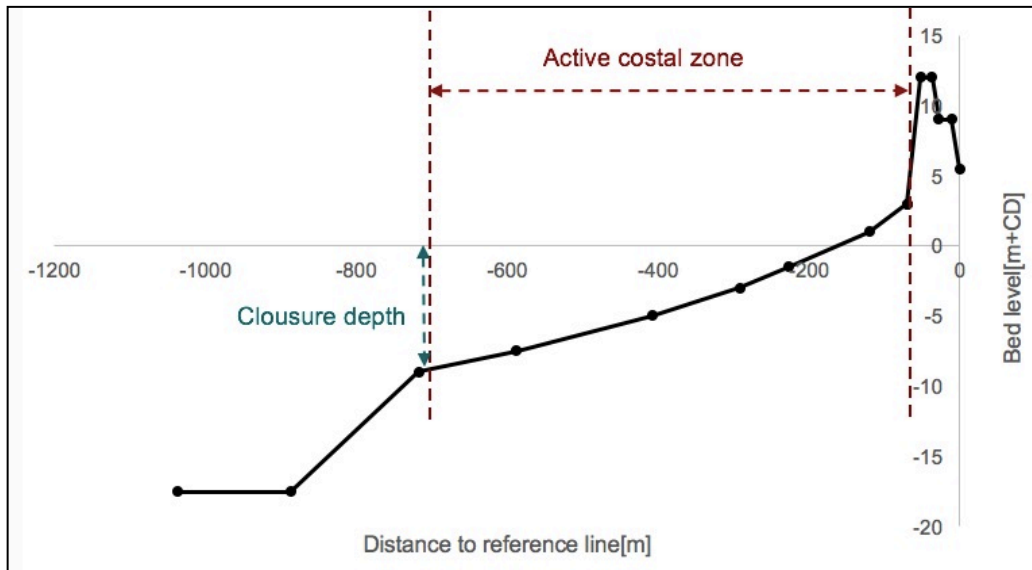


Figure 18: Cross-shore depth profile marked with closure depth and active height

4.2.3 Closure depth and active height

There are other two important parameters of LT model input are the closure depth and the active height. For the calculation of UNIBEST LT-model, sediment transport in the area within the closure depth is considered. So the value of “dynamic boundary” will effect the sediment transport rate along the sandy beach exported by UNIBEST LT-model. The active coastal zone associated with the active height is where the profile deformation happens. The calculated sediment transport rate and the active height is saved in the result file, which is used in the CL-model the simulation of shoreline deformation.

The closure depth in the model is estimated according to the Hallermeier-equation (1981) .

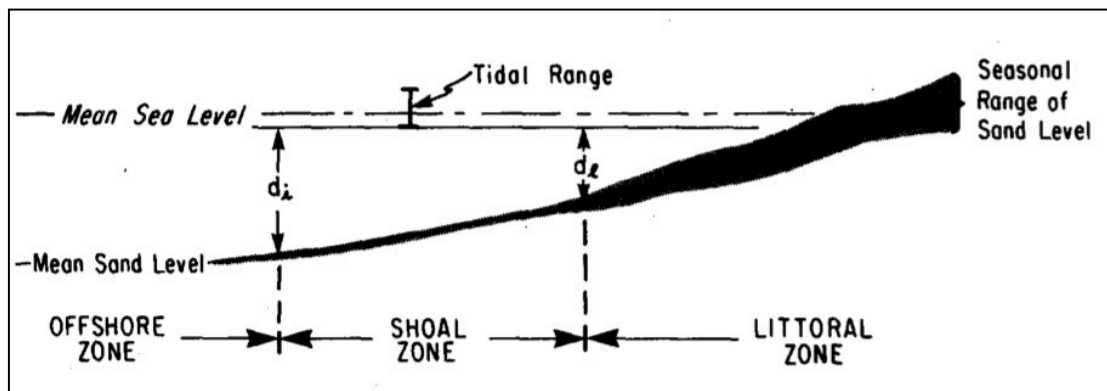


Figure 19 : Proposed annual zonation of seasonal sand beach profile (Hallermeier, 1981)

$$d_i = 2.28H_{sx} - 68.5 \frac{H_{sx}^2}{g * T_{sx}^2} \quad (11)$$

$$H_{sx} = \bar{H}_s - 0.3\sigma$$

$$T_{sx} = \bar{T}_s$$

Where:

- d_i : The closure depth d_i is defined as the depth to which significant sediment transport by waves is occurring. At depths larger than d_i , sediment transports are expected to be non-relevant.
- H_{sx} : The extreme wave height that is exceeded 12 hour per year.
- T_{sx} : The period associated with extreme wave height.
- \bar{H}_s : Mean significant wave height.
- \bar{T}_s : Mean significant wave period.
- σ : Standard deviation of significant wave height.

According to Hallermeier equation, the closure depth is related to the wave climate. The closure depth for two wave climates is calculated in Table 4.

Table 4: The calculation of closure depth

Wave climate	\bar{H}_s	\bar{T}_s	σ	H_{sx}	T_{sx}	d_i
Southwest	0.87	9.25	0.60	4.23	9.25	8.18
Northwest	0.96	9.68	0.65	4.63	9.68	8.95

The active height defines the area where the cross-shore coast zone is highly dynamic by the hydraulic process. It can be calculated as the closure depth plus profile height beyond the water level. According to the previously calculation, the extreme wave height reach up to 3 m. And the water level raise during flood tide is about 1 m. Therefore, above the water level, a 4 m profile height is added to the active height. The closure depth and active height for the two wave climates is listed in Table 5.

Table 5: Closure depth and active height in LT-model

Wave climate	Closure depth(m)	Active height(m)
Southwest	8.18	12.18
Northwest	8.95	12.95

4.2.4 Sediment transport parameters

For the calculation of the sediment transport, the transport formula is select to be Van Rijn (1993) equation. According to the design of DELTA 21, the dredged material from the Valmeer will be used for the dune construction. For the design of Maasvlakte 2, D_{n50} of 0.37mm and D_{n90} of 0.58mm was applied at the soft defense. The same grain size distribution will be applied for the sandy beach of Valmeer in this study.

4.3 Setup of UNIBEST CL-model

The UNIBEST CL-model computes the coastline evolution and sediment transport at predefined location along the coastline. There are two main steps to set up a CL-model, creating the coastline and defining the global climate.

4.3.1 Definition of the coastline

The coastline in the UNIBEST CL-model is defined based on the sketch of the DELTA 21 layout. The figure imported in the model need to be scaled and rotated to couple with the real spatial dimension. This done by adjusting the coordinates of three geo-referencing points on the figure. As the real world coordinates applied at these three points, coordinates of other points on this figure also fits in the real world. To define the real spatial dimension for both original and improved layout, three points near Maasvlakte 2 is specified as geo-referencing points. Three point are located at the tip of the Hook of Holland, the eastern boundary of Haringvliet dam and a bend of the water way in Maasvlakte 2, as shown in Figure 20.

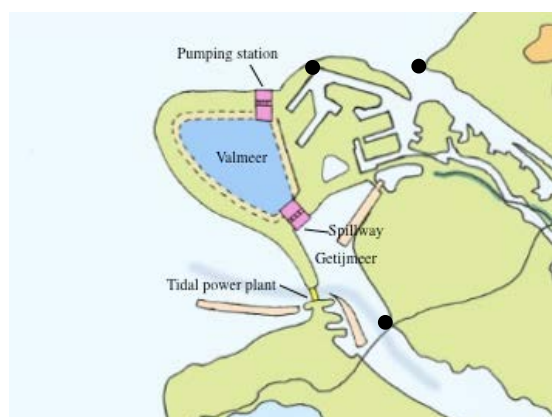


Figure 20: Location of three geo-referencing points

The coastline in the UNIBEST CL-model is define by a reference line (basic model) and a support line (coast model). The support line shows the exact shape of the shoreline. The reference line follows the general contour and fitted to the shoreline. The grid is generated along the reference line, as shown in Figure 22 and Figure 23.

The coastline range for the original layout covers the sea defense of Valmeer and soft defense of Maasvlakte 2. This study deals with the morphological development at northern side, so the southern boundary doesn't reach the barrier of the tidal lake. The northern boundary is at the transmission of soft defense and hard defense of Maasvlakte 2. At this location, the sand is transported in and along the hard sea defense (see Figure 21). Such process cannot be simulated by the UNIBEST CL-model and is therefore not included in this study.

The UNIBEST CL-model for the improved layout covers the sea defense of the Valmeer and also involves the outlet of the pumping station. By doing this, the deposition which may happen near the breakwater of the pumping station can be considered as well. Within the model, the pumping station and outlet is modeled as a section of sea defense. No water discharge through the outlet is included.

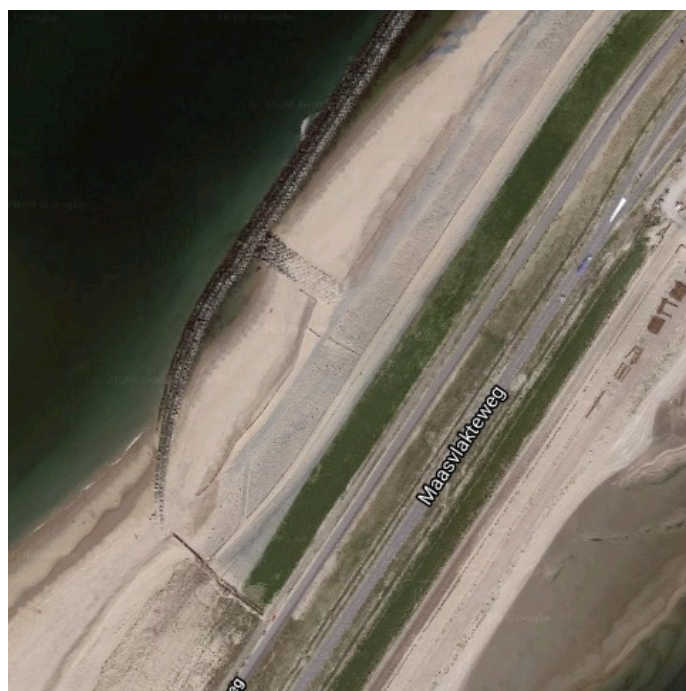


Figure 21: The structure to block sediment between soft defense and hard defense (earth.google.com)

4.3.2 Definition of the global climate

To define the global climate in the UNIBEST CL-model, the RAY-file that generated from UNIBEST LT-model is used. The RAY-file describes the schematized sediment transport and contains information about the depth profile. In CL-model, the RAY-file will then fitted to the specific location according to the wave climate and costal orientation.

For the original layout, the RAY-files are coupled in the following way:

- the RAY-file as applicable for the 250°N coast is coupled to the southwest coastline.
- the RAY-file as applicable for the for 305°N coast is coupled to head of Valmeer and also the soft defense of Maasvlakte 2.
- the RAY-file for 360°N coast is coupled to the northern part of Valmeer

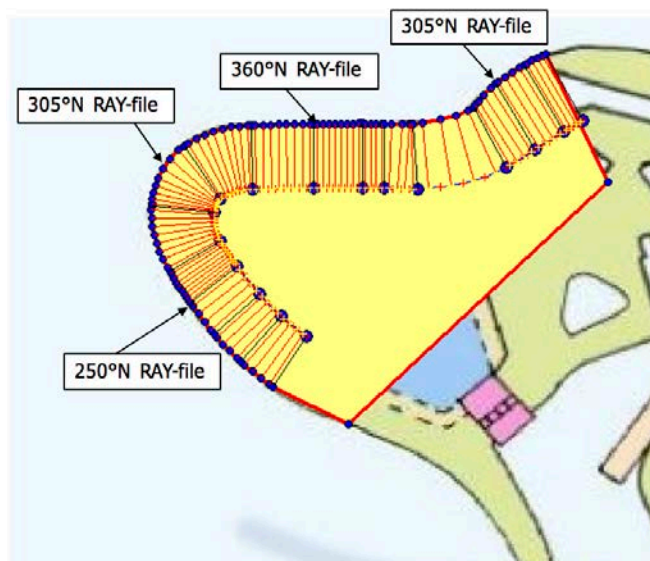


Figure 22: The CL-model of the original layout

For the improved layout, the RAY-files are coupled in the following way:

- the RAY-file as applicable for the 250°N coast is coupled to the southwest coastline.
- the RAY-file as applicable for the for 305°N coast is coupled to northern part.

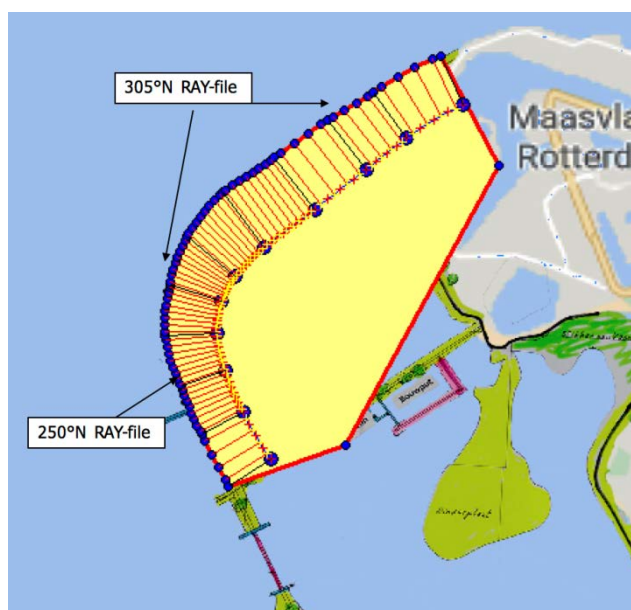


Figure 23: The CL-model of the improved layout

5

Local-scale model results analysis

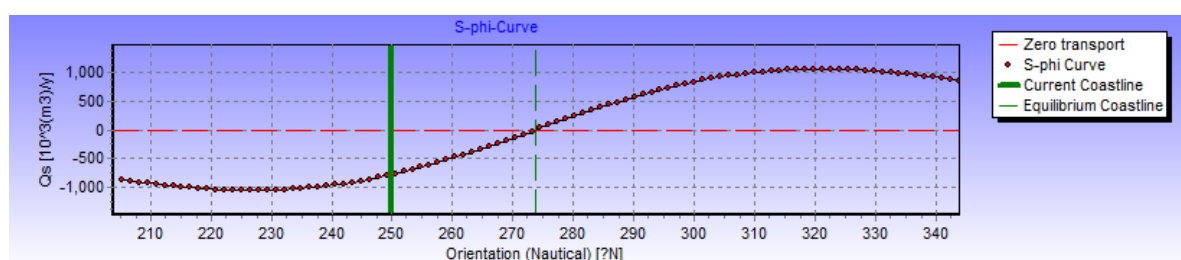
5.1 Introduction

Sediment transport distributions for three different coast segment have been generated from the UNIBEST LT-model calculation. With the transport distributions, the 1 year, 3 year, 5 year and 10 year coastline deformation along the sandy beach of Valmeer has been simulated in UNIBEST CL-model, for both the original layout and improved layout. Section 5.1 deals with the theoretical prediction of the coastline evolution based on the sediment transport rate along the sandy beach. In Section 5.2, the coastline deformation is quantitatively analyzed based on the result of CL-model simulation. By comparing the CL-model simulation result with theoretical conclusions in Section 5.1, the process of coastline evolution is better understood. Synthesize the conclusions from Section 5.1 and Section 5.2, the necessity and efficiency of the layout improvement is summarized in Section 5.3.

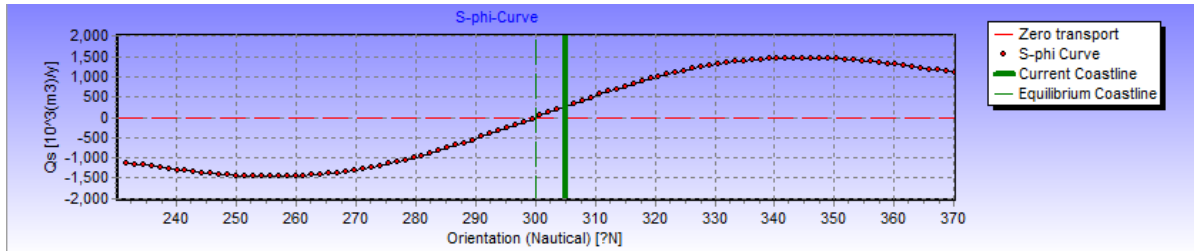
5.2 Theoretical analysis

5.2.1 Sediment transport curve

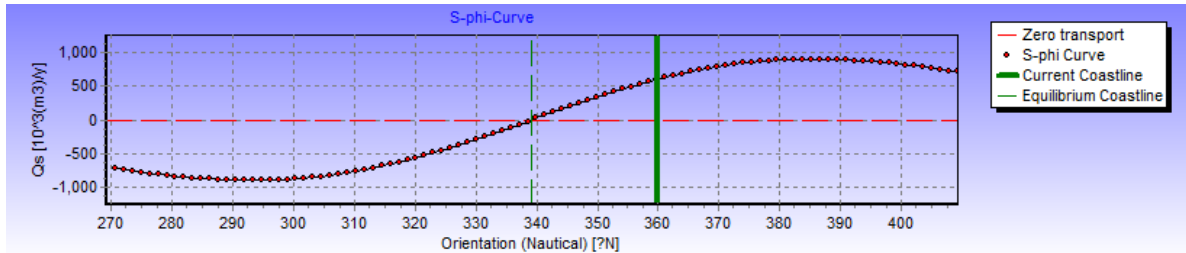
Three S- ϕ curves that describe the sediment transport distribution along different coastline orientation has been generated from LT-model, as shown in Figure 24. The curve of sediment transport distribution along the sea defense is produced by reading the sediment transport rate at different locations from the S- ϕ curves. Along the coastline of original and improved layout, several points is selected and the coastal orientation is measured.



(1) S- ϕ curves for the 250°N coast



(2) S-φ curves for the 305°N coast



(3) S-φ curves for the 360°N coast

Figure 24: S-φ curves generated from Lt-model

For the sediment transport rate at some area that between 250°N, 305°N and 360°N, two different S-φ curves gives completely different result. For these coast orientations, the accurate sediment transport rate is achieved by additional UNIBEST LT-model run. According to measured coastal orientation, the calculated sediment transport rates are listed in Table 6 and Table 7.

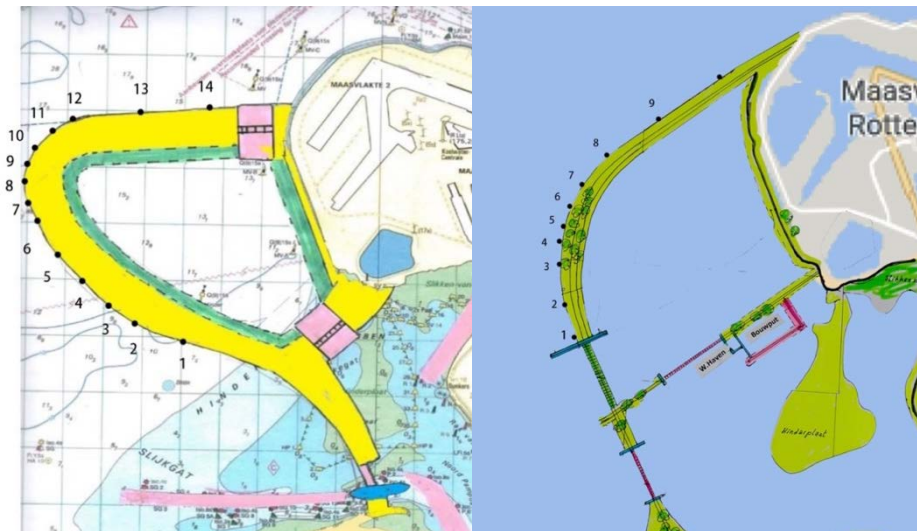


Figure 25: The points selected on the original and improved layout

Table 6: Sediment transport rate along original layout

	Coast orientation	Wave climate applied	Sediment transport[m³/y]
1	195.7°N	Southwest	-784.391
2	209.4°N	Southwest	-980.909
3	216.6°N	Southwest	-1000.943
4	225.3°N	Southwest	-1050.815
5	229.8°N	Southwest	-1030.305
6	244.9°N	Southwest	-900.223
7	249.1°N	Southwest	-750.138
8	269.7°N	Southwest	-164.264
9	290.3°N	Northwest	211.302
10	308.6°N	Northwest	430.624
11	322.7°N	Northwest	1030.32
12	342.3°N	Northwest	1340.441
13	356.5°N	Northwest	750.114
14	360.0°N	Northwest	680.114

Table 7: Sediment transport rate along improved layout

	Coast orientation	Wave climate applied	Sediment transport[m³/y]
1	246.6°N	Southwest	-860,451
2	255.3°N	Southwest	-700,568
3	270.7°N	Southwest	-656,654
4	277.3°N	Southwest	-501,940
5	282.2°N	Northwest	-367,180
6	293.9°N	Northwest	-41,452
7	303.9°N	Northwest	212,501
8	318.2°N	Northwest	492,138
9	325.6°N	Northwest	588,801

Then the curves of the sediment transport along sandy beach of original layout and improved layout is given in Figure 26 and Figure 27, respectively. The x-axis gives the distance of these locations from south to north and y-axis shows the sediment transport rate at these locations. The positive value stands for sediment transported towards northern boundary. Negative transport is directed towards the southern boundary. The coastline evolution can then be estimated according to change of sediment transport. Deposition occurs at location where the sediment transport rate is decreasing along the transport direction. On the contrary, the coastline is eroded if the sediment transport is increasing.

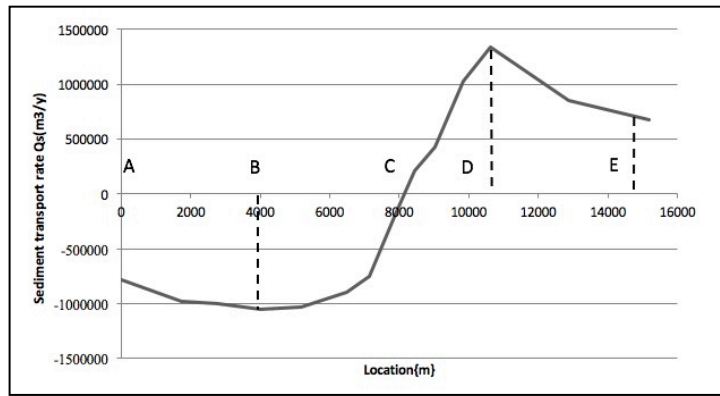


Figure 26: The sediment transport along the sandy beach for the original layout

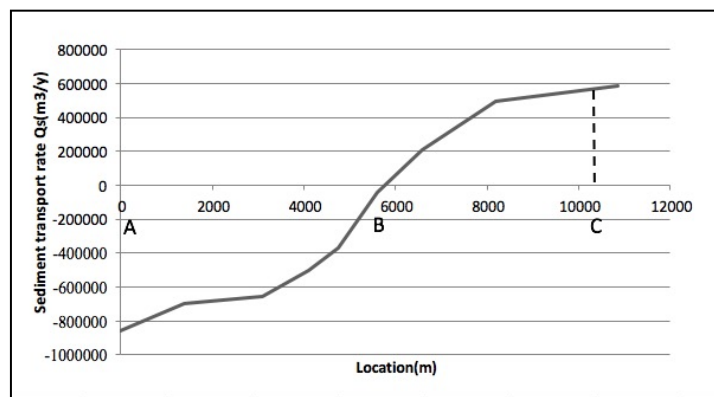


Figure 27: The sediment transport along the sandy beach for the improved layout

5.2.2 Result for the original layout

To be analyzed, the sandy beach of the Valmeer is divided into several sections. Along the original layout, six points are picked along the coastline and form five sections as shown in Figure 28. Location A and E are the southern boundary and northern boundary, respectively. At location C, the direction of sediment transport is changed from negative to positive. Location B is the peak point of sediment transport towards southern boundary. Location D is the peak point of sediment transport towards northern boundary.

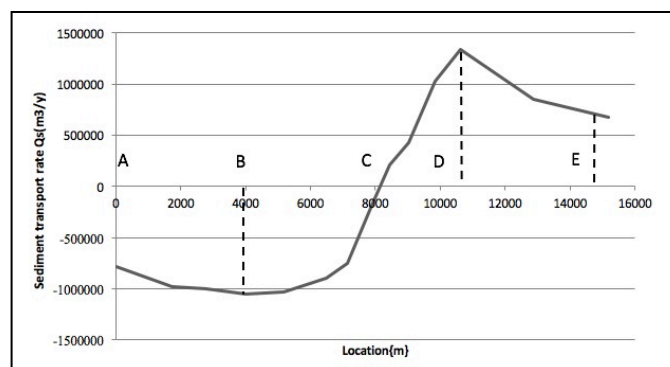


Figure 28: The sediment transport along the sandy beach for the original layout

According to Figure 29(a), at southwest side, the sediment is transported towards southern boundary. With point B holds the maximum sediment transport rate, sediment transport is decreasing in section AB and increasing in section BC. So there will be deposition in section AB and section BC will be eroded. Furthermore if look at gradient of curve, the volume of the sedimentation in section AB will be very limited with a gentle slope of the curve. The erosion around point C will be quite noticeable. In section CE, the sediment is transported toward the Maasvlakte 2 as shown in Figure 29(c). With a rapid increasing of the sediment transport rate, section CD will be eroded seriously at the head of Valmeer. At the sandy beach at the northern side, there will be some sedimentation in section DE. At the joint of the Valmeer and Maasvlakte 2, the sediment transport direction changes which may cause deposition similarly as a groyne.

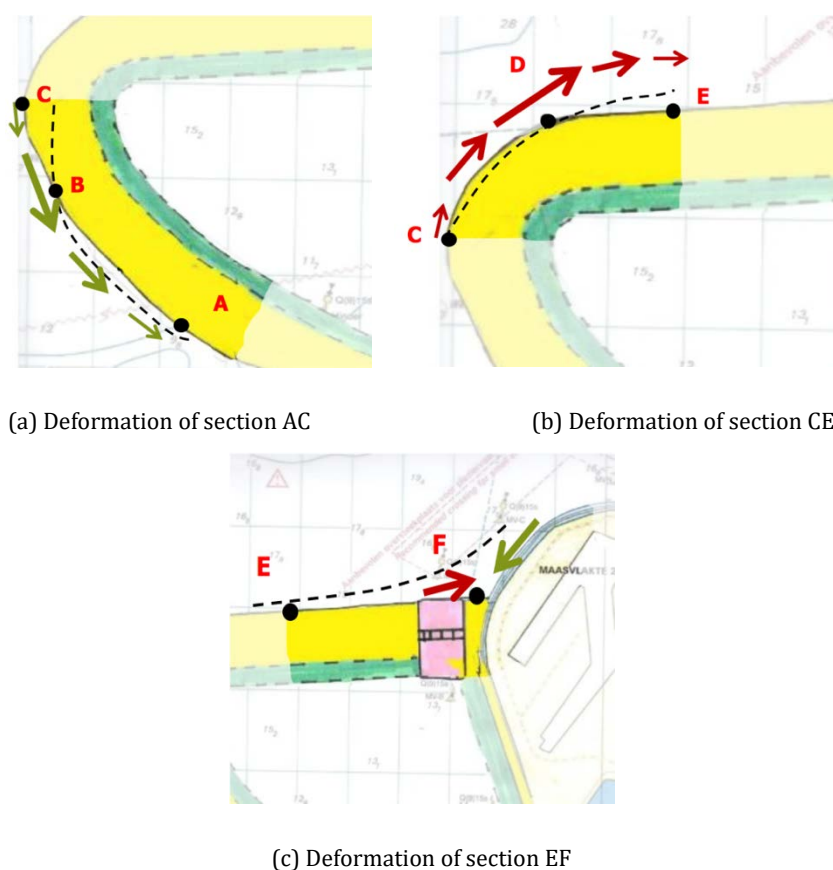


Figure 29: The coastline deformation of original layout at different sections

Combining deformation in all sections, the coastline evolution as a whole is demonstrated in Figure 30. There will be some deposition, at the sea defense of northern side as the sediment transport towards the northern boundary is decreased in section DE and change of transport direction at location F. The head of the Valmeer will be seriously eroded due to increased sediment transport in both section CD and BC. At the southern part of the sandy beach, sediment is deposited due to decreased sediment transport in section AB. On the whole, the sediment transport along the sea defense is smoothing the bulge shape of the Valmeer and the angle at the transmission part. The shape of the layout is transformed towards the shape similar as Maasvlakte 2.

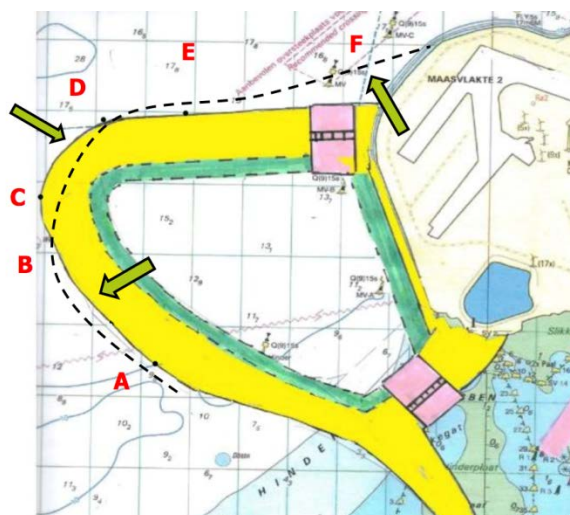


Figure 30: The coastline deformation of original layout

While processing the theoretical analysis, several facts is not considered:

- At point F, the flow and turbulence caused by the discharge from the pumping station may make it hard to keep deposition at the joint.
- Along the sea defense at southwest side, tidal current may have more effect on the sediment transport after the reopening of the Haringvliet Dam.

5.2.3 Sandy hook development

On the northern side of the sea defense, there may develop a unpredictable sedimentation, which is known as sand spit. Spits are known as an accumulating form attached at one end of the mainland, as shown in Figure 31. Spits are common morphological features on interrupted coastlines that can typically be found at locations where the coast makes a sudden change in its orientation (King, 1972). For the accumulation of sand spit, it requires a sediment transport capacity to decrease as the wave angle increase. So the angle between the incoming wave and the base of the spit needs to be larger than 45° , as shown in Figure 32, where the transport has its maximum. The spit will be formed down-drift a coastline with a wave incidence angle of less than 45° .



Figure 31: Sandy hook (spit) at Jibei island

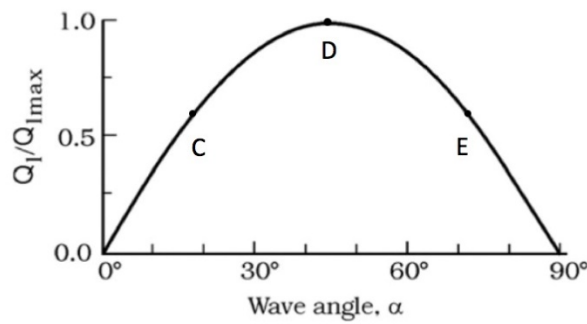
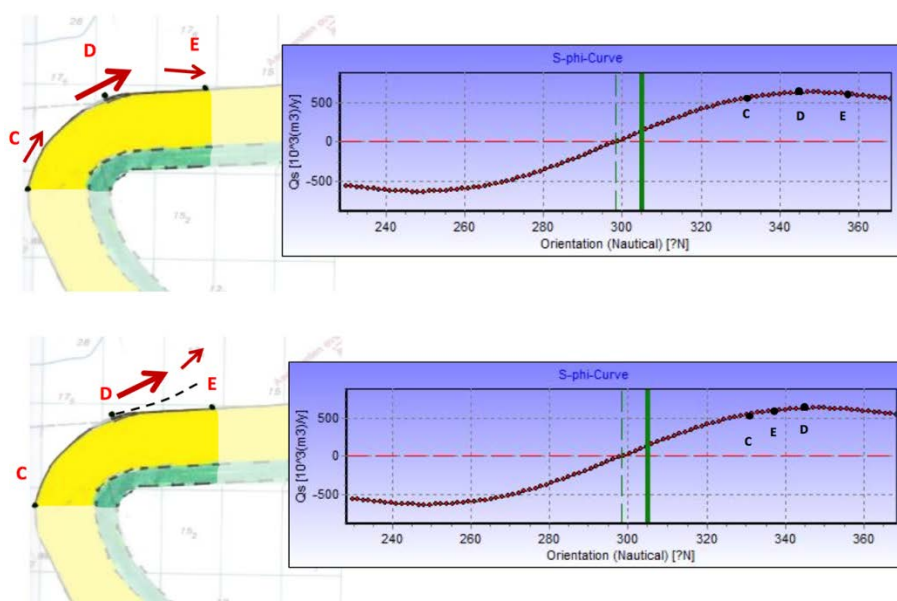


Figure 32: The qualitative relation between the wave direction and the littoral drift for a given offshore wave height (Petersen, 2008)

In the original layout, the head of the Valmeer has a bulge shape, which lead to a rapidly changing of the coastline orientation from Point C to point E. According to the $S-\varphi$ curve in Figure 33, the direction of incoming wave from northwest is about 300° . So incidence angle of section DE is larger than 45° and incidence angle of section CD is smaller than 45° .

Along Section C-E, the sediment transport rate increases to a maximum value at Point D and decreases again towards the east. As shown in Figure 33, Point D is at the peak point of the $S-\varphi$ curve, where the transport has its maximum. On the $S-\varphi$ curve, Point E is located on the right side of Point D. From Point D to E, there is some deposition in Section D-E due to decreasing of sediment transport. The deposition results in the change of coastal orientation at Point E, which means Point E switch to the upward slope. However, there is still a decreasing of the sediment transport from Point D to E as read from the $S-\varphi$ curve. The deposition in Section D-E will carry on, and so does the moving of Point E towards the left side in the the $S-\varphi$ curve. The process of sedimentation is further encouraged by the change of coastal orientation. Unpredictable sedimentation can form a structure so-called sandy hook or a coastal spits, as shown in Figure 12, which is a hidden trouble for the maintenance of DELTA 21 project.



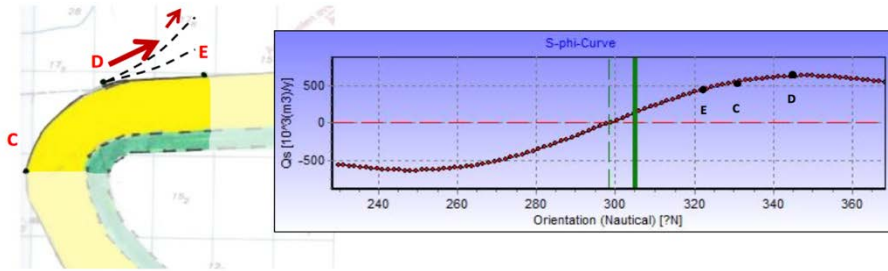


Figure 33: The morphological process of sandy hook occurrence

5.2.4 Result for the improved layout

Condition for the improved layout is less complex. The curve of sediment transport along the coastline demonstrated in Figure 34 has a simple positive slope. The point A is located at the breakwater of the pumping outlet. Location B is around the head of the Valmeer, where sediment start to transport towards the northern boundary. Location C is at the northern boundary.

Along section AB, sediment transport towards the pumping station is increasing, which results in the erosion within section AB. At the head of groyne, some deposition is expected as the sediment is blocked by the groyne. Along section BC, erosion is again caused by the increase of sediment transport towards the Maasvlakte 2. The predicted coastline deformation is shown in Figure 35.

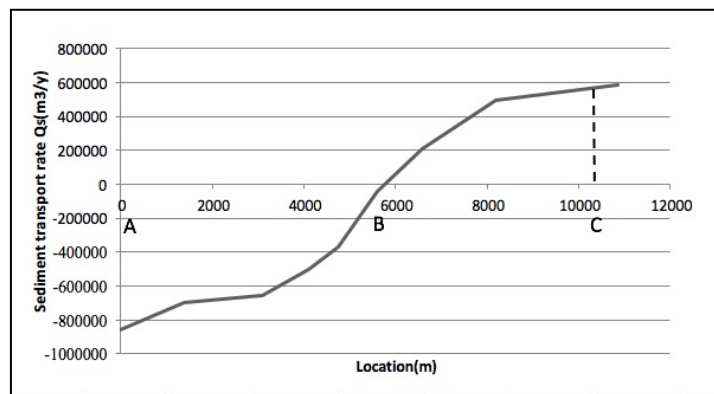


Figure 34: The sediment transport along the sandy beach of improved layout

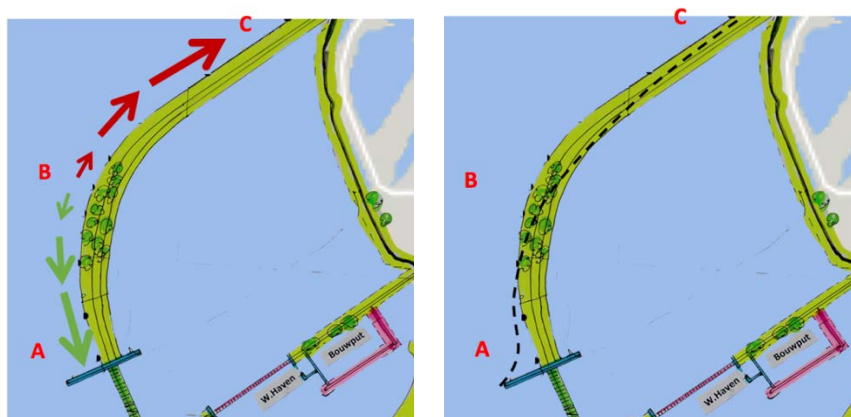


Figure 35: The coastline deformation of improved layout

5.3 UNIBEST CL-model results

The 1 year, 3 years, 5 years and 10 years' coastline deformation is simulated in the UNIBEST CL-model. The result is analyzed and compared with the conclusion of theoretical analysis. The UNIBEST CL-model is constructed based on the design sketch of the DELTA 21 project. In the model, parameter Y stands for the distance between the coastline and reference line. At each point, the deviation of this parameter ΔY is stands for the coastal deformation, with positive ΔY indicates deposition and negative ΔY indicates erosion.

5.3.1 Result of original layout

After 10 years' simulation, the evolution of the coastline along the Valmeer is shown in Figure 36. The large erosion at the head of the Valmeer is one of the expected appearance based on the explanation in Section 4.2. Along the sea defense, the maximum shoreline retreat is reaching up to 448m after 10 years, as shown in Figure 37. On the southwest side, the coastline is hardly changing due to the more or less constant sediment transport rate.

At the head of Valmeer with maximum coastline retreat, the average erosion rate is calculated based on the shoreline retreat from the model result and listed in Table 8. The erosion rate decreased rapidly from 72m/year to 54 m/year in the first 3 years. The decreasing of the erosion rate slows down in following years. For the last 5 years, the erosion rate of the sandy beach still gives a considerable value as 35.8 m/year.

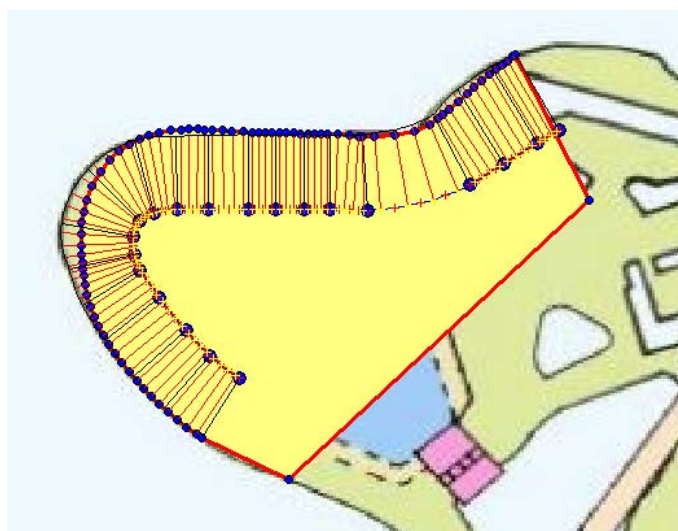


Figure 36: The coastline deformation of original layout after 10 years simulation

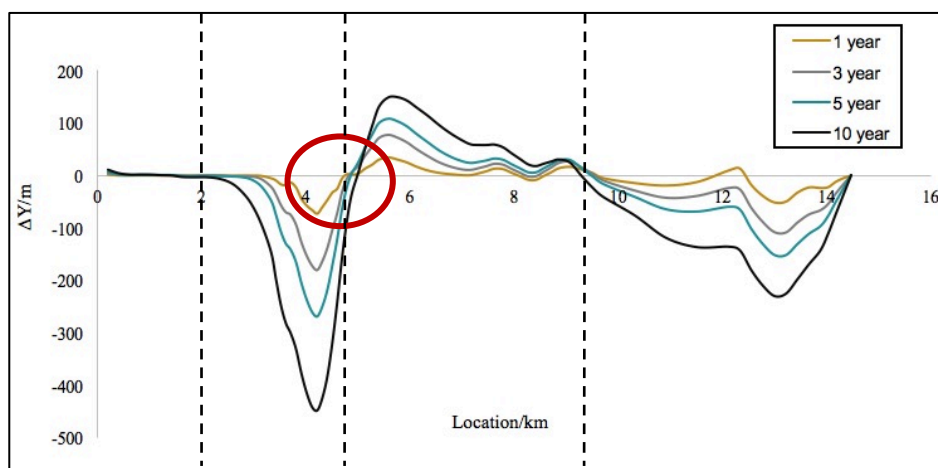


Figure 37: The coastline deformation of original layout after 1 year, 3 years, 5 years and 10 years simulation

Table 8: Average erosion rate at maximum retreat location of original layout

Year	Coastline retreat (m)	Erosion rate (m/year)
1	71.9332	71.9
2	125.9332	54.0
3	179.8413	54.0
4	224.8413	45.0
5	269.0787	45.0
6	304.8787	35.8
7	340.6787	35.8
8	376.4787	35.8
9	412.2787	35.8
10	448.2711	35.8

At the northern side, the hidden threaten of unpredictable sedimentation in section 3 does not occur in the model simulation result. According to the deformation curve, the turning point between the erosion in Section 2 and depositing in Section 3 is moving to the east (towards the Maasvlakte 2). Figure 38 demonstrates the coastline deformation and erosion rate after 1, 3, 5 and 10 years. The long string that surrounded the outer contour of the coastline shows the erosion rate (in m/y), with the red line indicate erosion rate and yellow line indicate deposition rate (in m/y). The deposited area is gradually decreasing with the development of time, especially from 5 years to 10 years. This signifies the pick point of the S- φ curve as introduced in Section 5.1 is moving towards Maasvlakte 2, as shown in Figure 38.

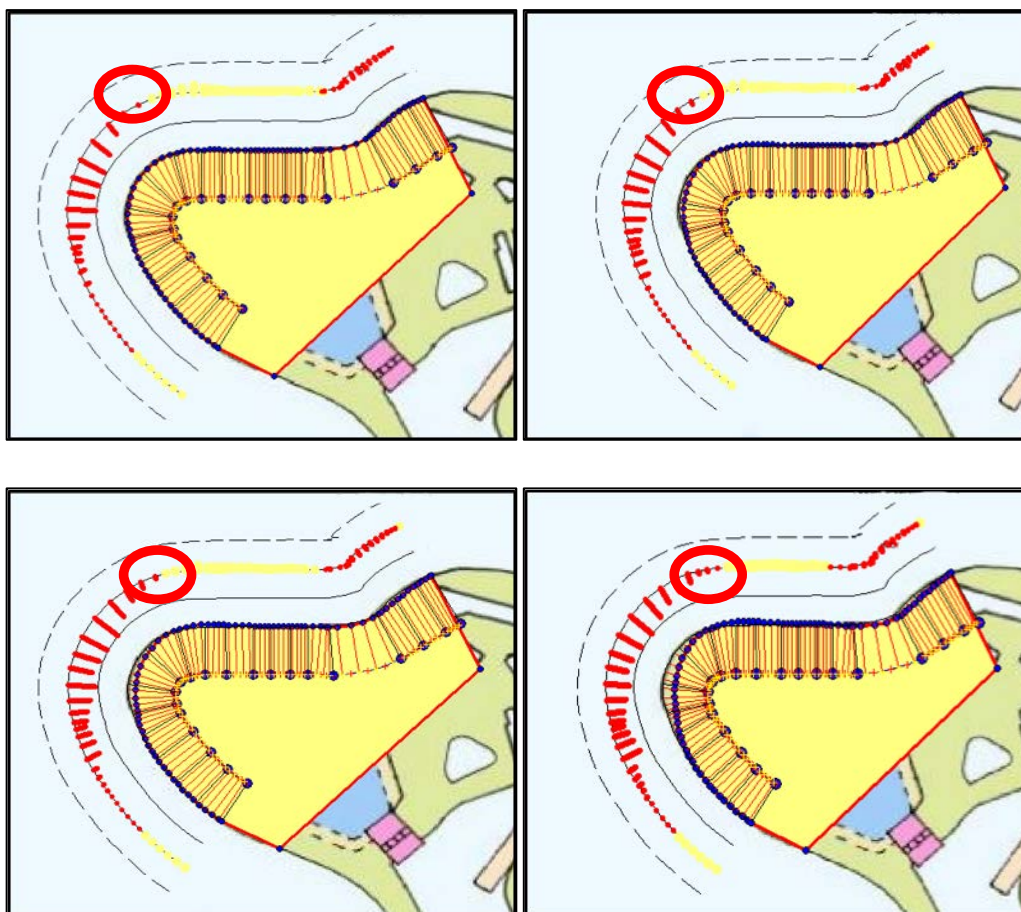


Figure 38: The coastline deformation and erosion rate after 1 year (upper left), 3 years (upper right), 5years (lower left) and 10 years (lower right) simulation of original layout

With erosion in Section CD and deposition in Section DE, the costal orientaion at both D and E has changed. In the the $S-\varphi$ curve, both points moves to the left side. Instead of point E change to the left side of D and cause sediment transport decreasing, the sediment transport rate may come to a stage as shown in Figure 39. Because the erosion rate of section CD is the predominant factor that decides the costal orientation at D. Start with a rapid erosion in section CD and limited deposition in section DE, point D can stay at the left side of point E in the $S-\varphi$ curve. Another pick point is generated in section DE and repeat the process above. This cyclic process makes the turning point transport towards the Maasvlakte 2 direction and prevents the occurrence of unexpected sedimentation.

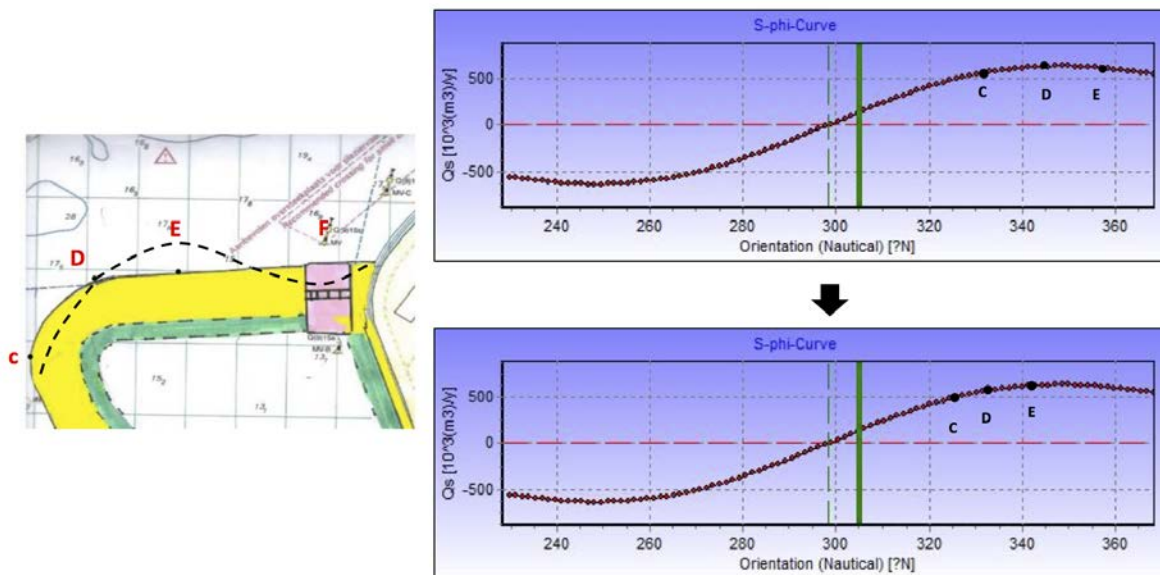


Figure 39: The morphological process in section DE

5.3.2 Result of improved layout

The coastline evolution of the improved layout after 10 years simulation is shown in Figure 40. The section between the southern boundary and the groyne is the pumping station outlet, which is included to study the effect of the groyne. The deformation in this section is not considered. Near the pumping station, a large amount of sedimentation is blocked by the groyne as expected. As shown in Figure 41, section 2 that covers most part of the sandy beach is eroded with maximum shoreline retreat still happens at the west head of Valmeer and reach up to 165 m.

Same for the improved layout, the average erosion rate at the location of maximum shoreline retreat is calculated. As listed in Table 9, the erosion rate start with 36.4 m/year and reduced by half in the first three year. From the three to ten years, the erosion rate only decreased from 15 m/year to 12.2 m/year. The erosion rate after ten years simulation gives relatively stable and acceptable value.

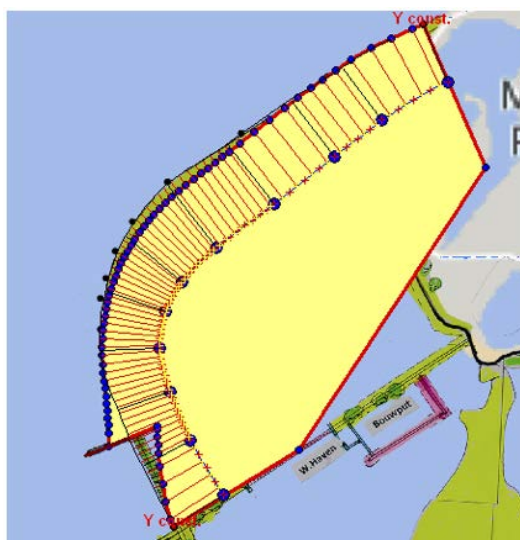


Figure 40: The coastline deformation of improved layout after 10 years simulation

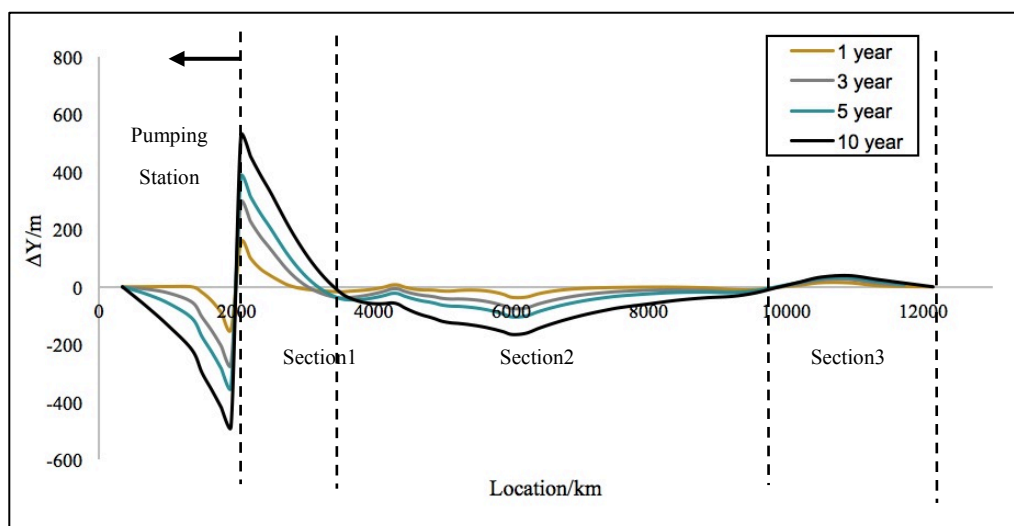


Figure 41: The coastline deformation of improved layout after 1 year, 3 years, 5 years and 10 years simulation

Table 9: Average erosion rate at maximum retreat location of original layout

Year	Coastline retreat (m)	Erosion rate (m/year)
1	36.3865	36.4
2	55.3865	19.0
3	74.329	19.0
4	89.329	15.0
5	104.2135	15.0
6	119.2135	12.2
7	131.4135	12.2
8	143.6135	12.2
9	155.8135	12.2
10	165.9628	12.2

Near the northern boundary, some deposition is generated with negligible value. Similar as previous problem for the model of original, this may be the compensate for the Y constant boundary. This phenomenon can also be spotted at the southern boundary of the model, where a yellow dot indicates a little sedimentation happens at that location. The erosion rate pattern in Figure 42 demonstrate that this error will be reduced with the increasing simulation period. Generally, the CL-model result of the improved layout is very consistent with the theoretical conclusions in section 4.1.

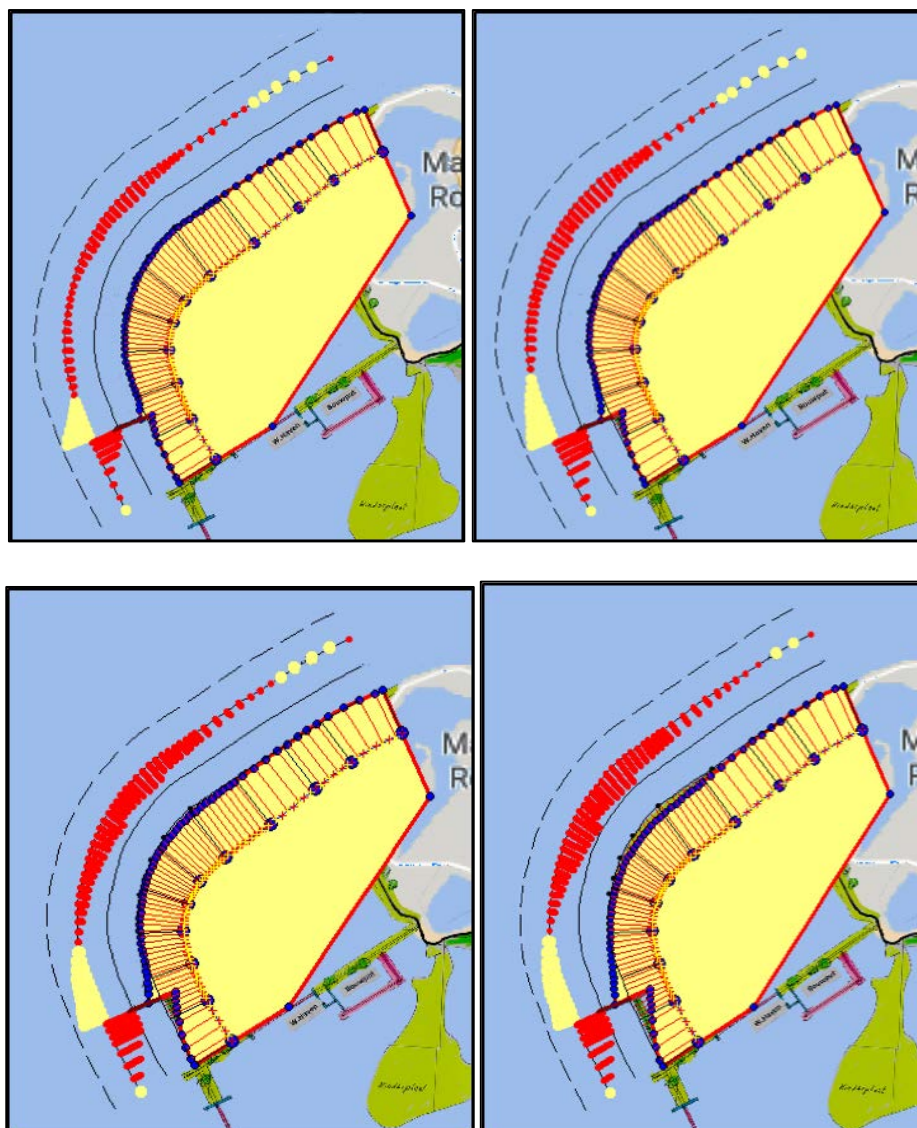


Figure 42: The coastline deformation and erosion rate after 1 year (upper left), 3 years (upper right), 5 years (lower left) and 10 years (lower right) simulation of improved layout

5.3.3 Assessment of layout improvement

To assess the necessity and effect of the layout improvement, the morphological development along the sandy beach of Valmeer in case of the original layout and improved layout is compared in this section. Based on the theoretical analysis and the CL model result, the design of these two layouts are compared in the aspects of shoreline evolution and sediment balance.

The coastline evolution of original layout and improved layout is compared in Figure 43. On the whole, the deformation of the original layout has a more complicated shape which has three different sections of erosion and deposition. The erosion at the head of Valmeer is very serious and intensive, which makes the layout structure quite unstable. The erosion of the improved layout is almost distributed along the entire sea defense. In addition, the shape of the original layout makes the deformation hard to be predicted, which is demonstrated by less consistency in the theoretical conclusions and model results. The maximum shoreline retreat of the original design and improved

design is 448m and 165m, respectively. The erosion at the head of Valmeer is reduced dramatically by optimizing the coastline cure.

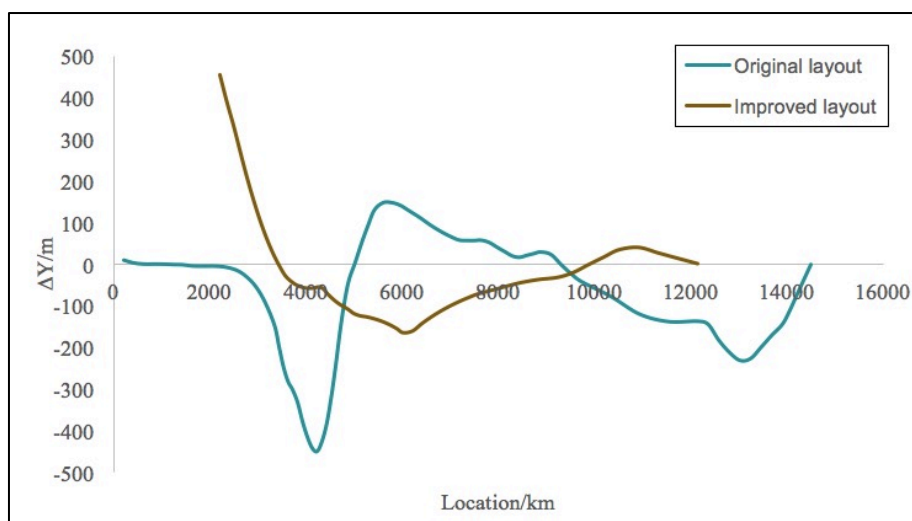


Figure 43: The coastline deformation of original layout and improved layout after 10 years simulation

The sediment balance is compared based on the sediment transport rate after 1 years' simulation. Sediment gain and loss of different sections are shown schematically in Figure 44 and Figure 45 and listed in Table 10 and Table 11. In the southwest side of the original layout, the deposition value 6,000 m^3/y can hardly exist. The sand loss in the seriously eroded area reach up to 2165,000 m^3/y over around 3km sandy beach. The overall sediment balance along the sea defense of original layout is -2402,000 m^3/y , which means the sandy beach of Valmeer is losing 2402,000 m^3 per year after 1 years.

The sediment balance of the improved layout is computed from the location of groyne with 0 sediment transport. The eroded section of improved layout is around 7km and has 1140,000 m^3 sediment loss per year. The volume of sand that is lost from the head of the Valmeer in the original layout is almost two times the volume of improved layout. The total sediment loss is 178,000 m^3 per year. This mainly due to 787,000 m^3 is blocked by the breakwater of pumping station. The sediment transported towards the Maasvlaket 2 for original and improved layout is 1013,000 m^3 and 178,000 m^3 , respectively. Adjustment in the outline of Valmeer also dramatically reduced the sediment that is transported towards the Maasvlakte 2.

Table 10: Sediment balance of the original layout after 1 years simulation

	Sediment transport [m^3/y]	Sediment gain and loss [m^3/y]
Section1	-1054,000	6,000
Section2	-1060,000	-2165,000
Section 3	1105,000	240,000
Section 4	530,000	-483,000
Total	1013,000	-2402,000

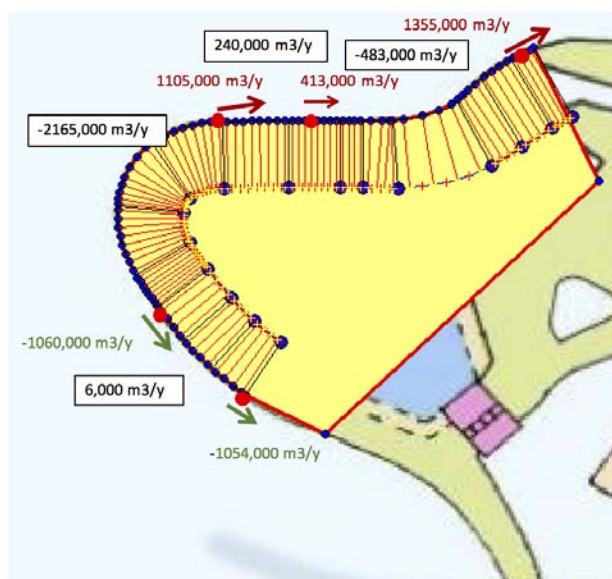


Figure 44: Sediment balance of the original layout after 1 years simulation

Table 11: Sediment balance of the improved layout after 1 years simulation

	Sediment transport [m ³ /y]	Sediment gain and loss [m ³ /y]
	0	
Section1	-787,000	787,000
Section2	354,000	-1141,000
Section 3	178,000	176,000
Total		-178,000

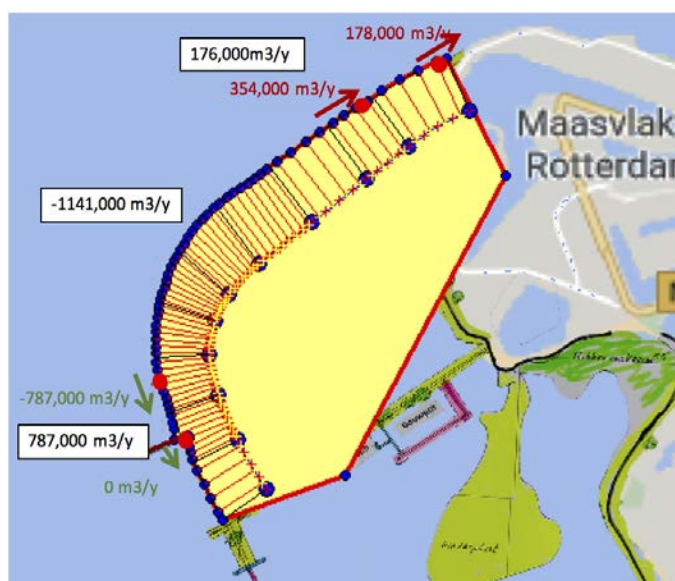


Figure 45: Sediment balance of the improved layout after 1 years simulation

5.4 Conclusion

The predicted evolution of coastline in case of the improved layout gives more gentle and stable shape. Except for the deposition near the groyne, the sandy beach of the improved layout is constantly eroded. In case of the original layout, there is three different sections of erosion and deposition. The shape of deformation at the head of Valmeer is very sharp and threatens the stability of the structure. The maximum shoreline retreat of original layout is 448m which is almost three times larger than the improved layout (being 166m). At the northern side of original layout, the occurrence of a sand spit is still to be discussed and need to be modeled with more detailed hydraulic conditions.

Furthermore, the calculated average erosion rate at the head of Valmeer demonstrated coastline evolution after 10 years simulation. For the first year, the original layout has a erosion rate of 71.9 m/year and the improved layout has a erosion rate of 36.4 m/year. The average erosion rates during last 5 years for the original layout and improved layout are 35.8 m/year and 12.2 m/year, respectively. The coastline of the original layout is still going to retreat three times faster after ten years simulation, which is adverse to the stability of project layout.

When looking at the sediment loss along the sea defense of Valmeer, the improved layout gives better performance. In case of the original layout, 2165,000 m³ sand is eroded at the head of Valmeer along 3km sandy beach in the first year. The eroded section of improved layout is around 7km and has 1141,000 m³ sediment loss per year. The original layout results in larger sediment loss over a shorter section and requires more maintenance work after the construction of DELTA 21 project. Also at the northern boundary, less sediment is transported towards the hard defense of Maasvlakte 2 and reduced the maintenance work in that region.

Based on previous discussion, the improvement in the layout of DELTA 21 project has remarkable influence on coastline evolution and sediment balance. With a regular shape of the coastline, the morphological process happens along the sandy beach is more predictable. Maximum shoreline retreat and sediment loss is reduced dramatically after the improvement. Overall, the DELTA 21 layout improvement is quite effective.

6

Large-scale model setup

6.1 Introduction

This chapter deals with the setup of the DELTA21 project in the Delft3D model, according to the previous described method. The grid and bathymetry are demonstrated in Section 6.2. The boundary conditions are given in Section 6.3. Other parameter settings for Delft3D morphodynamic model are described in Section 6.4. In Section 6.5 the sensitivity study is performed for different morphology scale factors.

The model used in this study is established by another graduate student in DELTA21 group (IJntema, 2020). The Maasvlakte model calibration and validation has been done in his study. Model calibration and validation is not included in this report.

6.2 Grid and bed schematization

Delft3D-FLOW supports two kind of co-ordinate systems in the horizontal: the Cartesian co-ordinates and Spherical co-ordinates. In Delft3D, the equations are numerically solved based on the curvilinear staggered grids. The depth points are defined in the center of the grid (Deltares, 2014a). The model grids applied in this study used the Cartesian co-ordinates. The grids are developed based on a Maasvlakte 2 model grid as provided by Arcadis. The model is extended southwesterly direction to cover the coastal region of Nature 2000. The model covers the coast of Zuid-Holland and on the south reach to the estuaries of Eastern Scheldt, as shown in Figure 46. A more refined grid is applied in the region around the DELTA21 and Maasvlakte 2 to give better performance.

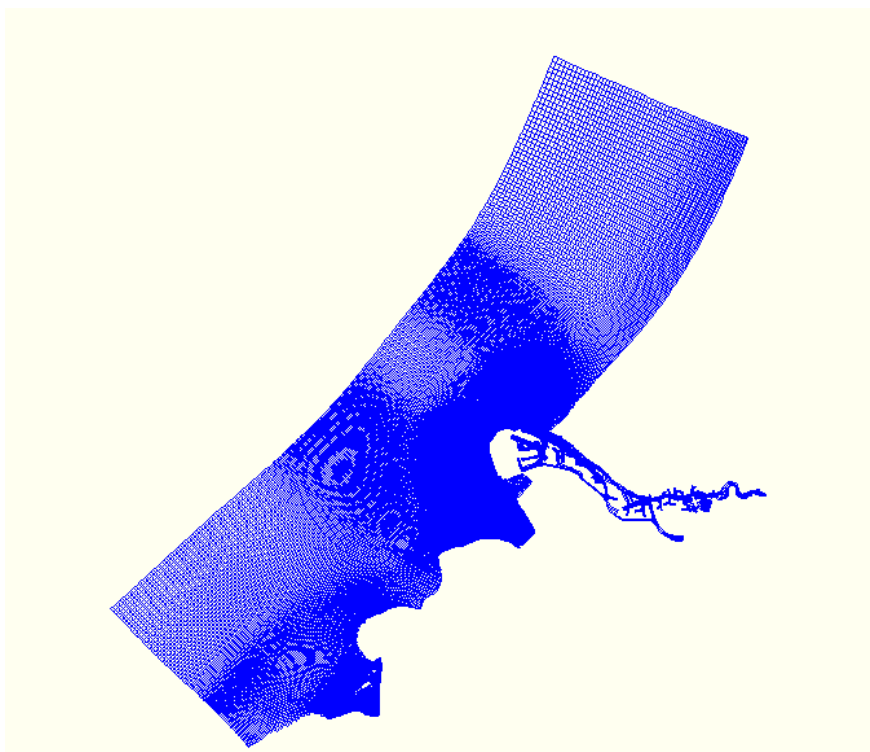


Figure 46: Model grids for Maasvlakte 2 model

The bathymetry data of 2015 from the Vaklodingen set is applied to schematize the bathymetry. To include the layout of the DELTA 21 into the model, (IJntema, 2020) applied dry points at the location of dam's highest elevation. At the location of pumping station and spill way, thin dams are applied to block water. The bed level is adapted at the location of dune structure, with 10 meters above the water level at the top of dune structure and around 1:50 slope for cross-shore profile. The inner side of the Valmeer becomes a closed area, since analysis for the performance of the pumping station and Valmeer is not included in this study.

The DELTA21 model of the original layout is developed in this study. Dry points are located along the sea defense according to original layout design. Thin dams are applied at the northern side pumping station and the spill way between Valmeer and Getijmeer to block waters in the deep Valmeer. The bathymetry is adapted along the dune structure. The original layouts and improved layout of DELTA 21 in Delft3D are given in Figure 47 and Figure 48.

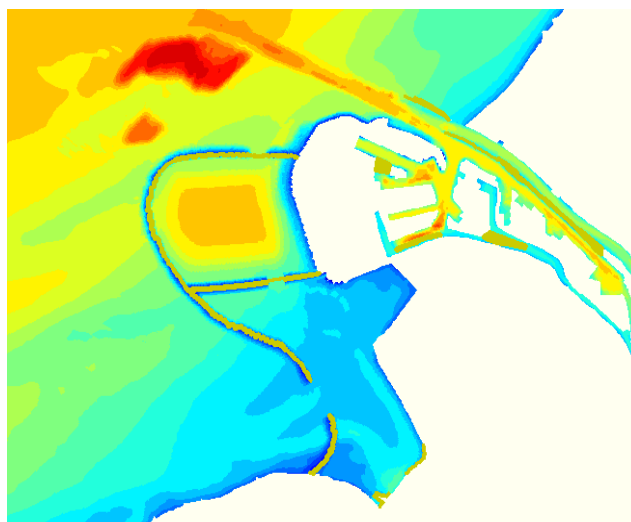


Figure 47: Delft3D model of DELTA 21 project in case of original layout

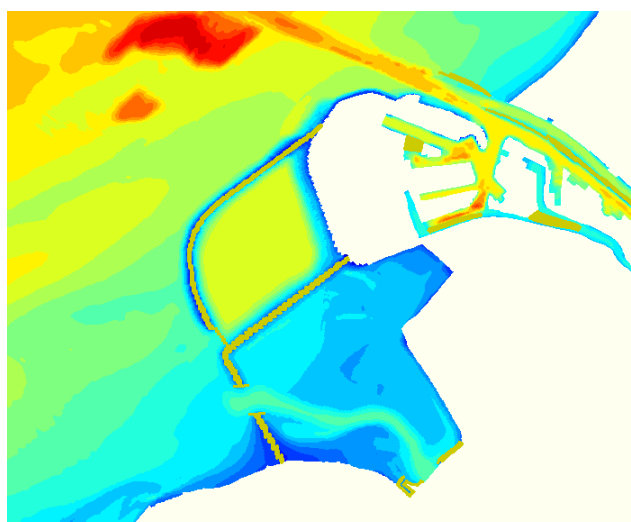


Figure 48: Delft3D model of DELTA 21 project in case of improved layout (IJntema, 2020)

6.3 Boundary conditions

The open boundaries of the model consist of several types of boundary conditions, including discharge, water level and current. For all boundaries, time-series forcing type is applied. On the land boundary side, total discharge boundary is given at the outlet of Eastern Scheldt. At the outlet of Haringvliet and Nieuwe Waterweg. The boundary condition is given as discharge per cell. For the seaward boundaries, a water level boundary is applied at the north boundary perpendicular to the coastline and the offshore northwest boundary. A current boundary is applied at the southwest boundary perpendicular to the coastline. All boundaries conditions are presented by means of a 15 days' times-series data from 10th August to 25th August. With a 1 days' spin-up interval, the hydraulic boundaries support 14 days simulation. The locations of boundaries are given in Figure 49.

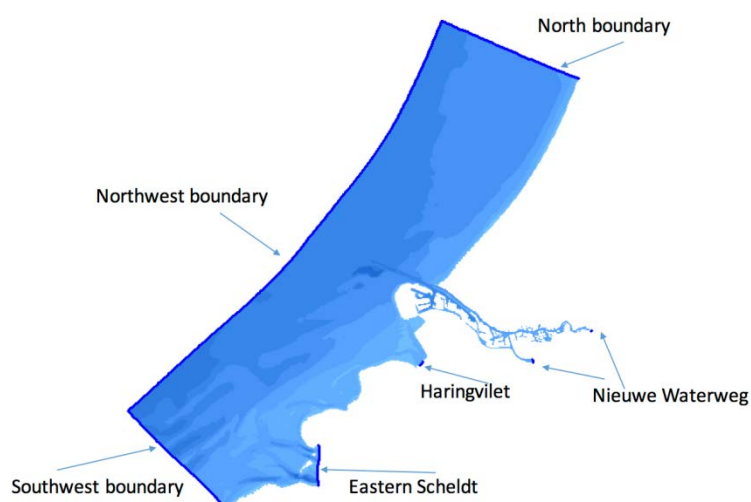


Figure 49: Open boundaries for Delft3D model

For the model of the DELTA21 project, the discharge at the pumping station and the reopening of the Haringvliet dam is not included. According to (IJntema, 2020), the effect of the pumping station has very limited range near its outlet. Changes caused by the discharge of Haringvliet are situated within the Haringvliet tidal delta at the southern part of DELTA 21. Therefore, effect of the reopening of the Haringvliet is not considered in this study.

6.4 Model setup

The long-term morphodynamic simulations are performed with use of the calibrated Delft3D-FLOW model. For the hydrodynamic module, the model is used in a 2DH depth averaged area mode, which means the vertical momentum equation is reduced to the hydrostatic pressure relation. A time step of $\Delta t=30s$ is chosen for a stabilized and accurate simulation.

The process of sediment transport is included in the Delft3D-FLOW model by means of a morphological model. The Delft3D computes bed changes by summation of the gradients the suspended load and bed load transports. Within the morphodynamic model, the bathymetry is updated every time step when the sediment transport is computed. At the boundaries, an equilibrium sand concentration profile is applied to get the sediment concentration at inflow boundaries. This means that the sediment load entering through the boundaries will be near-perfectly adapted to the local flow conditions, and very little accretion or erosion should be experienced near the model boundaries (Deltares, 2014a). In this study the transport of non-cohesive material (sand), is considered. The grain size in the model is set to be 0.2 mm according to previous study of Maasvlakte 2 (Van den Berg, 2007) and the background information about the study area in previous Chapter 5. A uniform grain size is applied. The erodible layer is set to be 20 meters according to the geological information for the study area.

6.5 Morphological scale factor

The morphological acceleration factor is a scalar quantity applied to the sediment continuity equation, assuming that morphodynamic evolution occurs at longer time scales than the hydrodynamic processes (Lesser et al., 2004). To perform a long-term morphological study, a proper morphological scale factor should be applied in the Delft3D morphodynamic model. By implementing a morphological time scale factor, the erosion and sedimentation fluxes from bed to the flow during each computational time-step is multiplied by time scale factor. In this way, the bed-level changes are accelerated according to the hydrodynamic flow calculations (Deltares, 2014a). A sensitivity study is done to set the proper Morphological time scale factor for this study. The simulations for this sensitivity study are listed in Table 12.

Table 12: Simulations for sensitivity study

Simulation	Duration of Hydrodynamic process (days)	Morfac value (-)	Duration of Morphodynamic process (days)
1	10	1	10
2	1	10	10
3	14	10	140
4	7	20	140
5	2	70	140
6	1	140	140

The sensitivity study starts with comparing the performance of the model with a morphological scale factor (morfac) equal to 1 and 10. By doing a 10-days simulation with morfac equals 1 and a 1 days simulation with morfac equals 10, bed-level changes in 10 days is compared. The bed-level changes along three cross-sections are compared in Figure 52. The locations of the cross-sections are given in Figure 50. The difference of the bed-level after 10 days between the simulation with morfac equals 10 and 1 in the interest area is shown in Figure 51.

The result of these two simulations are more or less similar. There is hardly any difference noticeable in Figure 50, except for one point on the soft defense of Maasvlakte 2. Based on the simulation result, it is concluded that Morfac=10 is acceptable.

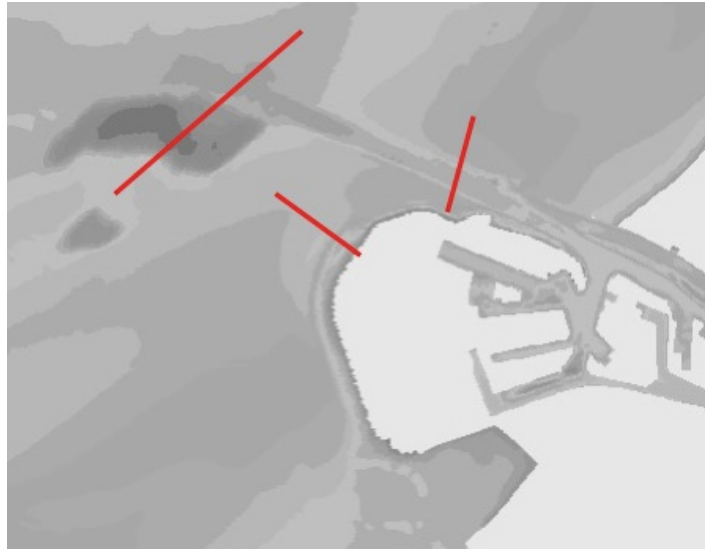


Figure 50: Locations of three cross-sections

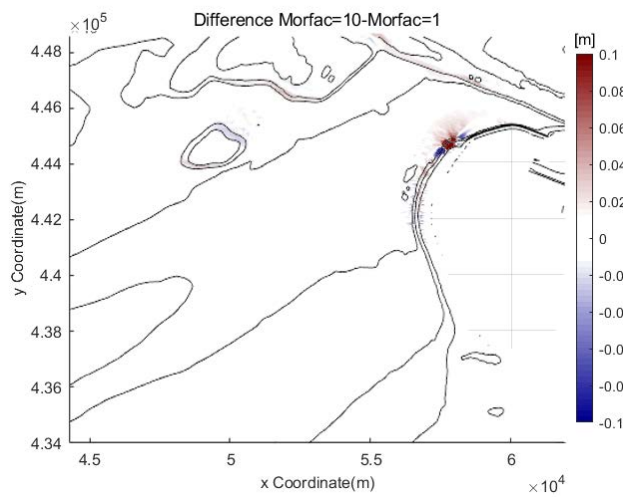
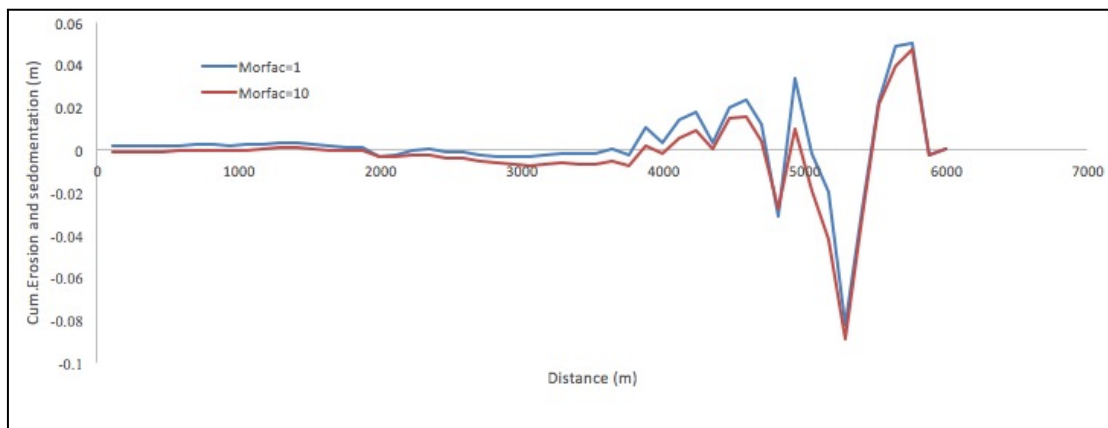
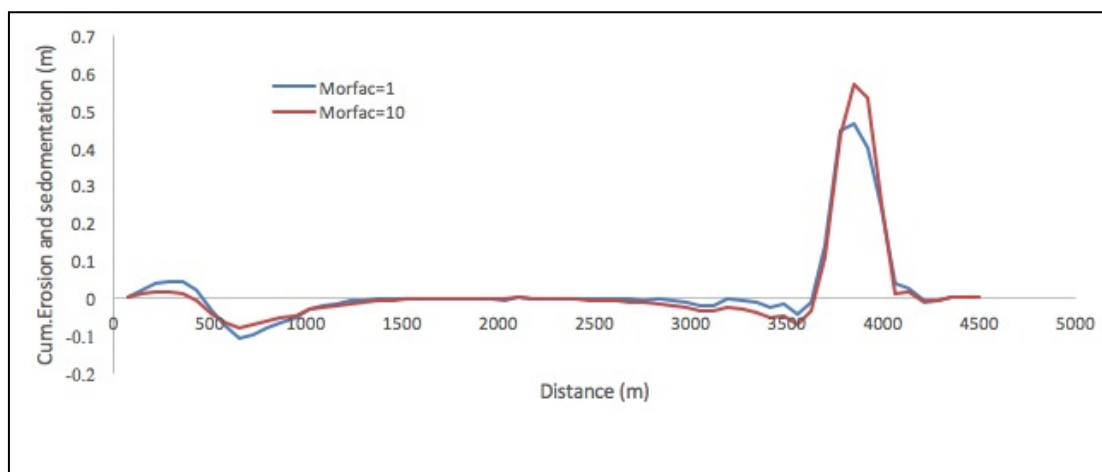


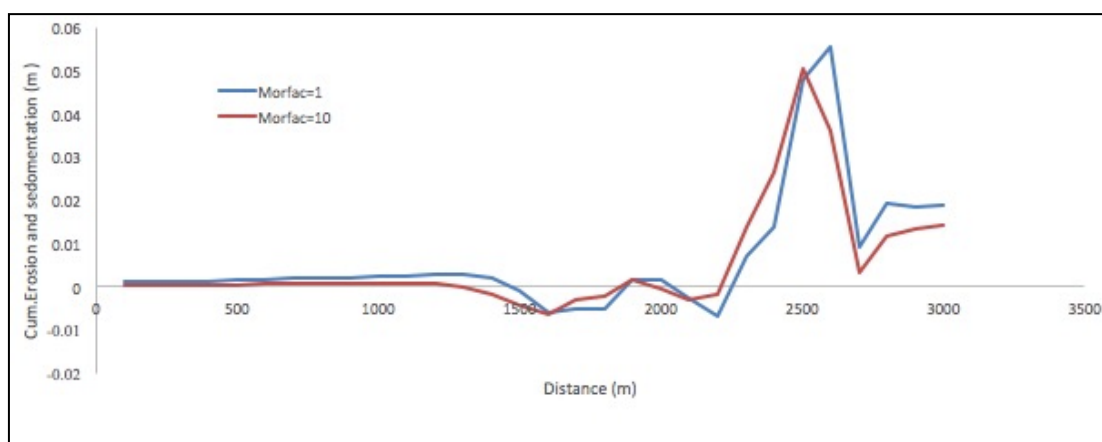
Figure 51: 10 days bed-level difference between simulation Morfac=1 and Morfac=10



(a) The northern side of Maasvlakte 2



(b) The shipping channel



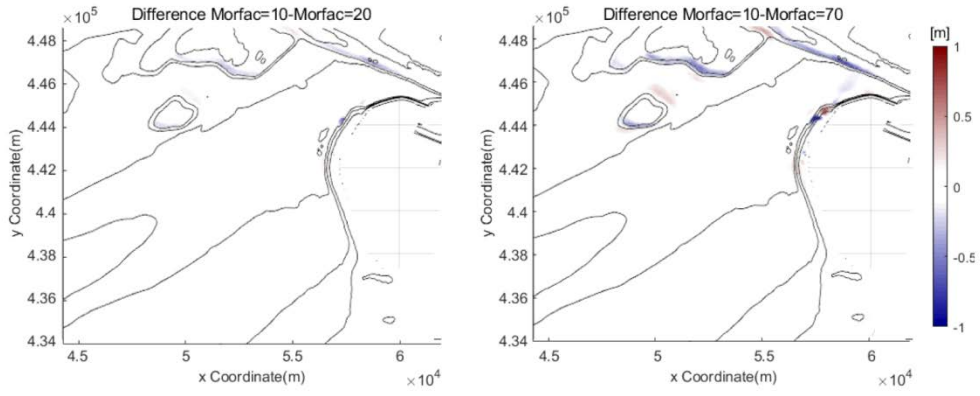
(c) The dredging point

Figure 52: Bed level changes along the cross-sections for simulation morfac=1 and 10 at (a) the northern side of Maasvlakte 2, (b) the shipping channel and (c) the dredging point.

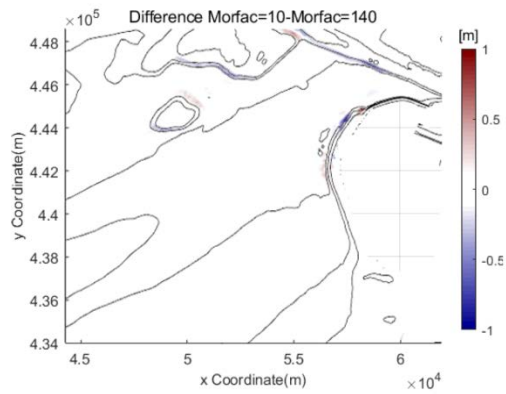
With trusted result of morfac equals 10, larger morfac values can be tested. Simulation 3 to 6 compares bed-level changes in 140 days with a morfac=10, morfac=20, morfac=70 and morfac=140, respectively.

Figure 53 represent the difference of 140 days bed level changes, simulation results of larger morfac values are compared with the result morfac=10. For simulation 4, 5 and 6, the results are more or less the same. Some difference can be seen near the dredging location for Maasvlakte 2, the edge of the shipping channel and some location on the profile of soft defense. Based on the bed level difference, simulation 4,5 and 6 gives similar result and the differences is acceptable.

Based on the result in Figure 54, the bed-level changes have a same trend along the three cross-sections. At locations of relatively large amount of erosion and sedimentation, some differences are noticeable however. At such locations, the result does not give a consistent conclusion about the performance of the larger morfac values. From Figure 53(a), at the location of max erosion result of morfac=140 has better consistency with result of morfac=10. However, morfac=20 and morfac=70 gives better performance at the location of deposition.

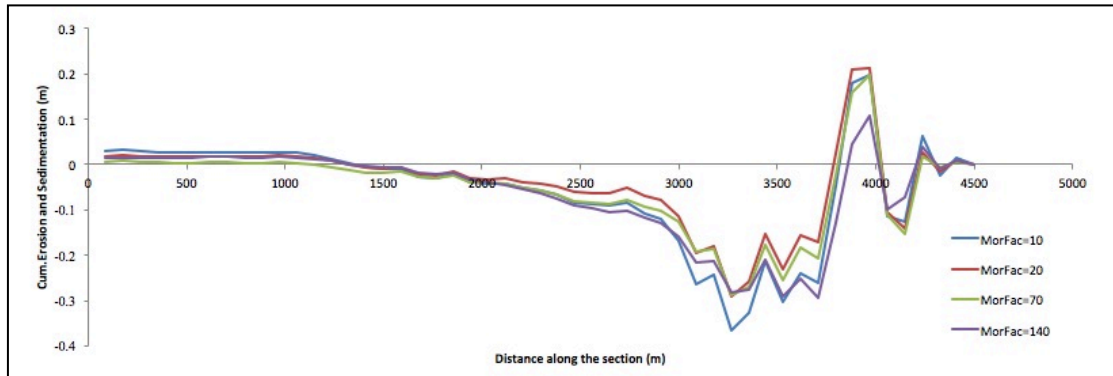


(a) Difference between Morfac=10 and Morfac=20 (b) Difference between Morfac=10 and Morfac=70

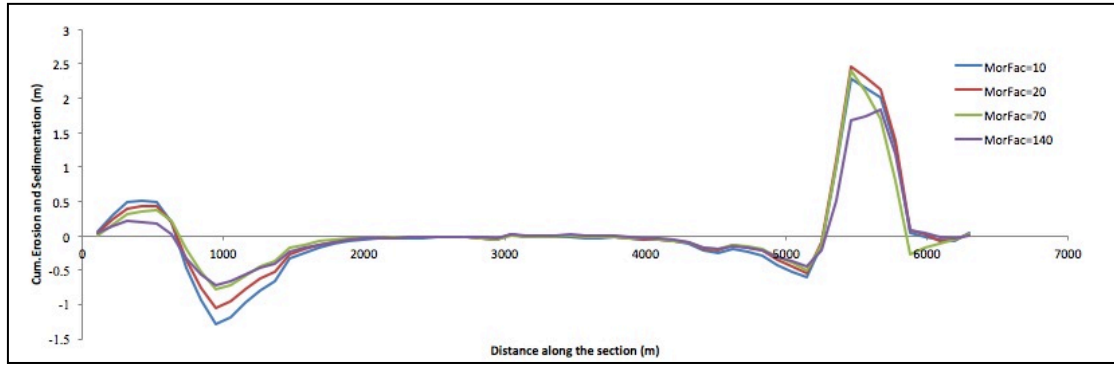


(c) Difference between Morfac=10 and Morfac=140

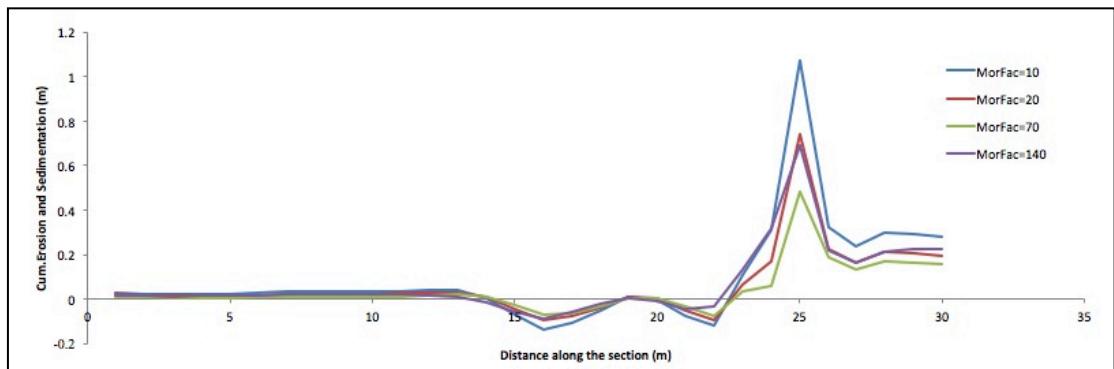
Figure 53 : 140 days bed-level change difference



(a) The northern side of Maasvlakte 2



(b) The shipping channel



(c) The dredging point

Figure 54: Bed level changes along the cross-sections at for simulation morfac=10 ,20, 70 and 140 (a) the northern side of Maasvlakte 2, (b) the shipping channel and (c) the dredging point.

On the whole, simulation with morfac=20, morfac=70 and morfac=140 can well predict the morphodynamic process and the resulted bed level changes with accepted difference at some locations. Therefore, morfac value of 140 will be used in the long-term morphodynamic simulation of this study to reduce the simulation time.

7

Large-scale model results analysis

7.1 Introduction

This chapter deal with the simulation results of Delft3D model. A 20 years' long-term morphodynamic simulation has been performed for the Maasvlakte 2 model and the DELTA 21 model (for both original layout and improved layout). In Section 7.2, the flow pattern the three different layouts at the beginning of the simulation is analyzed. Subsequently, Section 7.3, 7.4 and 7.5 demonstrates the tide induced long-term morphological development under three different conditions. The Maasvlakte 2 model as a reference case is discussed in Section 7.3. Section 7.4 and 7.5 deal with the the long-term bed level change under DELTA 21 original layout condition and improved layout condition, which is done by analyzing the underlying sediment transport patterns as well as the residual current patterns. An overview of the impact of DELTA 21 project on the flow pattern and resulted morphological changes is given in Section 7.6.

7.2 Flow patterns

7.2.1 Flow pattern during over tidal cycles

As previous discussed, the implementation of the DELTA 21 project may result in contraction of tidal currents at the head of Valmeer. In this section, the flow pattern after the construction of original layout and improved layout is demonstrated. Water level and depth averaged velocity at several observation points are compared with the Maasvlakte 2 model result to analyze the change in both horizontal tide and vertical tide.

The flow pattern in the Maasvlakte 2 is given as a reference case. In Figure 55, flow patterns of representative ebb current and flood current are plotted for the Maasvlakte 2 model. Locations of four observation points are marked on Figure55 (a), including the head of Maasvlakte 2, shipping channel, the head of Valmeer for both original layout and improved layout. Time series of water level and depth averaged velocity is plotted in Figure 56 and 57.

During an ebb tide, tidal current along Dutch coast is on general directed towards southwest. Around the Maasvlakte 2, the flow concentrated and follows the shape of Maasvlakte2 sea defense at northern side, which induced shifting of the current direction toward seaward. The velocity direction turning back to the

original direction after passing the Maasvlakte 2. The same accounts for the northeast directed flood current shown in Figure 55(b).

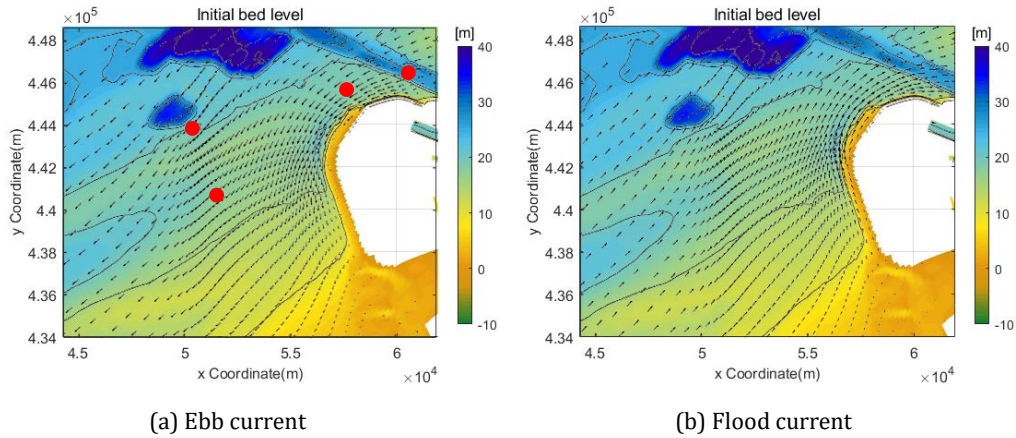
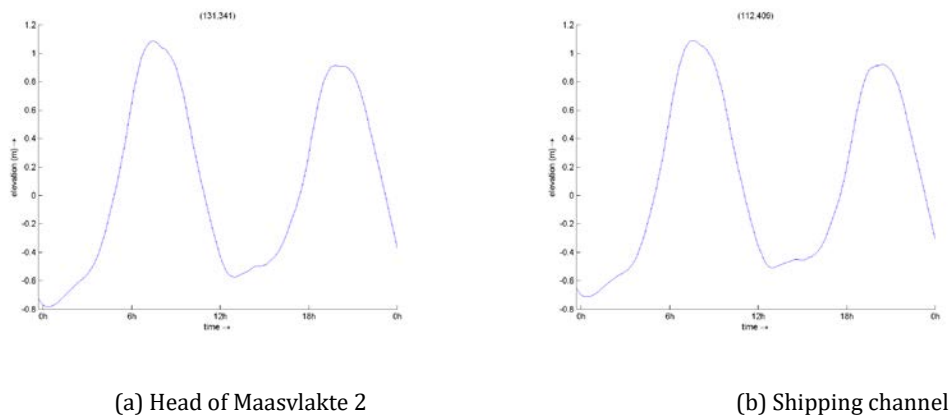
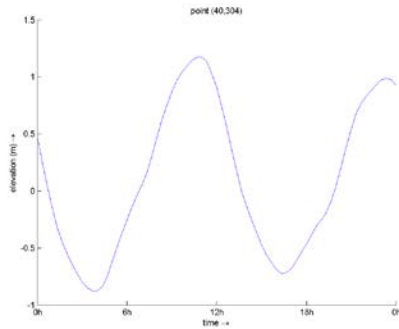


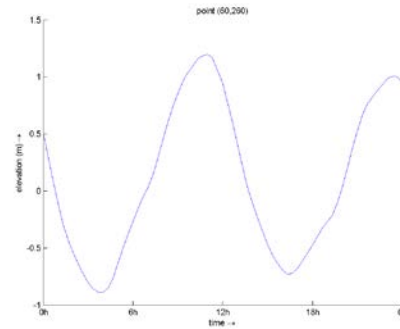
Figure 55: Flow pattern over a tidal cycle of Maasvlakte 2 model

The time-series of velocity and water level includes two tidal cycles. The tidal range at the four considered locations is around 1.8 m. At the near shore locations, tidal signal becomes asymmetric and has longer duration for ebb tide. The horizontal tide is shown in Figure 57 as depth average velocity. The figures give only the magnitude with the negative velocity stands for ebb tide directed southwest and positive velocity stands for flood tide directed towards northeast. The velocity at the head of Maasvlakte 2 has maximum value that up to 1.1 m/s during flood tide due to contraction of the tidal currents. Similarly, horizontal tide also has a asymmetric signal at onshore location.



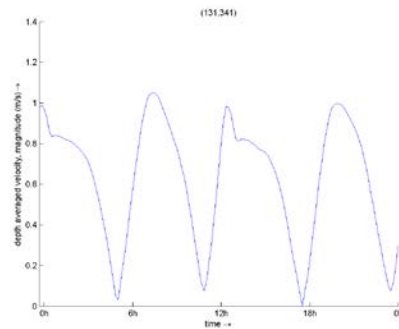


(c) Head of Valmeer (original layout)

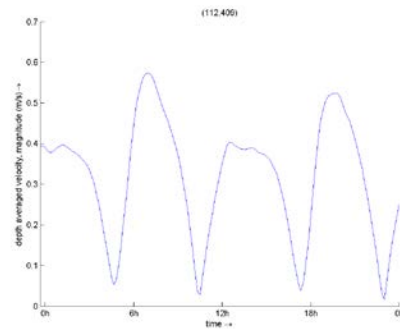


(b) Head of Valmeer (improved layout)

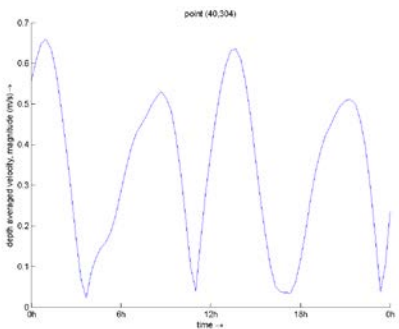
Figure 56: Water level at observation points over two tidal cycle of Maasvlakte 2 model



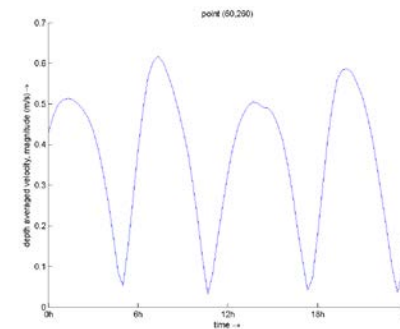
(a) Head of Maasvlakte 2



(b) Shipping channel



(c) Head of Valmeer (original layout)



(b) Head of Valmeer (improved layout)

Figure 57: Depth average flow velocities at observation points over two tidal cycle of Maasvlakte 2 model

When include the improved layout design of DELTA 21, noticeable contraction of the tidal current can be seen mainly at the corner of Valmeer on northern side. Consistent with what is described in Section 3.3, the flood current is onshore bended and the ebb current is offshore bended. Therefore, during both flood tide and ebb tide, the flow is concentrated at northern side and sheltered at southern side. The intensity of flow vectors decreased before reaching the northern side of the pumping station. Since the area of Valmeer is blocked by thin dam at the pumping station and spillway as described in Section 6.2, no flow can be found inside of the Valmeer (the thin dam is not shown in the flow pattern plot).

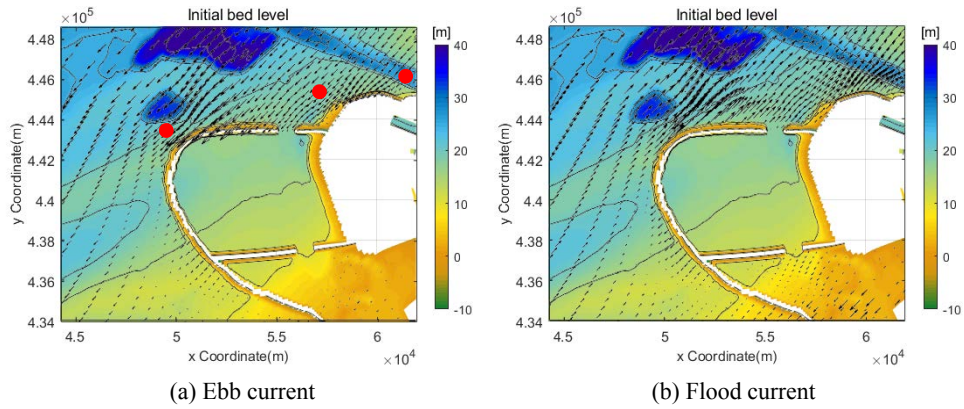


Figure 58: Flow pattern over a tidal cycle in case of original DELTA 21 layout

The water level and depth averaged velocity is measured at the same locations near the head of Valmeer (original layout), Maasvlakte 2 and in the shipping channel, as shown in Figure 59. The magnitude of water level and flow velocity are also listed in Table 12. The vertical tidal range is barely affected by the change of the flow pattern. But tide at the head of Valmeer start to be asymmetric. By comparing the velocity at same location in Figure 57 and Figure 60, it can be concluded that the DELTA 21 project has impact on the horizontal tide. At the head of Valmeer, the maximum velocity increased from 0.65m/s to 1.30 m/s due to flow concentration. Instead, at the northern side of Maasvlakte 2, the peak velocity decreased from 1.15 m/s to 0.43 m/s due to sheltering of the Valmeer. The rate of change is about 50 % in model of the original layout.

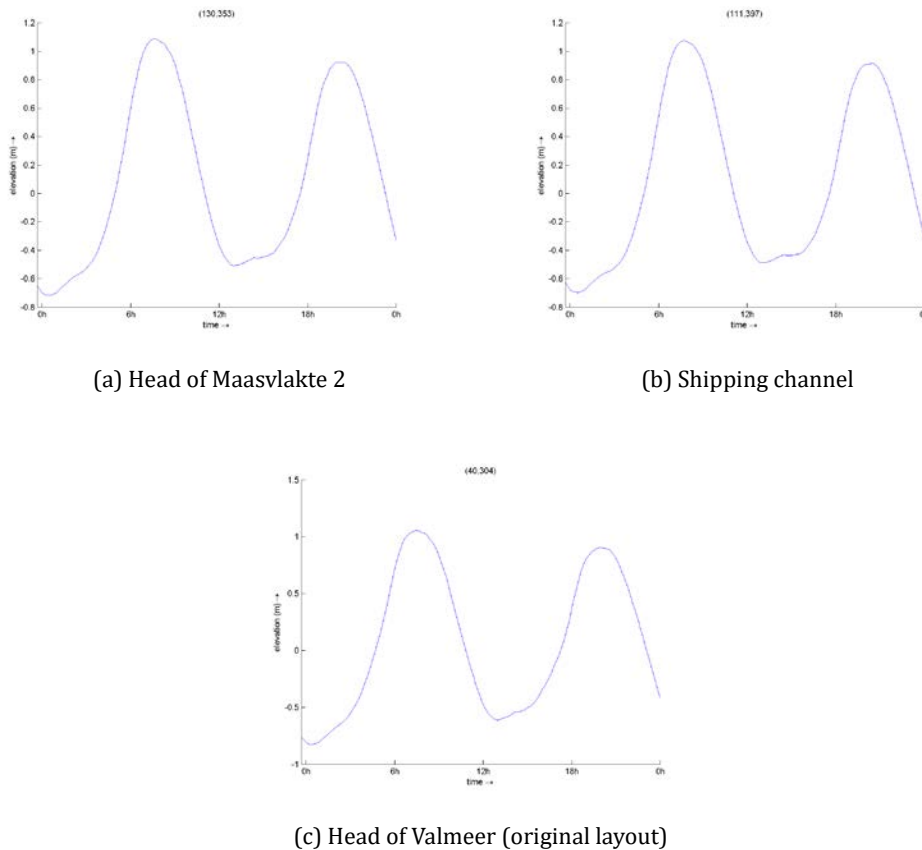


Figure 59: Water level at observation points over two tidal cycle in case of original DELTA 21 layout

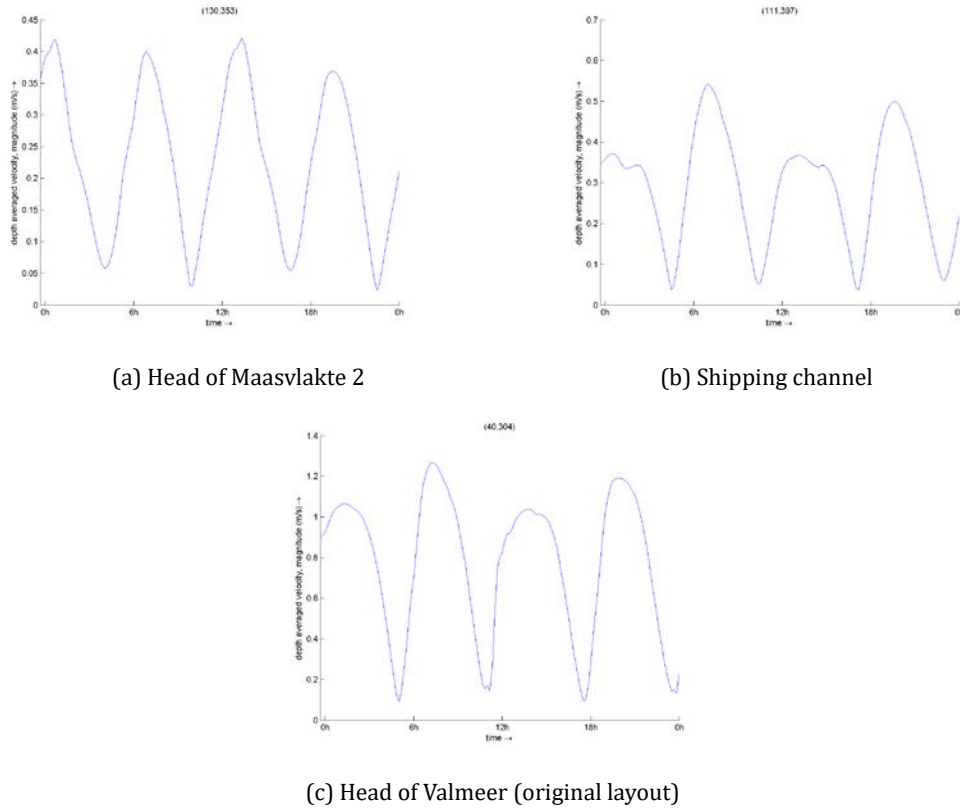


Figure 60: Depth average velocity at observation points over two tidal cycle in case of original DELTA 21 layout

In the model of improved layout, flow concentration can also be found at the northern side of Valmeer. Since the improved layout is less extended in seaward direction, some intensive vectors can also be found around Maasvlakte 2 in Figure 61. The improved layout has same impact on the vertical tide signal as demonstrated in Figure 62, with only change in the shape of tidal signal near the curved section of Valmeer. As shown in Figure 63, the maximum velocity at the head of Valmeer increased from 0.65 m/s to 0.8 m/s and decreased from 1.15m/s to 0.8 m/s at northern side of Maasvlakte 2. The ratio of changing is about 20% at both locations. The velocity in the shipping channel slightly changed from 0.575 m/s to 0.55 m/s in both model of original layout and improved layout. At the inlet of Port of Rotterdam, the flow is also decided by the discharge from Nieuwe Waterweg.

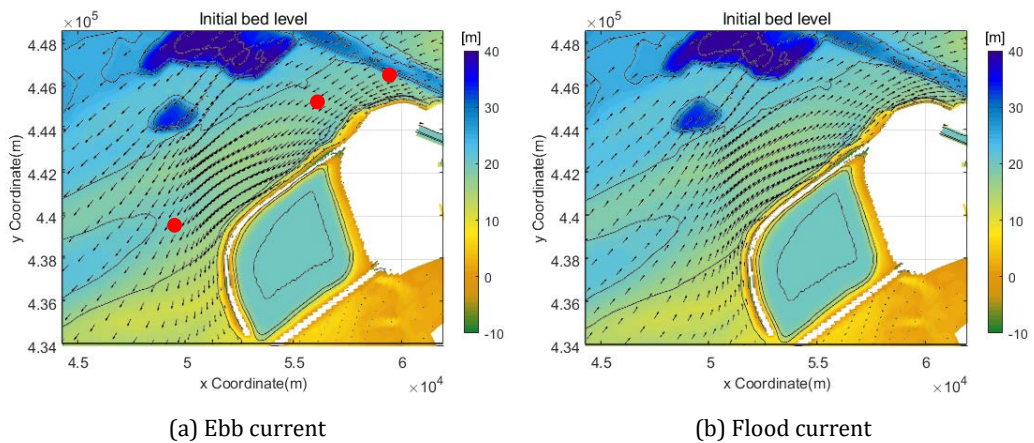


Figure 61 Flow pattern over a tidal cycle in case of improved DELTA 21 layout

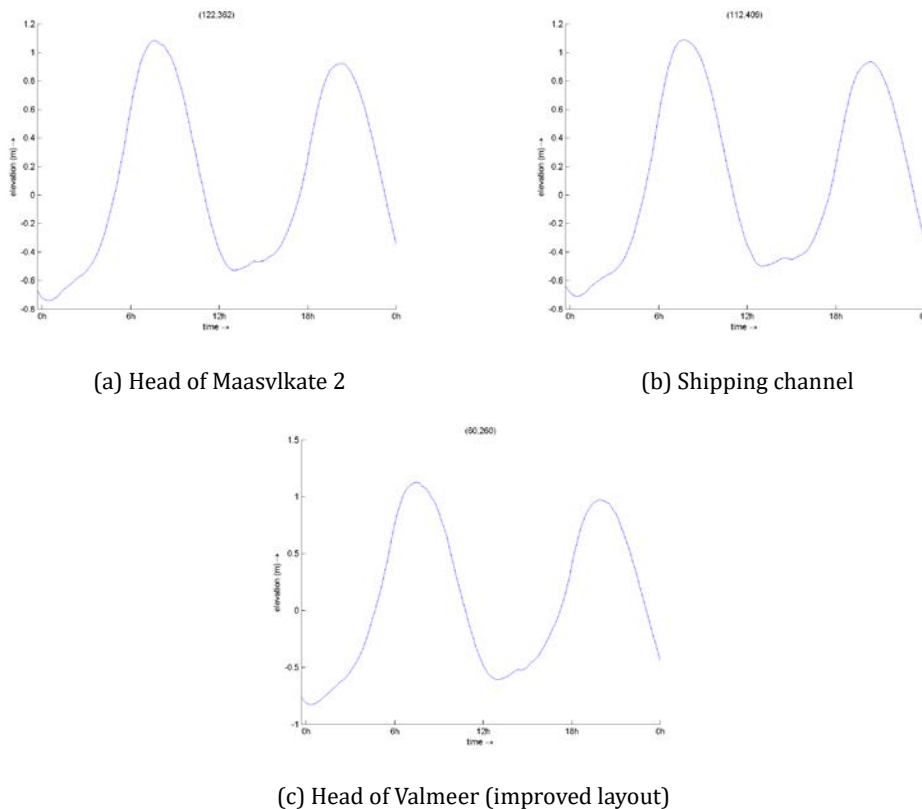


Figure 62: Water level at observation points over two tidal cycle in case of improved DELTA 21 layout

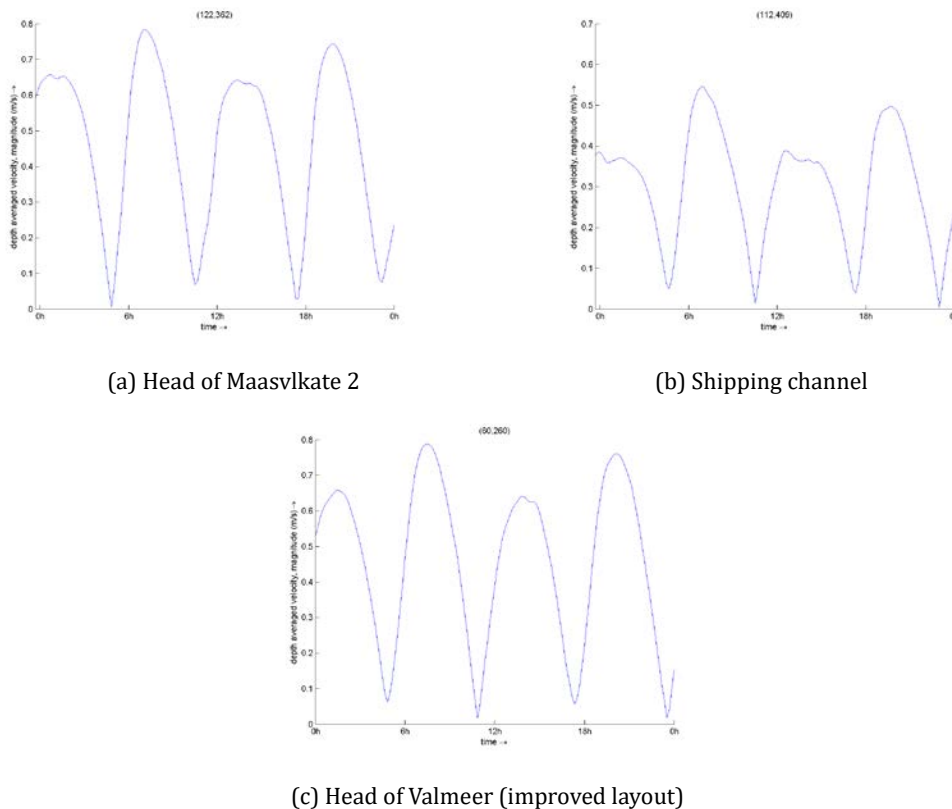


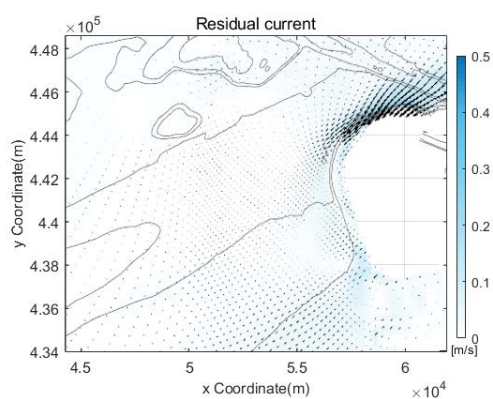
Figure 63: Depth average velocity at observation points over two tidal cycle in case of improved DELTA 21 layout

Table 12: Magnitude of vertical tide and horizontal tide

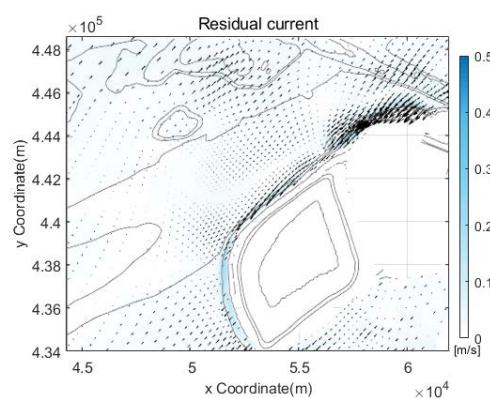
Water level(m)	Maasvlakte 2		DELTA 21(original layout)		DELTA 21(improved layout)	
Simulation	Flood	Ebb	Flood	Ebb	Flood	Ebb
Maasvlakte 2	1.10	-0.55	1.10	-0.50	1.10	-0.75
Shipping channel	1.10	-0.55	1.10	-0.55	1.10	-0.70
Valmeer (original layout)	1.25	-0.80	1.15	-0.80	-	-
Valmeer (improved layout)	1.24	-0.82	-	-	1.20	-0.80
Maximum Velocity(m/s)	Maasvlakte 2		DELTA 21(original layout)		DELTA 21(improved layout)	
Simulation	Flood	Ebb	Flood	Ebb	Flood	Ebb
Maasvlakte 2	1.06	-0.97	0.42	-0.37	0.78	0.65
Shipping channel	0.58	-0.39	0.56	-0.37	0.55	-0.38
Valmeer (original layout)	0.65	-0.54	1.31	-1.05	-	-
Valmeer (improved layout)	0.63	-0.52	-	-	0.79	-0.65

7.2.2 Residual currents

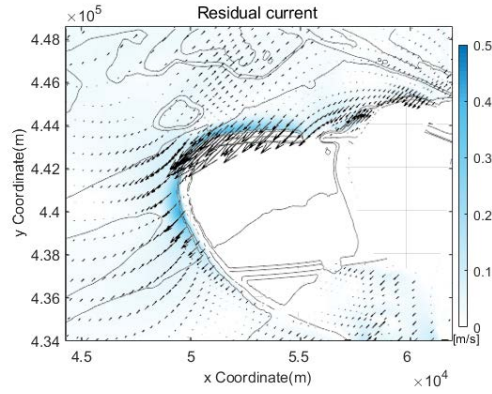
Residual currents during the first tide cycle of the simulations is demonstrated in this section. Figure 64 shows the residual current in the three different models. In the deep offshore area, the magnitude of the residual current is very limited due to the symmetric tidal signal. The flow vectors only can be noticed at a limited area around the sea defense of Valmeer and Maasvlakte 2. The residual current along the sea defense is mainly directed towards southwest, which is coupled with ebb current direction. Also based on the tidal signal plotted in Section 7.2.1, the ebb tide has lower velocity but longer duration. It can be concluded that, at the beginning of the simulation for the three models, the tidal currents along the coastline in a near shore range is mainly ebb dominant and result in southwest directed residual currents. But as described in Section 2.3, the residual current does not have decisive influence on the non-cohesive sediment transport. The non-cohesive is mainly bed transported which is mainly affected by the direction of highest velocity.



(a) Model of Maasvlakte 2



(b) Model of original layout



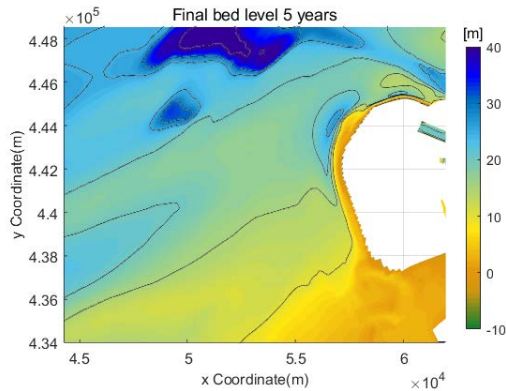
(c) Model of improved layout

Figure 64: Residual current over first tidal cycle

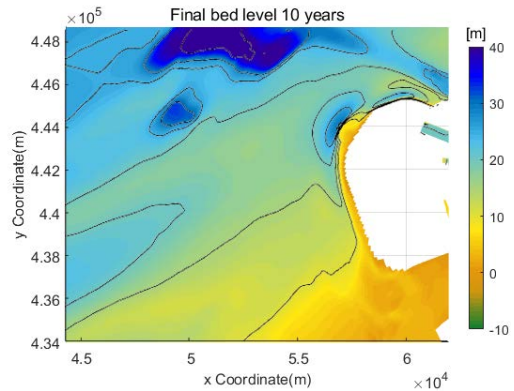
7.3 Long-term simulation for Maasvlakte 2

7.3.1 Bed level change

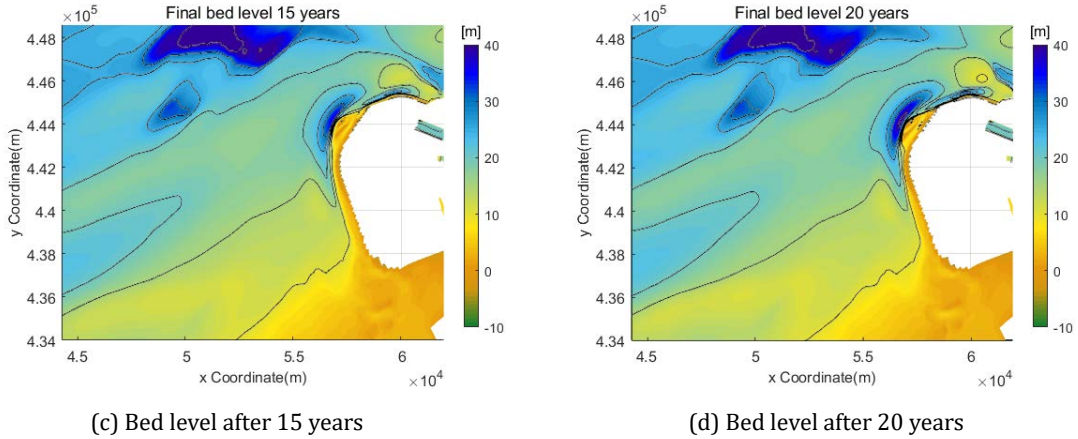
The bed level change during 20 years simulation is demonstrated in this chapter as a reference case. It contributes to evaluation of the influence in the area around Maasvlakte 2 and the shipping channel caused by the DELTA 21 project. Sediment transport caused by only tidal currents is considered. The bed level changes after 20 years simulation is given in Figure 65. A scour hole is not surprisingly developed at the northern side of Maasvlakte 2. Further northward in the shipping channel, large volumes of sedimentation is deposited. Even in the Figure 64(d), the depth contour that shows the shipping channel are cut off the middle, which means the channel is filled up at that section.



(a) Bed level after 5 years



(b) Bed level after 10 years

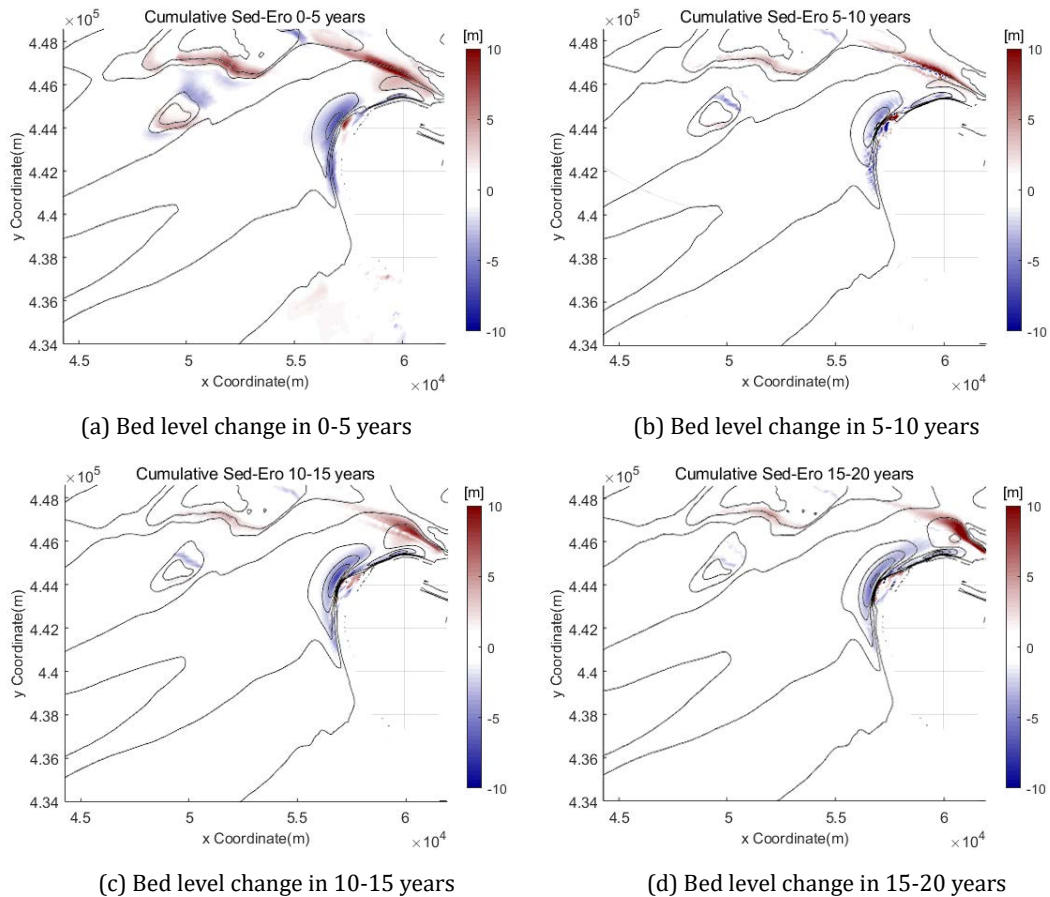


(c) Bed level after 15 years

(d) Bed level after 20 years

Figure 65: Bed level change in Maasvlakte 2 model after 5, 10, 15 and 20 years simulation of Maasvlakte 2 model

Figure 66 shows the cumulative sedimentation and erosion pattern during every 5 years within the simulation. The erosion at the head of Maasvlakte 2 and deposition in shipping channel occurs continuously throughout the 20 years simulation. Some sedimentation can also be found in the dredging location for Maasvlakte 2. The maximum erosion and sedimentation happened in the first five years and the ratio of change gradually decreased. This is also testified by the bed level change along the two cross-sections demonstrated in Figure 67.



(a) Bed level change in 0-5 years

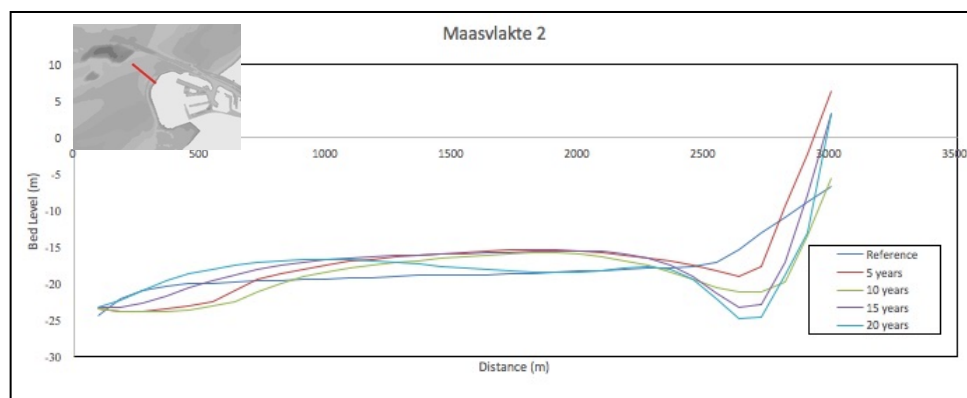
(b) Bed level change in 5-10 years

(c) Bed level change in 10-15 years

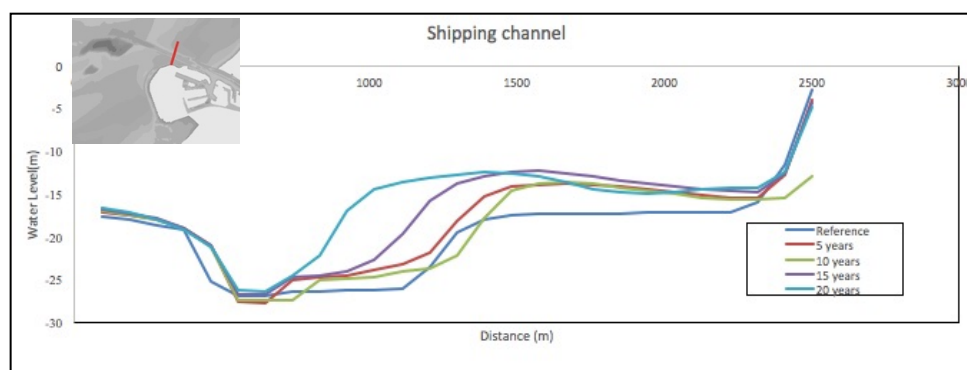
(d) Bed level change in 15-20 years

Figure 66: Cumulative bed level change in every five years simulation of Maasvlakte 2 model

The two cross-sections are located at the head of Maasvlakte 2 and shipping channel. As shown in Figure 66(a), at the northern side of Maasvlakte 2 a scour hole is developed and the depth is over 10 m after 20 years. In the first five years, the bed change at eroded area is already 5 m. Over time, the erosion rate is decreasing and the bathymetry is tend to reach an equilibrium state. In the shipping channel, large amount of side is deposited at the edge on southwest side and results in narrowing of the channel. Without dredging, the width of the channel reduced by half at the cross-section.



(a) Cross section at the head of Maasvlakte 2



(b) Cross section at shipping channel

Figure 67: Bed level along two cross sections of Maasvlakte 2 model

The mean total sediment transport plotted in Figure 68 indicate the averaged transport rate over first five years simulation. The sediment transport also concentrated at the head of Maasvlakte 2. The mean sediment transport is mostly directed towards northeast which is in the opposite direction of residual currents as shown in Figure 63(a) in Section 7.2.2. This result agree with principle for non-cohesive sediment transport that the non-cohesive is usually transported in the direction with the highest peak velocity through bed-load transport. The transport rate decreases at the location of shipping channel. Therefore deposition happens in the channel as shown in Figure 67 (b).

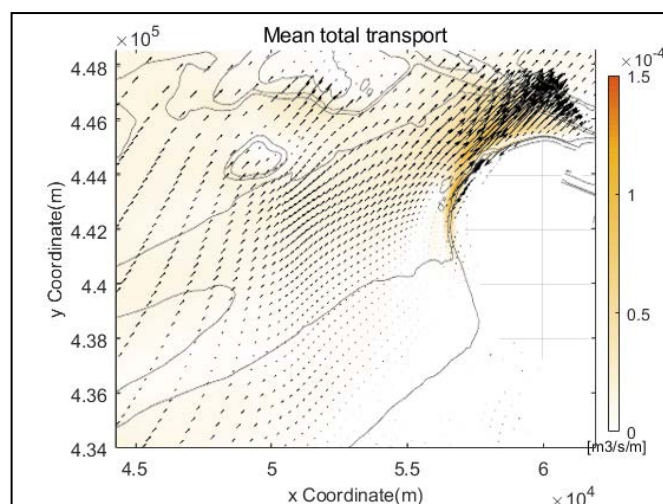


Figure 68: Mean total sediment transport pattern in 0-5 years simulation of Maasvlakte 2 model

7.4 Long-term simulation for the original layout of DELTA

21

7.4.1 Bed level change

Based on the considerably increased velocity and intensive flow vectors at the head of Valmeer as shown in Section 7.2, strong erosion is expected in case of original layout. The estimation is consistent with the simulation result given in Figure 69. Already after 5 years, a noticeable scour hole is formed at the head of Valmeer. Further to the north a large-scale sediment deposition area exists. From the pattern of bed level change provided in Figure 70(a), the maximum erosion is at least 10 m in first five years. Also the height of the deposition further to the north is larger than 10 m.

In the following 15 years, the eroded scour hole grows depth and also in surface area. The profile of the dune structure is completely eroded after 20 years. The expansion of scour hole is blocked by the dry points in the model as shown in Figure 69(d). Without well designed bed protection and/or and adequate maintenance strategy, sea defense of Valmeer is likely to become unstable. From the every five years bed level changes shown in Figure 70, it can be concluded that the erosion rate at the head of Valmeer decreases over time.

The large deposition is also growing over time and migrates in the direction towards shipping channel. Instead of rising in the vertical direction, the deposited sediment expands in the horizontal area and formed a submerged sand bar. The expansion of the deposited sediment can also be confirmed with the cumulative sedimentation pattern given in Figure 70. After the large deposition formed, it start to be eroded from the southwest side through the center of the deposition. More sediment is deposited at the edge of the sand bar on northeast side. In this way, this sand bar expanded and migrated. Also at the landward side of the sandbar, some intensive erosion also developed along the sea defense. The reason behind this kind of sedimentation and erosion pattern around the large scale deposition is further explained with flow pattern and sediment transport in Section 7.4.2.

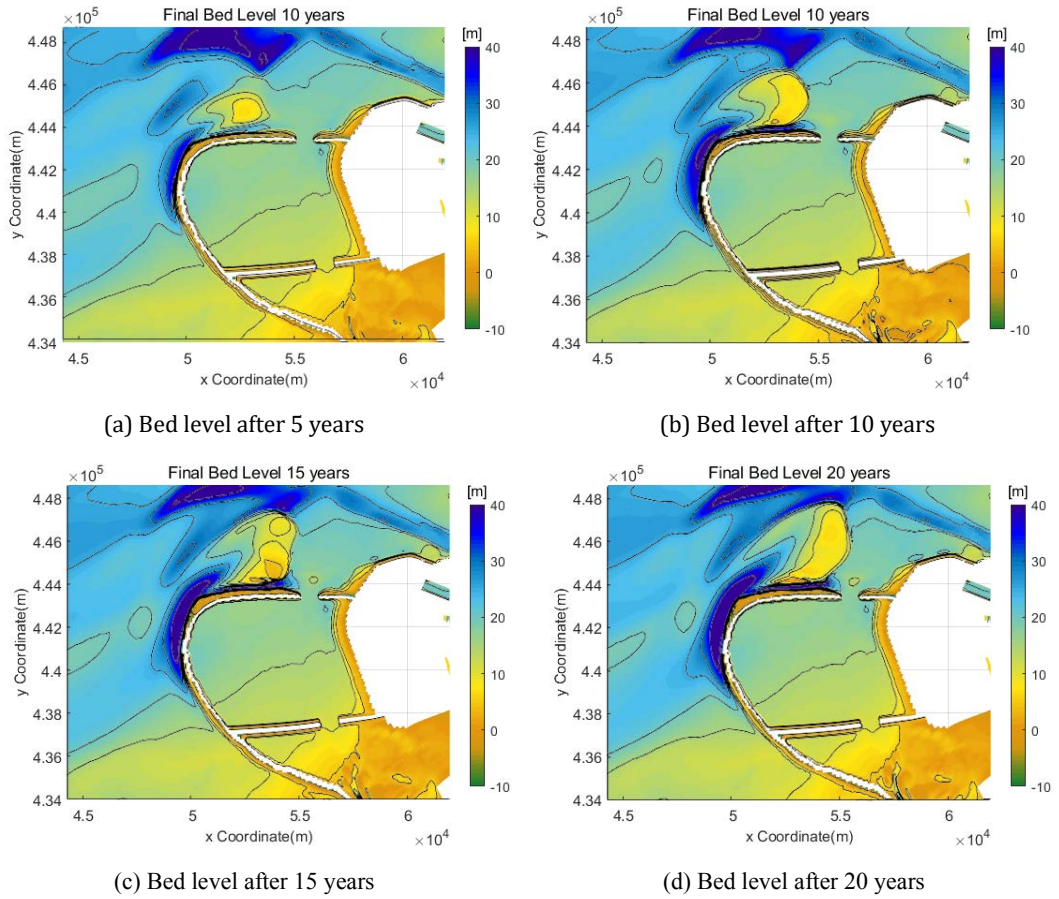
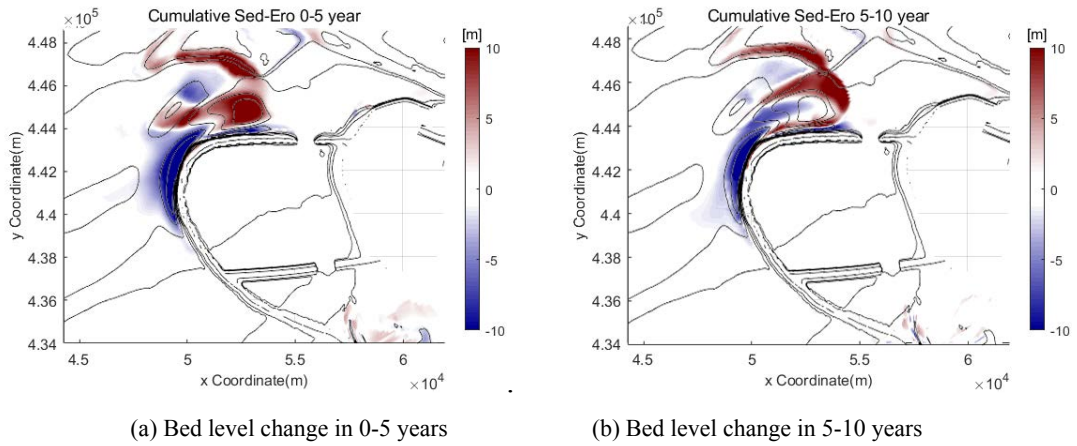


Figure 69: Bed level change in Maasvlakte 2 model after 5, 10, 15 and 10 years simulation in case of original DELTA 21 layout



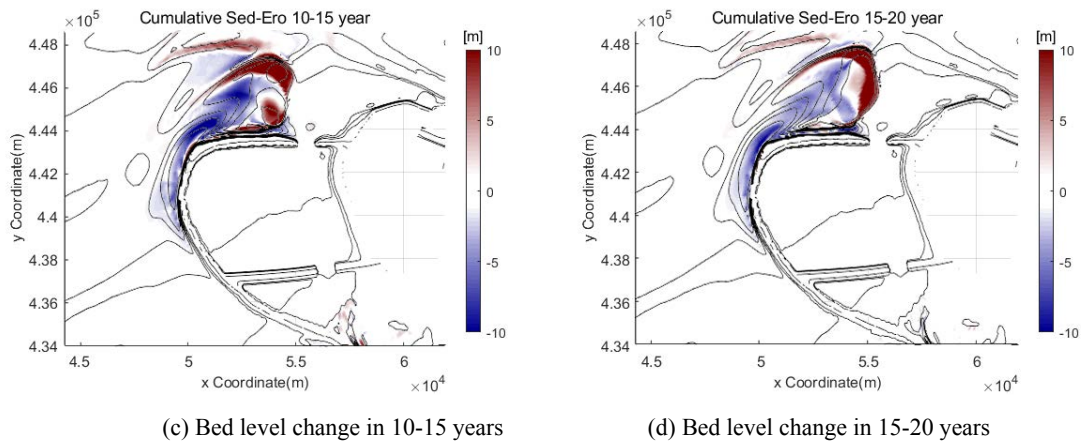
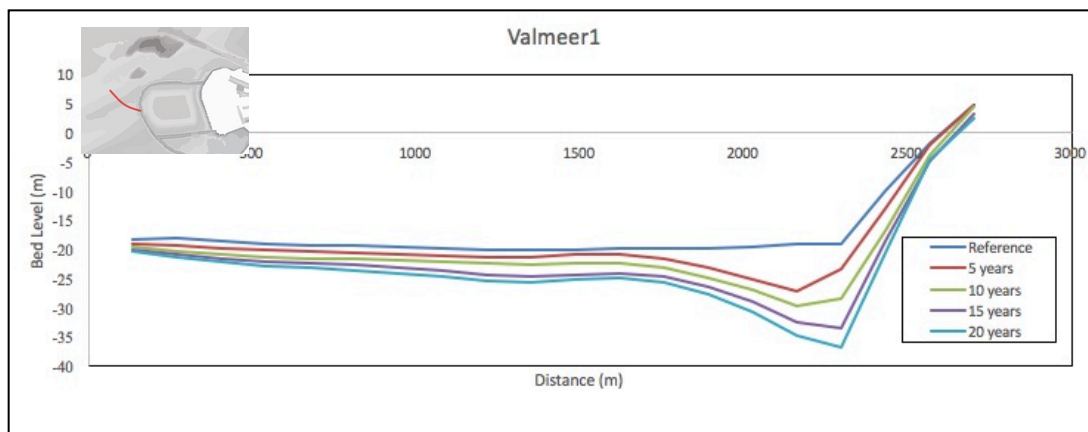


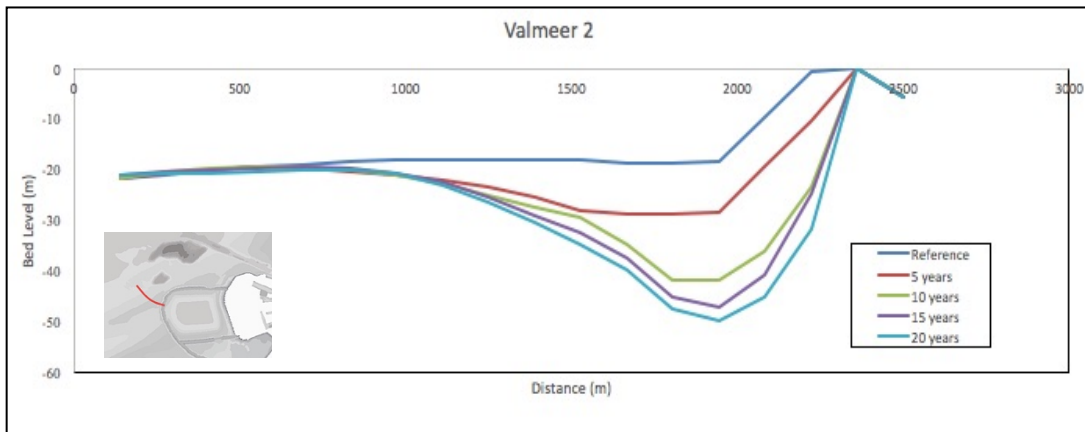
Figure 70: Cumulative bed level change in every five years simulation in case of original DELTA 21 layout

For a detailed analysis of the bed level changes, several cross-sections were selected around the interesting features. In case of original layout, four cross-sections are selected around the head of Valmeer shown in Figure 71 from (a) to (d). Cross-sections at Maasvlakte 2 and shipping channel are defined make a comparison with the result of Maasvlakte 2 model. Also a cross-section that cross the large scale deposition is selected to study the development of the feature. The development of scour hole can be spotted from bed level changes along all four sections at the head of Valmeer. The maximum scour depth is found at the cross-section Valmeer, where the bed level decreased up to 50 m. The erosion rate decreased over time as expected (eventually, an equilibrium will be reached).

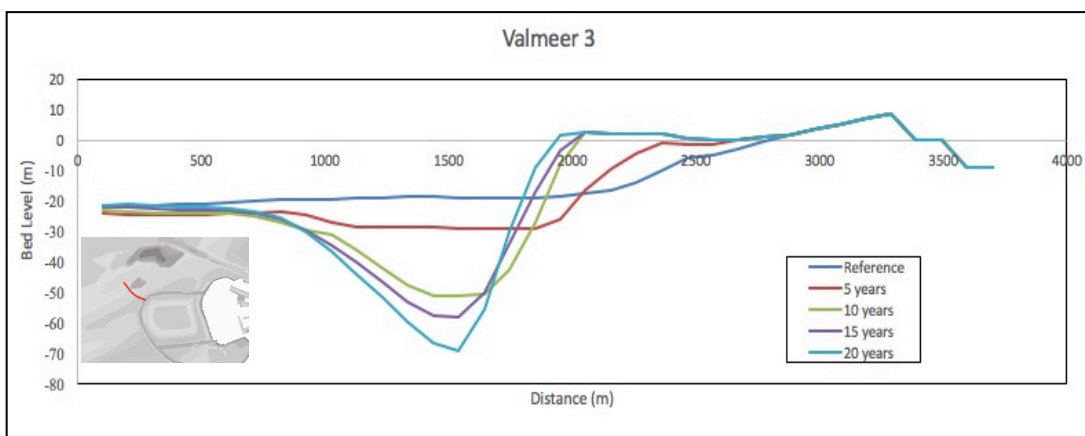
Figure 71 (e) and (f) provides bed elevation along the head of Maasvlakte 2 and shipping channel. In case of original layout, the distance that Valmeer extended in sea ward direction is almost double compare with Maasvlakte 2. Therefore, the onshore location is well sheltered which result in relative stable bathymetry around Maasvlakte 2. But with the newly developed sand bar transported towards the northeast, large amount of deposition may happen in the future (longer than 20 years). Intensive maintenance dredging work may be needed in the future.



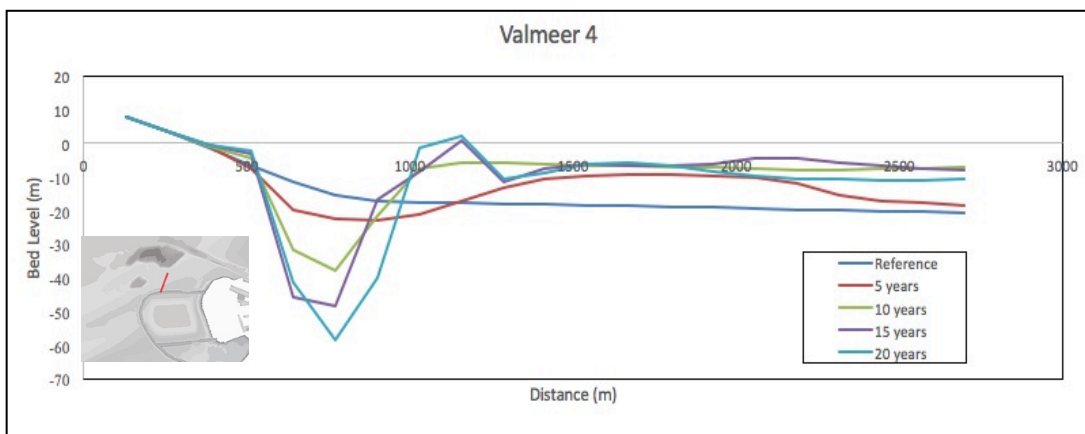
(a) Cross section at the head of Valmeer 1



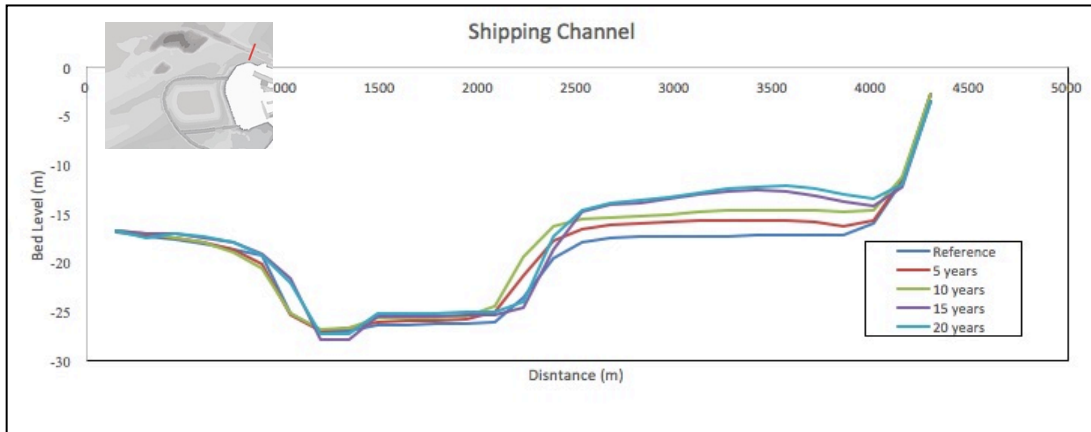
(b) Cross section at the head of Valmeer 2



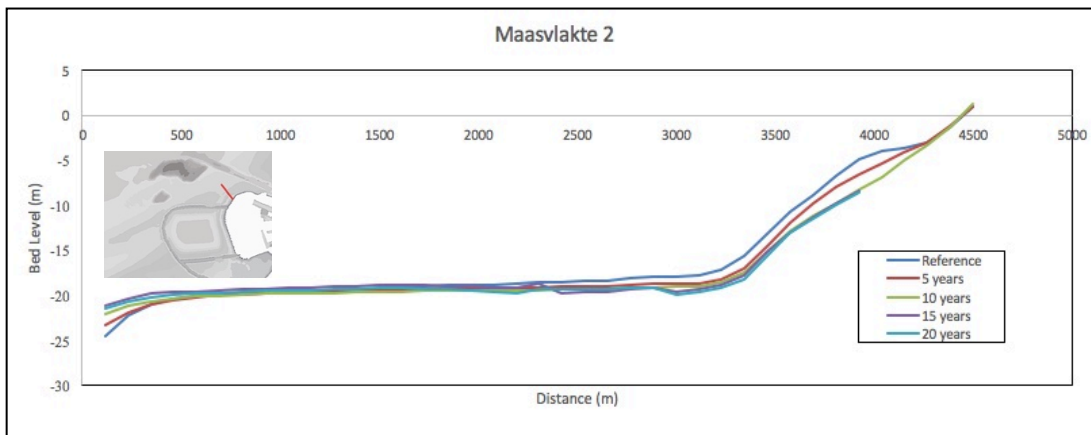
(c) Cross section at the head of Valmeer 3



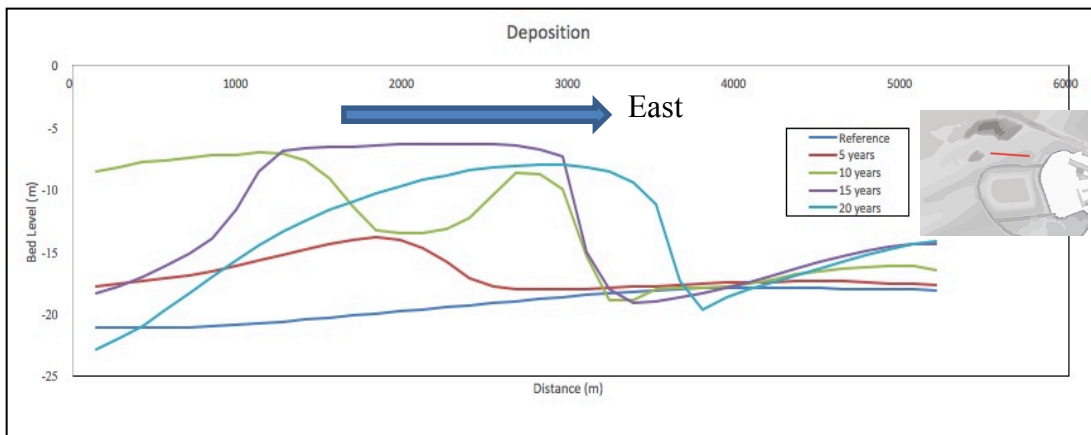
(d) Cross section at the head of Valmeer 4



(e) Cross section at shipping channel



(f) Cross section at head of Maasvlakte 2



(j) Cross section at large scale deposition

Figure 71: Bed level along different cross sections in case of original DELTA 21 layout

7.4.2 Residual currents and Sediment Transport

Carrying huge amount of sedimentation and may cause problem near Maasvlakte 2 and shipping channel, the development of the newly generated sand bar is analyzed in this section. The hydraulic processes and the morphological development are interactive process. With large horizontal dimension and bed level rising over 10 m, the sand bar alters the flow pattern during the tidal cycle. In return, the tide current decides the deformation of the sand bar in next step.

Figure 71(j) gives an impression of the development of this deposition in a long-shore direction. At the beginning of the simulation, sediment transport is directed towards the northeast as shown in Figure 72(a). This formed a deposition with a relative steeper slope at the east edge. Over times, the sand bar migrating towards the northeast direction and the steepness slope at east side is more distinct. The height of the sand bar exceeds 10 m and the remaining water depth is less than 10 m.

This large sedimentation feature result in large difference between flow pattern of ebb current and flood current, as shown in Figure 72. The ebb current transported southwest will face the steep edge. The reduced water depth increased the flow velocity due to concentration in vertical direction and decrease again while it flow past the mild slope on the west side. On the contrary, northeast directed flood is flow gradually concentrated in the vertical direction on the mild slope and suddenly decrease due to flow expansion. On the mild slope, the decreased ebb current and increased flood current velocity altered the direction of the residual current as provided in Figure 73. Between the sand bar and the soft defense, some ebb flow concentrated in the gap instead of flow through the steep edge. It gives a small gap where ebb current intensively concentrated and live part of area on the sandbar almost no flow passing. Consequently, residual current is ebb directed and has a large magnitude.

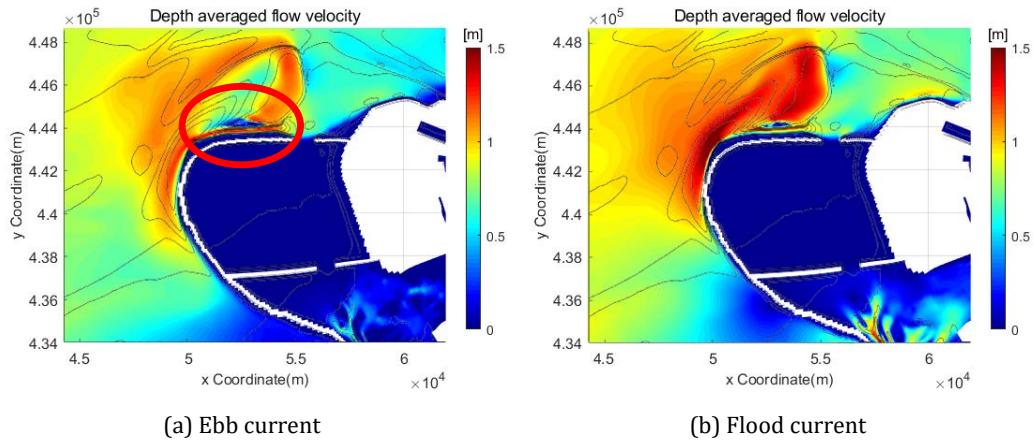


Figure 72: Magnitude over a tidal cycle in case of original DELTA 21 layout in 15-20 years simulation

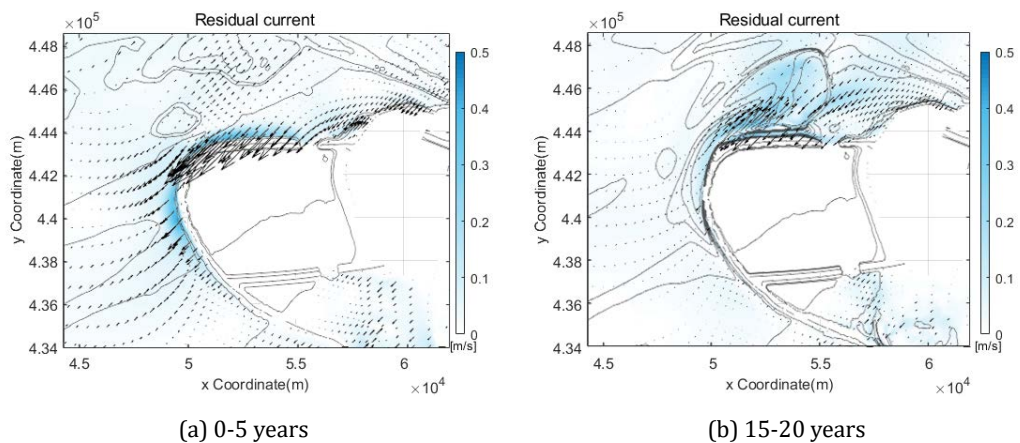


Figure 73: Residual currents in 0-5 years and 15-20 years simulation in case of original DELTA 21 layout

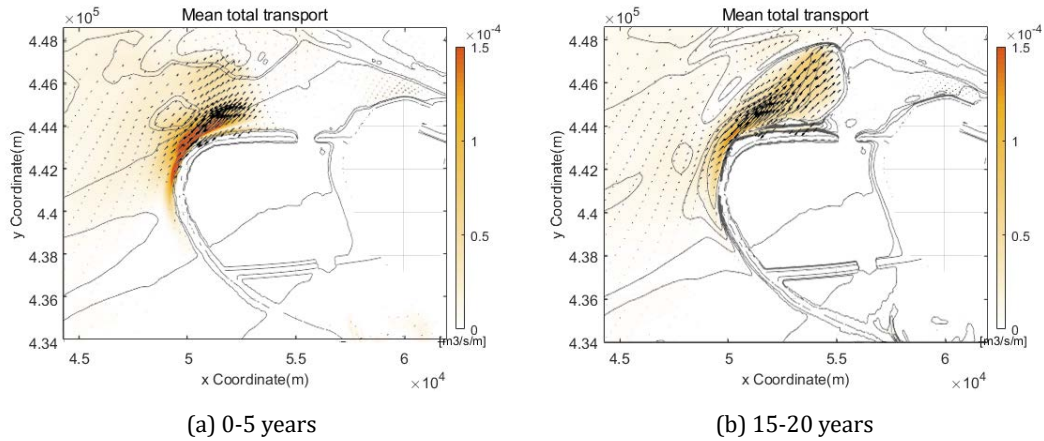


Figure 74: Mean total sediment transport in 0-5 years and 15-20 years simulation in case of original DELTA 21 layout

Figure 75 gives a detailed view of the sediment transport around the sand bar. On the west side, the decreased ebb current and increased flood current generate sediment transport directed towards the northwest. On the edge, the increased ebb current velocity and decreased flood current velocity provides a abruptly stop of sediment transport. In this way, the sediment is deposited around the east side of steep edge and eroded along the mild slope on the west side, which lead to a migration or this sand bar in flood current direction.

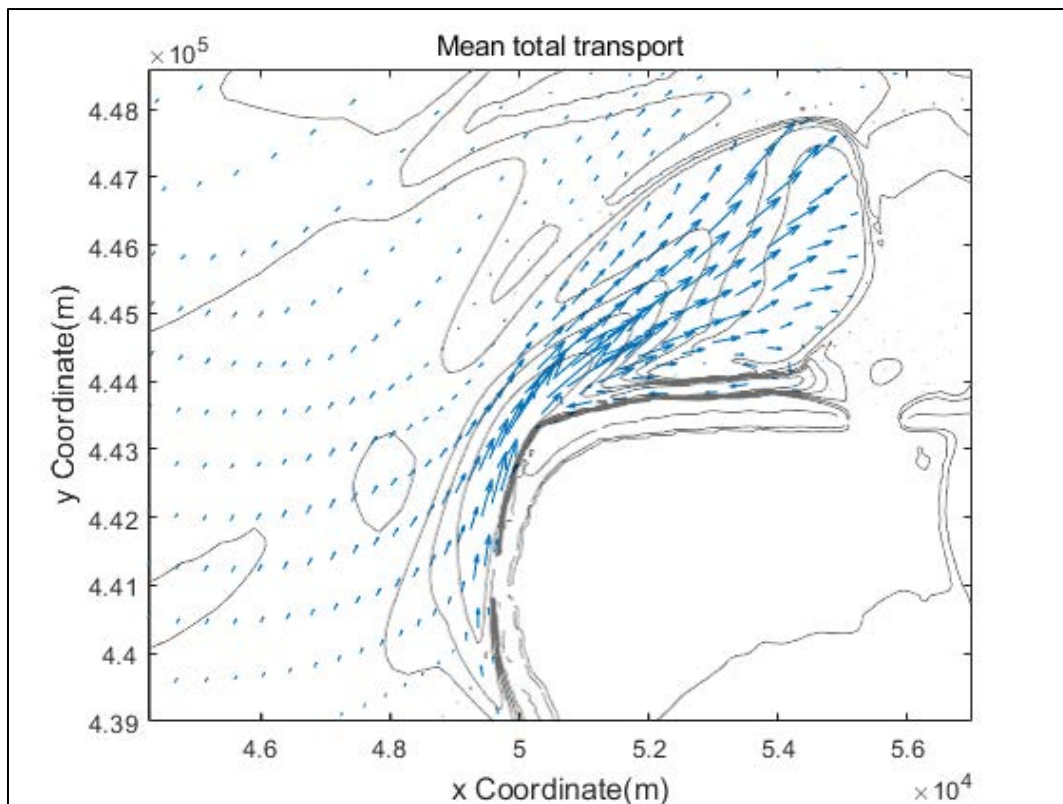


Figure 75: Residual sediment transport at the large scale deposition in case of original DELTA 21 layout

7.5 Long-term simulation for the improved layout of DELTA 21

21

7.5.1 Bed level change

Similar feature developed in case of improved layout of DELTA 21 project as given in Figure 76. Some erosion happens around the corner of Valmeer. This scour hole has limited surface area and depth compared to the original layout, since the flow contraction is less intensive as mentioned in Section 7.2.1.

Also, a deposition area with a noticeable scale is developed at the northern side of Valmeer. After 20 years cumulation and deformation, it forms a sand bar which is in line with the direction of the tidal currents. From the bed level change in every five years shown in Figure 77, the rate of sedimentation at the east side of this sand bar is increasing over time and also erosion pattern is developed and accelerated on the west side. Similar to the original layout, this is investigated through flow pattern and sediment transport pattern in Section 7.4.2.

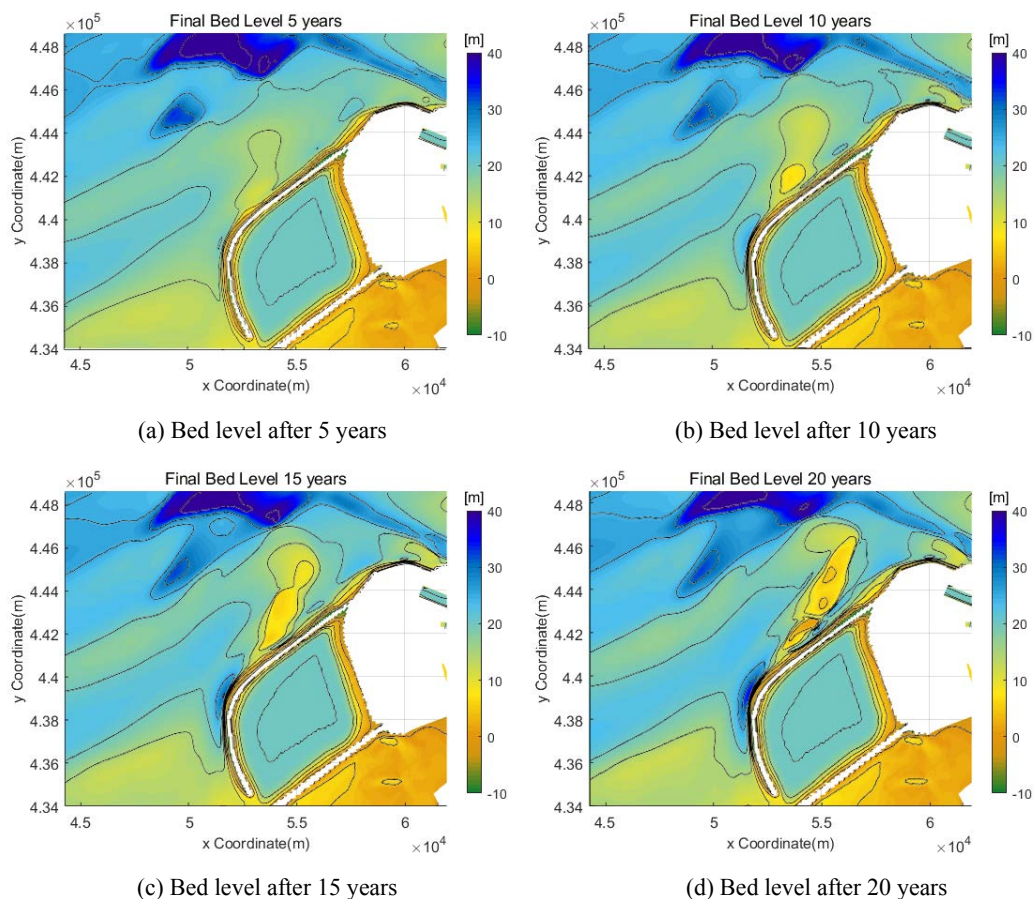


Figure 76: Bed level change in Maasvlakte 2 model after 5, 10, 15 and 10 years simulation in case of improved DELTA 21 layout

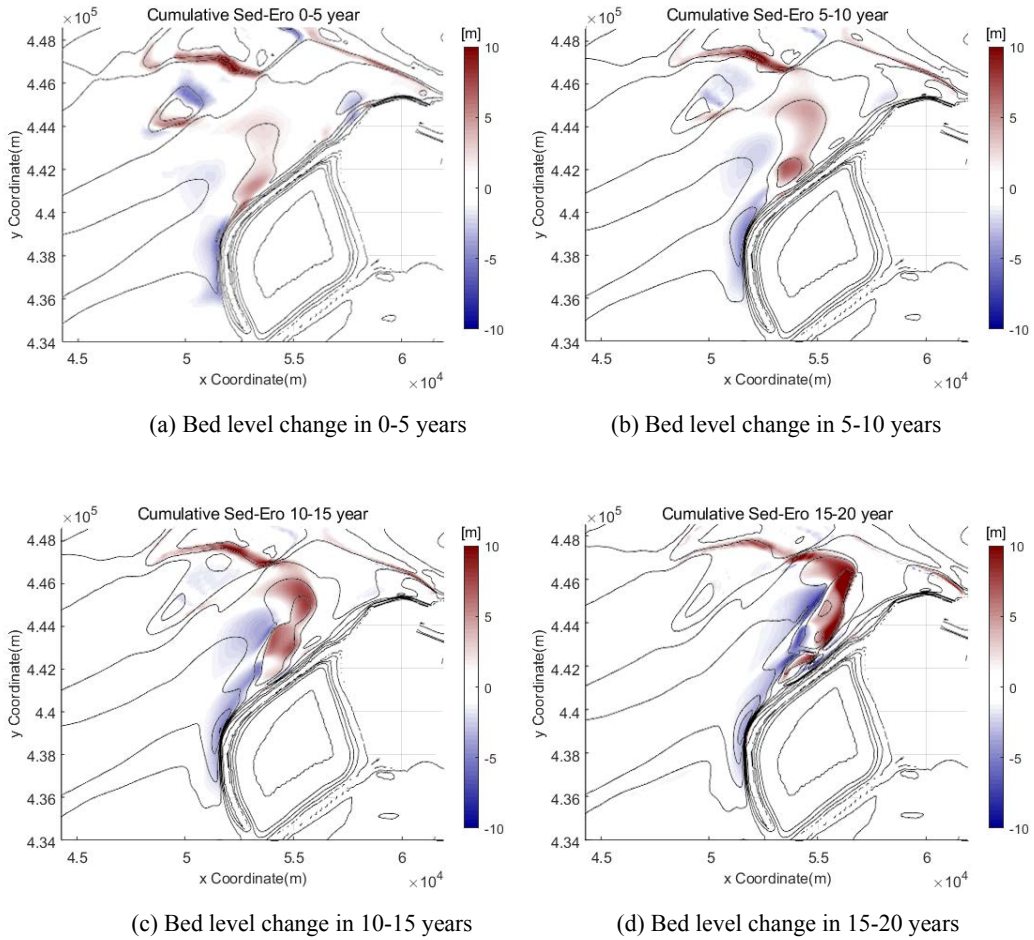
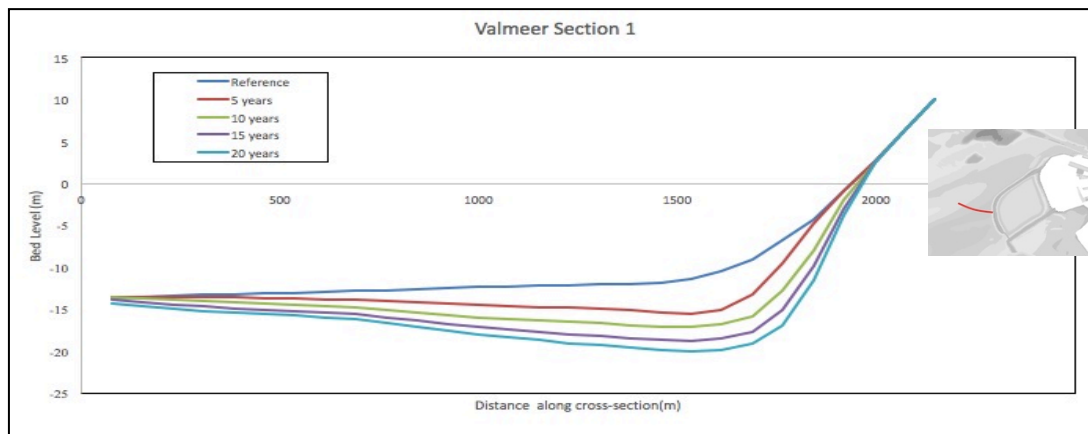
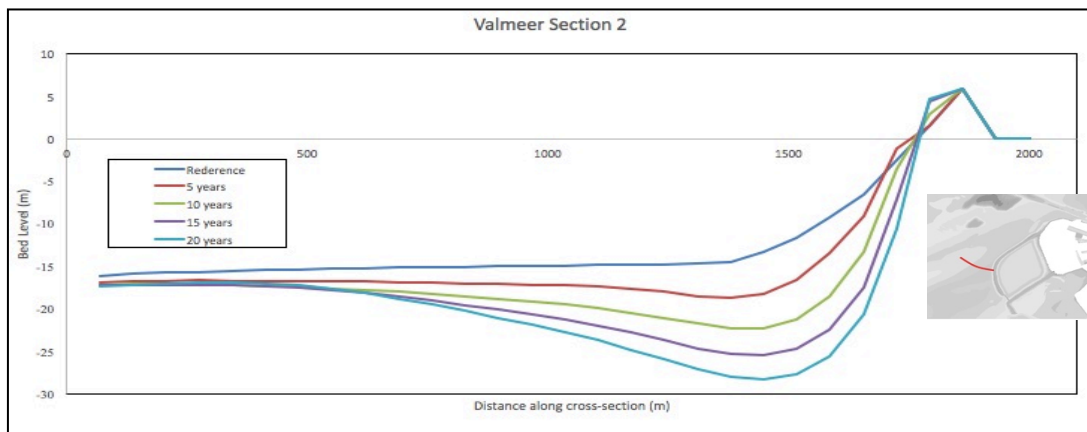


Figure 77: Cumulative bed level change in every five years simulation in case of improved DELTA 21 layout

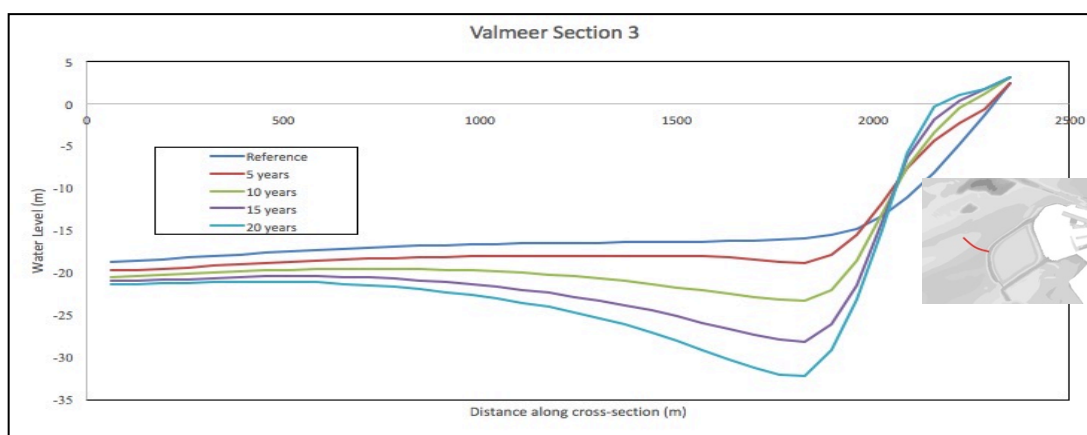
Similar to the original layout, four cross-sections are selected around the head of Valmeer. Shown in Figure 76 (a) to (c), the scour hole gradually develops and the maximum erosion depth given in Figure 76 (b) is about 15 m. The bed level change rate decreased over time. The development of the large deposition can be observed along the bed level change in section Valmeer 4 as shown in Figure 76 (d). Deposition in the shipping channel and erosion in the northern side of Maasvlakte is shown in Figure 76 (e) and (f). The shipping channel is narrowed about 30%. The scour hole at the head of Maasvlakte 2 hardly changes after 20 years simulation and indicate a quite equilibrium stage.



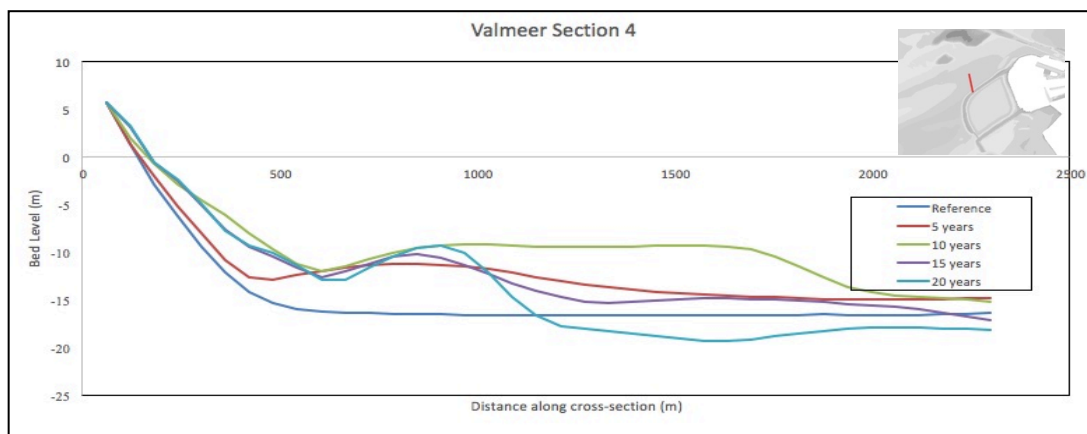
(a) Cross section at the head of Valmeer 1



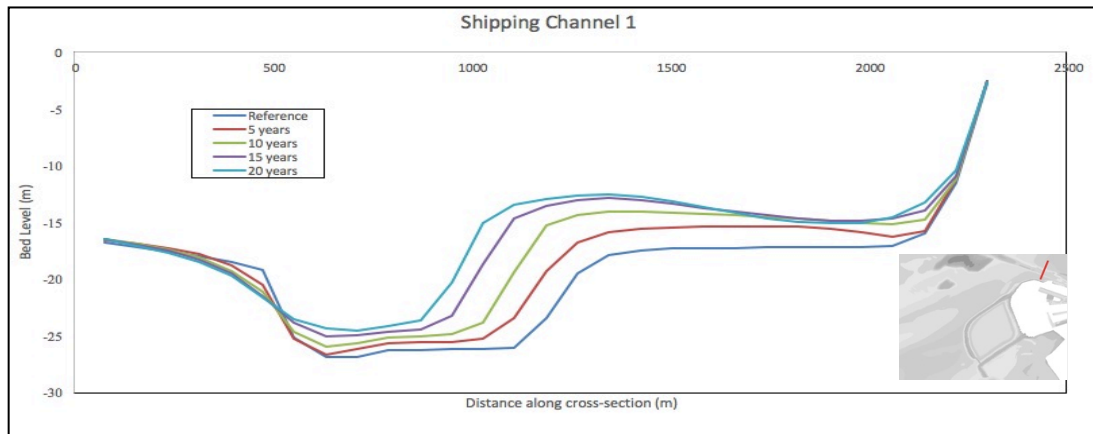
(b) Cross section at the head of Valmeer 2



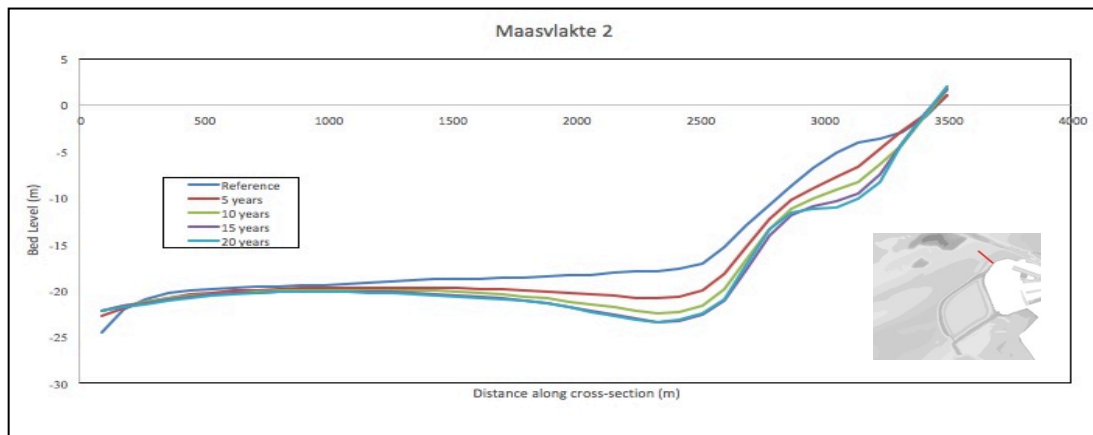
(c) Cross section at the head of Valmeer 3



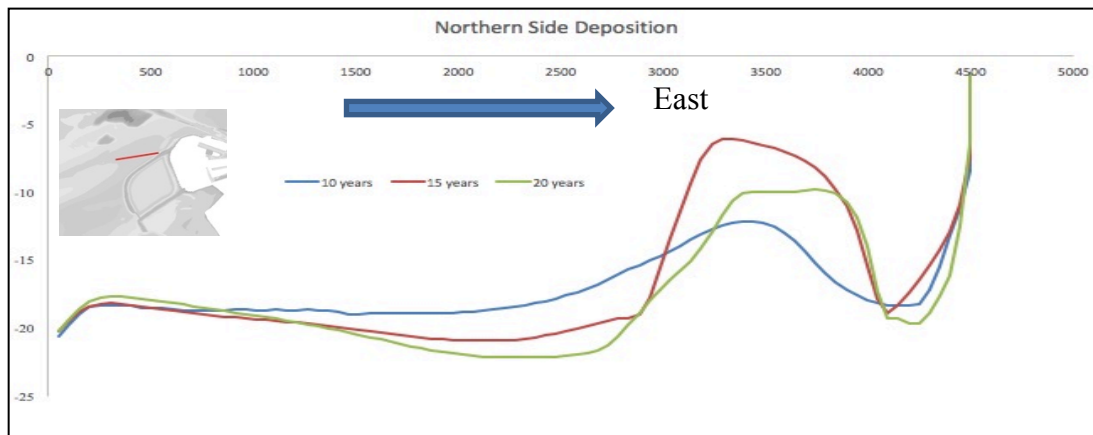
(d) Cross section at the head of Valmeer 4



(e) Cross section at the shipping channel



(f) Cross section at the head of Maasvlakte 2



(j) Cross section at large scale deposition

Figure 78: Bed level along different cross sections in case of improved DELTA 21 layout

7.5.2 Residual currents and Sediment Transport

The shape of the sand bar developed in case improved layout has a more rod-like shape. The shape in cross-section given in Figure 78 (j) shows a similar mild slope on the west side and steep edge on the east side as in case of original layout. The height of the sand bar rises to 15 m in case of improved layout. The principle behind the development of the sand bar is consistent with the condition in original layout. The ebb current is concentrated at the east edge and the gap between sand bar and soft defense. Flood current

accelerated on the mild slope on the west side. According to the sediment transport pattern in Figure 82 large amount of sediment is eroded on the slope surface on the west side and dropped on the east edge, result in migration of the deposition feature and constant sedimentation rate even after 20 years simulation.

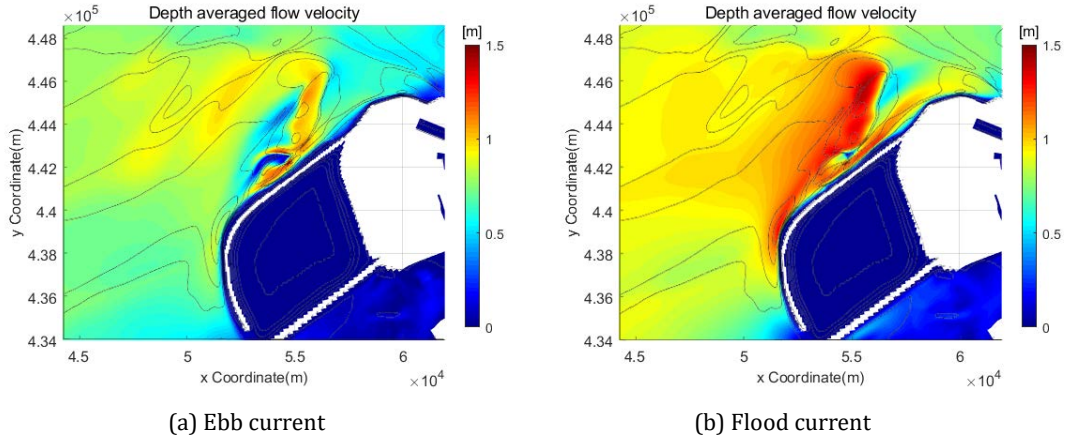


Figure 79: Magnitude over a tidal cycle in case of improved DELTA 21 layout in 15-20 years simulation

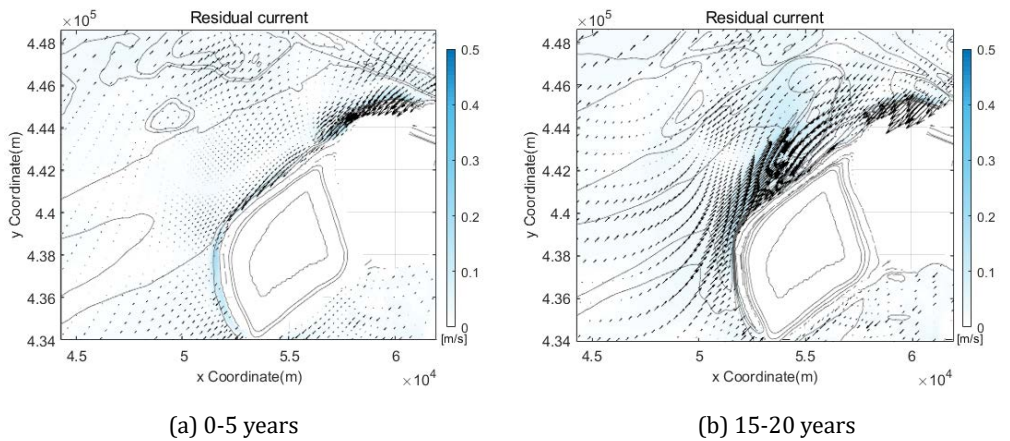


Figure 80: Residual currents in 0-5 years and 15-20 years simulation in case of improved DELTA 21 layout

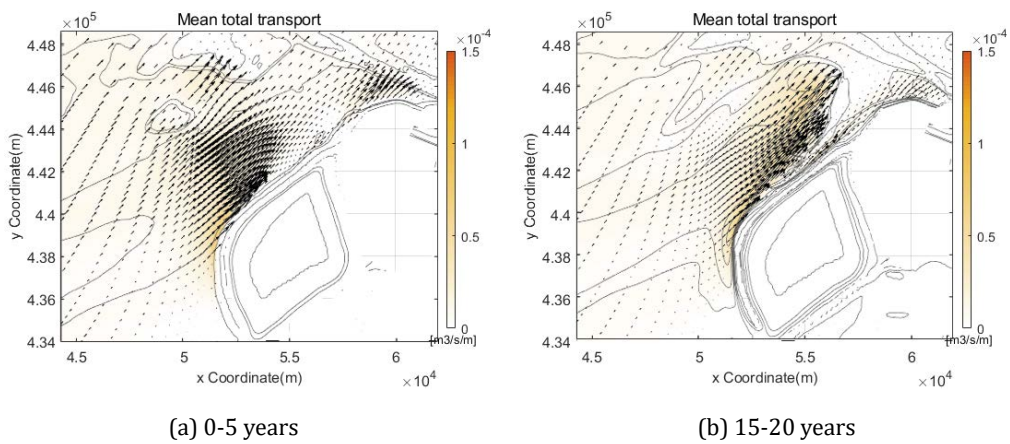


Figure 81: Mean total sediment transport in 0-5 years and 15-20 years simulation in case of improved DELTA 21 layout

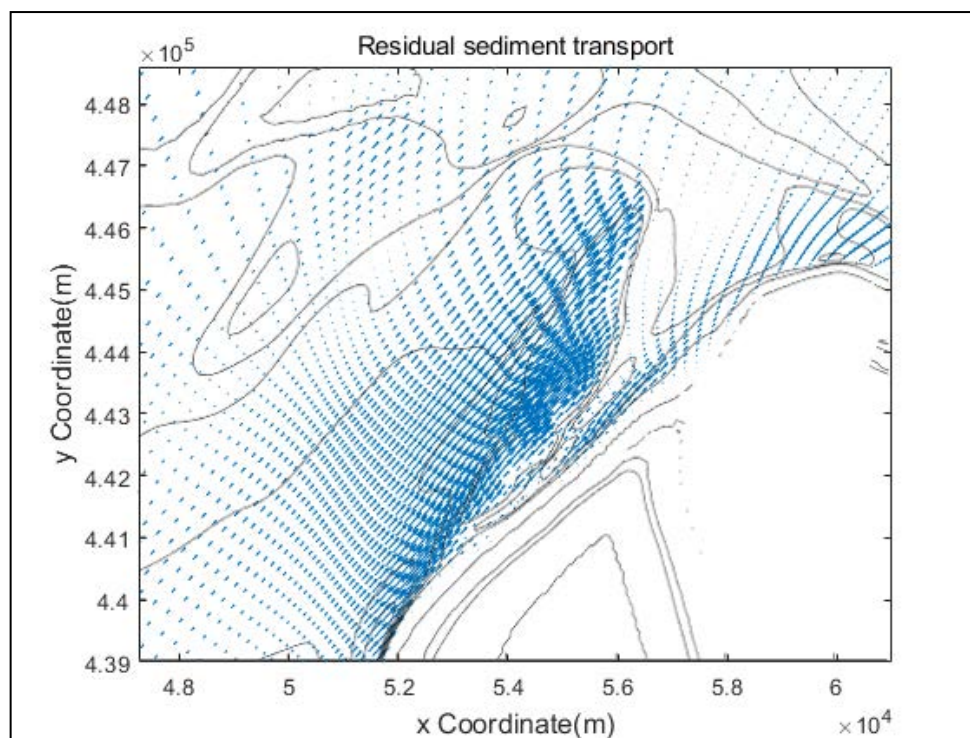


Figure 82: Residual sediment transport at the large scale deposition in case of improved DELTA 21 layout

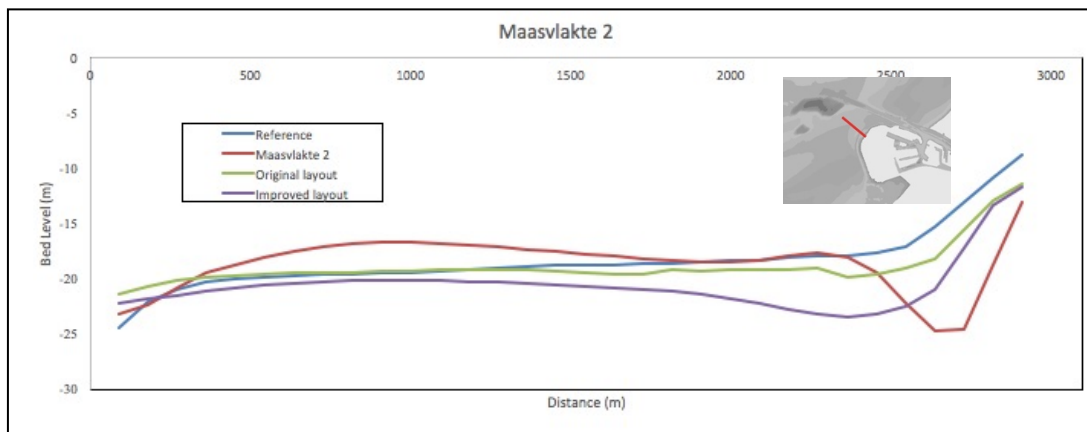
7.6 Conclusions

In this section, the conclusions of the long-term large scale morphological development are summarized. Considering the hydraulic process, the tidal current concentrated in case of both original layout and improved layout around the head of Valmeer and lead to an increasing in the magnitude of the horizontal tide. The increase in the velocity rate is about 50 % in case of original layout and 30% in case of improved layout.

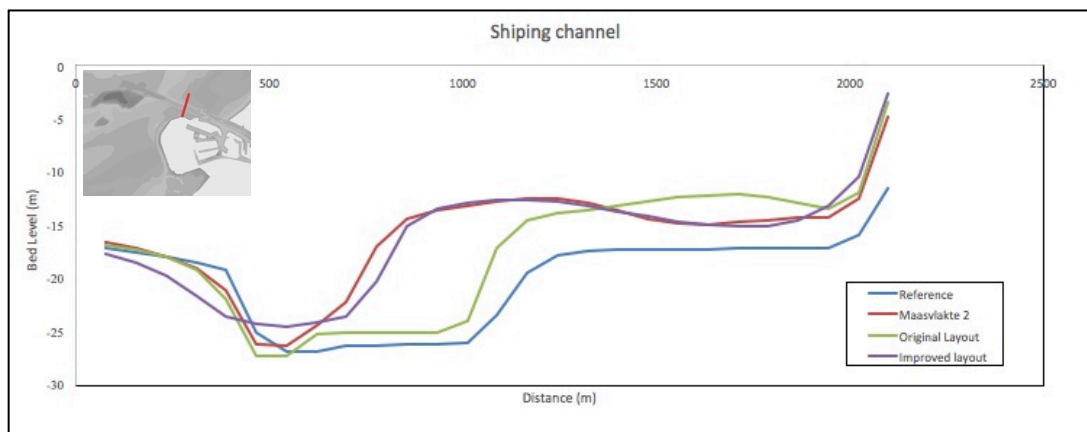
For the long-term morphological development in case of both original and improved layout of DELTA 21, two distinct morphological features can be found, namely the scour hole around the head of Valmeer and the large deposited sand bar at the northern side of Valmeer. The erosion depth in case of the original layout exceeds 50 m, which is over 3 time the value in case of improved layout (being 15 m). Also, the scour hole in case of original layout has a larger surface area. The dune structure is completely eroded at the corner of Valmeer. The development of the large scale deposition at the northern side of Valmeer is forced by the interaction between coastal morphology and flow pattern. While passing the large deposition, the ebb current accelerate at steep edge of the sand bar on the east side and decelerate along the mild slope on the west side. Flood current gradually accelerate on the mild slope and velocity speed dropped abruptly due to sudden flow expansion in the vertical direction. This kind of flow pattern leads to sedimentation on the edge of east side and erosion along the mild slope on the west side. Therefore, this sand bar is migrating towards northeast. This may eventually lead to large amount of sedimentation in the shipping channel.

Comparing the bed level change around Maasvlakte 2 with the result of 20 years simulation of Maasvlakte 2 model, as provided in Figure 83. the impact of DELTA 21 on the morphological

development in that area can be concluded. In case of original layout, shelter by the large seaward extension of the Valmeer, the bed level at the northern side of Valmeer and in the shipping channel is quite constant during 20 years simulation. In case of the improved layout, the development of scour hole is abated around the head of Maasvlakte 2. The sedimentation in the shipping channel gives similar result for the Maasvlakte 2 model and DELTA 21 model in case of improved layout. On general, the migrated sand bar will eventually lead to large amount of sedimentation in the area around Maasvlakte after longer times development in case of both original layout and improved layout.



(a) Cross section at the head of Maasvlakte 2



(b) Cross section at the head of shipping channel

Figure 83: Bed level of three model after 20 simulation at two sections

8

Conclusions and Discussions

8.1 Discussions

The DELTA 21 as a creative and completely new project, still needs to be evaluated in plenty of different aspects. Within this research certain assumptions are made and the following suggestions are proposed in order to decrease the model uncertainty of models as applied in this research project.

- The wave climate and grain size of bed material used for the local scale study in the UNIBEST model is obtained from the Maasvlakte 2 design. The applied wave climate may not be fully acceptable at the location and shape of the DELTA 21 project. It is recommended to prepare a more detailed nearshore wave climate, which is applicable for the DELTA 21 project.

Secondly, the sediment characteristics determine shape of the beach profile and the long-shore transports. At this moment it cannot be said which D50 grain size will be applied for the sea defense of Valmeer. With more detailed design for the dune structure, more accurate simulation should be done for the DELTA 21.

- For the long-term large scale morphodynamic prediction, the results still have large uncertainty range. The morphodynamic model setting can be further improved by calibration and validation with real bathymetry data. But still this study gives a good overview of future large-scale morphological development after construction of DELTA 21 project.
- In this study, the effect of wave motion on the sediment transport is not considered in the large scale morphodynamic simulations. At the location of the sand bar developed on the northern side of Valmeer, water depth is reduced to around 5-10 meters. In this case, the wave motion will contribute to the sediment transports process. In the area with limited water depth, turbulence caused by the orbital wave motion results in significant higher bed shear stress which will result into seabed agitation and sediment remobilization (Héquette, 2008). According to the sediment transport pattern in the area of the sand bar, erosion in the shallow area on the west side will be reinforced. Therefore, the development of sand bar in the vertical direction will be limited. But the process of its migration towards the shipping channel may be accelerated with larger erosion rate on west side, in the same time, larger deposition rate around east edge. To accurately predict the deformation of the large scale sand bar on the northern side of Valmeer, further research is needed.

- The material used in the large scale morphodynamic model is uniform non-cohesive sediment with $D_{n50} = 0.20$ mm. But based on the geological background information in the study area, the D_{n50} in most locations at the northern side of DELTA 21 is coarser than 0.20 mm. In reality, natural seabed sediments are non-uniform and therefore natural sorting of bed sediments occurs. The finer sediment will erode and the coarser material will stay behind forming an armour layer on the surface of the seabed. Higher flow velocity is required to transport coarser material. Therefore the morphological changes will be smaller which may result in a reduction of sediment transport. As a result, the development of large-scale scour hole and deposition in this study is overestimated.
- Sea level rise becomes to play an important role in the morphological development in coastal zone, which is not considered in this study. SLR can influence tidal hydrodynamics through increased tidal ranges (National Research Council, 1987). In addition, it has the potential to change circulation and sediment transport patterns. Increased tidal ranges have the potential to increase tidal current velocities (Stevens, 2010). Therefore, the sediment transport may be reinforced in both large scale and local scale. Also, wave height is limited by available water depth. Therefore deeper water in near-shore environments will cause wave heights to increase, which will lead to stronger erosion and shoreline retreat (Smith et al, 2010).

8.2 Conclusions

The objective of this research was to analyze the long-term morphological changes caused by the DELTA 21 project in case of both original layout and improved layout. This study focusses on the northern side of the DELTA 21 project. In this section, the research question is answered by presenting the answers and conclusions to the sub-questions as defined in Section 1.3.

- *What are the characteristics of the water motion and which mechanism should be included in the large scale and local scale morphology analysis, respectively?*

This study focusses on the morphological development induced by sand transport. As the northern side sea defense of Valmeer is located in deep water, the large-scale morphological development is governed by tidal currents. At such depth, only very severe wave conditions will affect the bottom shear stress which is important for the transport of non-cohesive material. For this reason, only the effect of tidal forces on the large-scale morphology is assessed.

When zooming into the local scale along the sandy beach of Valmeer, waves start to be the dominant process for sediment transports. Sand is stirred up by the wave orbital motion near the bed and transported by long-shore currents (both tidal currents and wave-induced currents). Both the significant wave height and the wave direction in the wave climate affect the long-shore sediment transport and coastline deformation. To assess the nearshore morphology and shoreline evolution, both the wave and tide are included in the local scale morphological study.

- *How will the layout of the Valmeer affect the morphological change at a local scale in case of the original layout?*

In case of the original layout, the coastline deformation has several distinct sections. The coastline is eroded at the most western location of the Valmeer and deposition occurs at the southwest side and northern side. The significant erosion at the head of Valmeer eventually threatens the stability of

the structure if no maintenance is performed to compensate the erosion. The maximum shoreline retreat of original layout is 448m in 10 years' time. Part of the eroded sediment deposits at the northern side sandy beach, as shown in Figure 84. In the eroded section 2,165,000 m³ sand is lost at the head of Valmeer along 3 km sandy beach in the first year only.

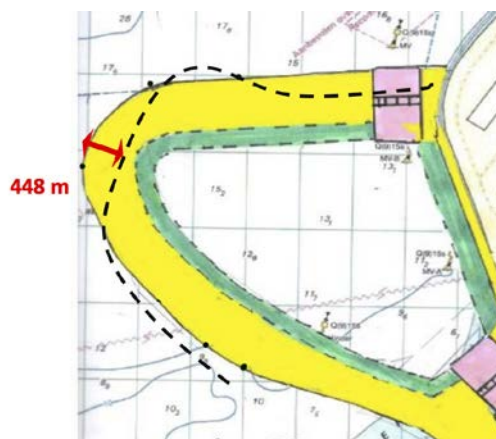


Figure 84: Coastline deformation after 10 years in case of original layout

- *How will the layout of the Valmeer affect the morphological change at a local scale in case of the improved layout?*

The predicted evolution of coastline for the improved layout gives more gentle and stable shape. Except for the deposition near the groyne, the sandy beach of the improved layout is constantly eroded, with a maximum shoreline retreat of 165 m in 20 years' time, as provided in Figure 85. The eroded section of improved layout is around 7 km and has 1,141,000 m³ sediment loss in the first year. In comparison with the original layout less sediment is transported towards the hard defense of Maasvlakte 2 and the required maintenance to compensate for the erosion along Valmeer is less.



Figure 85: Coastline deformation after 10 years in case of improved layout

- *How will the DELTA 21 influence the coastal morphological evolution at a large scale on the northern side of Valmeer?*

At the northern side of Valmeer, two distinct morphological features are developed after 20 years. The first feature is the scour hole near the most western location of the Valmeer. For the original layout, the maximum scour reaches up to 50 m in 20 years' time. With an original bed level of NAP-20 m, the local water depth inside the scour hole reaches NAP-70 m after 20 years. In the improved layout, the maximum scour after 20 years is approximately 16 m deep. With an original bed level of NAP-17 m, the local water depth inside the scour hole reaches NAP-33 m after 20 years. The rate of erosion around the head of Valmeer decreased over time and likely to reach an equilibrium state.

The second feature is a large deposition area (sand bar), which develops just north of the Valmeer. This deposition has a height (with respect to the original bed level) of 10 m in case of original layout and 15 m in case of improved layout. In both cases, the sand bar is gradually migrating in the direction of flood current. One thing to be noticed is that the deposition can reduce the water depth to around 5-10 meters, where the wave motion starts to play a role in the sediment transports. But in this study, the wave effect is not included in the large scale morphodynamic simulation.

- *How will the DELTA 21 influence the coastal morphological evolution at a large scale around Maasvlakte 2?*

In case of original layout, the bed level at the northern side of Valmeer and in the shipping channel is quite constant due to the sheltering of Valmeer. In case of the improved layout, the development of scour hole is abated around the head of Maasvlakte 2 and seems no effect on the deposition in the shipping channel in the first 20 years. The migrating sand bar will however eventually reach the shipping channel and high sedimentation rates are expected. This conclusion holds for both original layout and improved layout.

8.3 Recommendations

- According to the discussion about the limitation of this study, future study on the large-scale morphological development on the northern side of Valmeer can be improved by including the following aspects.
 - Include the wave motion to study its effect on the bed shear stress and large-scale morphological feature development.
 - The armouring effect of larger grain size in the seabed can also be studied with sensitivity study.
 - The process of sea level rise can also be included in the morphodynamic model and investigate on its impact of large scale morphological development.
- For local-scale coastline deformation, the model can be improved by determining near-shore wave climates at the location of Valmeer and including the process of sea level rise. The near-shore wave climate can be obtained by transformation of the offshore wave climate to near-shore wave climates (by means of SWAN for example). Also, a detailed beach profile should be designed and applied for the sandy beach of Valmeer after the design of the DELTA 21 project goes more into details.

- Silt transport is also an important part of coastal morphology study. The fine material transport is greatly influenced by the residual current as discussed in section 2.3. Based on the result of Delft3D simulations in this study, the transport pattern of fine cohesive material can be completely different with the sand transport. Further study can be done for the transportation and deposition for cohesive material along the coastline of Valmeer caused by residual current.

Reference

- Bagnold, R., (1963). An approach of marine sedimentation. In: Hill, M.N. (Ed.), *The Sea*, vol. 3. Interscience, New York, pp. 507–528.
- Berke L., Lavooij H. (2019). DELTA21 en Waterveiligheid, DELTA21: Kostenbesparend alternatief voor dijkverhogingen. Retrieved from <https://www.delta21.nl/>.
- Bijker, E.W. (1968). Littoral drift as function of waves and currents, *Proceedings of 11th International Conference on Coastal engineering*, pp. 415-435, ASCE
- Bosboom J., Stive M.J.F. (2015). *Coastal dynamics I: Lecture notes CIE4305*. Delft, The Netherlands: VSSD.
- Camenen B., Larroude P. (2003). Comparison of sediment transport formulae for a coastal environment. *Coastal Engineering*, Elsevier, 2003, 48, pp.111-132.
- Church JA, Clark PU, Cazenave A, Gregory JM et al (2013). Sea level change. In: *Climate change 2013: the physical science basis. Contribution of Working Group I to the Fifth Assessment Report of the Intergovernmental Panel on Climate Change*. Cambridge University Press, Cambridge and New York, pp.1137–1216.
- Colina Alonso A. (2018). *Morphodynamics of the Haringvliet ebb-tidal delta*. Delft, The Netherlands: Delft University of Technology.
- Dalrymple R.W., Choi K. (1978) Sediment transport by tides. In: *Sedimentology. Encyclopedia of Earth Science*. Springer, Berlin, Heidelberg . https://doi.org/10.1007/3-540-31079-7_181
- Deltares (2014a). *Delft3D-FLOW user manual version 3.15, Simulation of multi-dimensional hydrodynamic flows and transport phenomena, including sediments*.
- Deltares (2014b). *Delft3D-WAVE user manual version 3.05, Simulation of short-crested waves with SWAN*.
- Deltares (2011). *UNIBEST-CL+ manual, Manual for version 7.1 of the shoreline model*.
- Dronkers, J. (1998). Morphodynamics of the Dutch Delta. In Dronkers, J. and Scheffers, M. B. A. M., editors, *Physics of Estuaries and Coastal Seas*, Rotterdam.
- De Vries, M. J. (2007). *Morphological modelling of the Haringvlietmonding using Delft3D*. Msc thesis, Universiteit Twente.

- Elias E., Aarninkhof S., Roelvink D. (2006). *Ontwikkeling ontgrondingskuil bij Maasvlakte 2*. Rotterdam, The Netherlands: Havenbedrijf Rotterdam.
- Hallermeier, R.J. (1981). A profile zonation for seasonal sand beaches from wave climate. *Coastal Eng.*, 4:253-277.
- Héquette A., Hemdane Y., Anthony E.J. (2008). Sediment transport under wave and current combined flows on a tide-dominated shoreface, northern coast of France. *Marine Geology* 249 (2008), pp. 226–242.
- Hijma M. (2015). *Geology of the Dutch coast, The effect of lithological variation on coastal morphodynamics*. Delft, The Netherlands: Deltares.
- Imasato, N. (1983): What is Tide-Induced Residual Current?. *J. Phys. Oceanogr.*, 13, 1307–1317, [https://doi.org/10.1175/1520-0485\(1983\)013<1307:WITIRC>2.0.CO;2](https://doi.org/10.1175/1520-0485(1983)013<1307:WITIRC>2.0.CO;2).
- Jenniskens M.J.J. (2001). *Comparison of the sediment transport formulae according to Bijker and Van Rijn*. Delft, The Netherlands: Delft University of Technology.
- Job Dronkers (2020): Active coastal zone. http://www.coastalwiki.org/wiki/Active_coastal_zone.
- Kemp P. H., Simons R. R. (1984). *Sediment Transport due to Waves and Tidal Currents*. *Seabed Mechanics*, B. Denness (ed.), pp. 197-206.
- Loman G.J.A., Hofland B., Van der biesen S.C., Poot J.G. (2012). *Integral design of hard sea defense of Maasvlakte 2 (Part II: Physical model testing of cube revetment & reef)*. Delft, The Netherlands: Deltares.
- Mann M. (2019). *Unravelling the sediment transport mechanisms in an artificial lagoon*. Delft, The Netherlands: Delft University of Technology.
- National Research Council (1987). *Responding to Changes in Sea Level: Engineering Applications*. The U.S., Washington, D. C.: The National Academies Press.
- Olthoff T. (2019). *Longshore transport of coarse-grained material*. Delft, The Netherlands: Delft University of Technology.
- Onderwater M. (2016). *Optimalisatie van beheer en onderhoud rondom noordelijke beeindiging van zachte zeewering van Maasvlakte 2*. Technical report, Arcadis, 2016.
- Passeri D.L., Hagen S.C., Medeiros S.C. (2015). The dynamic effects of sea level rise on low-gradient coastal landscapes: A review. *Earth's Future*, 159-181 May 2015.
- Petersen D., Deigaard R., Fredsøe J. (2008). *Modelling the morphology of sandy spits*. Lyngby, Denmark: Technical University of Denmark.
- PUMA (2008). *Zachte Zeewering: Prognose van onderhoudsuppletie*, Ontwerpnota puma-p-mo-onb07.

- Rijkswaterstaat (2017b). Waterbase. <http://live.waterbase.nl>
- Rijkswaterstaat (2014). Opzet Proef Slikken van Voorne: Natura 2000 Ontwerpbeheerplan Voordelta 2015- 2021. Technical report, Rijkswaterstaat.
- Ruiz R.A. (2020). Conceptual design of the Valmeer's pump storage station of the DELTA21 plan. Delft, The Netherlands: Delft University of Technology.
- Smith, J. M., M. A. Cialone, T. V. Wamsley, and T. O. McAlpin (2010), Potential impact of sea level rise on coastal surges in southeast Louisiana, *Ocean Eng.*, 37, pp. 37–47.
- Speer, P. E., and D. G. Aubrey (1985). A study of non-linear tidal propagation in shallow inlet/estuarine systems II: Thory. *Estuarine Coastal Shelf Sci.*, 21, pp. 207–224.
- Stevens, S. (2010), Estuarine shoreline response to sea level rise. Speers Point, Australia: Lake Macquarie City Council.
- Stolk A., Dijkshoorn C. (2009). Sand extraction Maasvlakte 2 Project: License, Environmental Impact Assessment and Monitoring. EMSAGG Conference, 7-8 May 2009
- Terwindt, 1973. J.H.J. Terwindt Sand movement in the in- and offshore tidal area of the S.W. part of the Netherlands. *Geol. Mijnbouw*, 52 (1973), pp. 69-77.
- Van der Werf J., Grasmeijer B., Hendriks E. et al (2017b). Literature study Dutch lower shoreface. Delft, The Netherlands: Deltares.
- Van den Berg A. (2007). Development scour hole Maasvlakte 1 & 2: data analysis and forecast. Delft, The Netherlands: Delft University of Technology.
- Van Ledden Ir.M. (2005). Effects of Maasvlakte 2 on the Wadden Sea and the North Sea coastal zone. Rotterdam, The Netherlands: Royal HaskoningDHV.
- Van Rijn, L.C., (1993). Principles of Sediment Transport in Rivers, Estuaries, and Coastal Seas. Amsterdam: Aqua Publications.
- Wachler, B., Seiffert, R., Rasquin, C. et al (2020). Tidal response to sea level rise and bathymetric changes in the German Wadden Sea. *Ocean Dynamics* 70, 1033–1052.
- Winterwerp J.C. (2006). Fluxes of fine sediment along the Dutch coast and the impact of Maasvlakte 2. Delft, The Netherlands: WL|Delft Hydraulics.

List of figure

Figure 1 : Layout version 2019 of DELTA 21 project (Berke and Lavooij, 2019)	1
Figure 2: Conceptual drawing of DELTA 21 project (Ruiz, 2020).....	2
Figure 3: Improved layout of DELTA 21 project (DELTA 21, 2020)	3
Figure 4: Maasvlakte 2 with hard sea defense design and built (Loman et al, 2012).....	4
Figure 5: Northern side of the DELTA 21 project	5
Figure 6: Bed load transport (Van Rijn, 1993)	10
Figure 7: Suspended transport (Van Rijn, 1993).....	10
Figure 8: Bedload transport by symmetric tidal current (left) and asymmetric tidal current (right) (Dalrymple, 1978).....	14
Figure 9: Longshore sediment transport and coastline deformation (Bosboom and Stive, 2015)	15
Figure 10: Coastal change in a cross-shore view (Bosboom and Stive, 2015).....	15
Figure 11: Geological borehole research identification and location from DINOloket (dinoloket.nl) ...	18
Figure 12: Sea defence of Maasvlakte 2 (Mann, 2019).....	19
Figure 13: Sand extraction area of Maasvlakte 2 (Stolk and Dijkshoorn, 2009).....	19
Figure 14: Tidal signal retrieved from Delft Dashboard measuring station: Xtide Tidal Station Haringvliet 10 (Colina, 2018)	20
Figure 15: Waves roses from 2013-2018 obtained from the Europlatform and a point 800m offshore from the sand layer area (Mann, 2019)	21
Figure 16: The coastal orientation and wave climate coupled with original layout (left) and improved layout (right)	23
Figure 17: Wave-rose for wave climates applied at southwest coast (left) and northwest coast (right) .	23
Figure 18: Cross-shore depth profile marked with closure depth and active height.....	25
Figure 19 : Proposed annual zonation of seasonal sand beach profile (Hallermeier, 1981)	25
Figure 20: Location of three geo-referencing points	27
Figure 21: The structure to block sediment between soft defense and hard defense (earth.google.com)	28
Figure 22: The CL-model of the original layout.....	29
Figure 23: The CL-model of the improved layout.....	29
Figure 24: S- ϕ curves generated from Lt-model	31
Figure 25: The points selected on the original and improved layout.....	31
Figure 26: The sediment transport along the sandy beach for the original layout.....	33
Figure 27: The sediment transport along the sandy beach for the improved layout	33
Figure 28: The sediment transport along the sandy beach for the original layout	33
Figure 29: The coastline deformation of original layout at different sections	34
Figure 30: The coastline deformation of original layout	35
Figure 31: Sandy hook (spit) at Jibei island	35
Figure 32: The qualitative relation between the wave direction and the littoral drift for a given offshore wave height (Petersen et al, 2008)	36
Figure 33: The morphological process of sandy hook occurrence	37

Figure 34: The sediment transport along the sandy beach of improved layout	37
Figure 35: The coastline deformation of improved layout	37
Figure 36: The coastline deformation of original layout after 10 years simulation	38
Figure 37: The coastline deformation of original layout after 1 year, 3 years, 5years and 10 years simulation.....	39
Figure 38: The coastline deformation and erosion rate after 1 year (upper left), 3 years (upper right), 5years (lower left) and 10 years (lower right) simulation of original layout	40
Figure 39: The morphological process in section DE.....	41
Figure 40: The coastline deformation of improved layout after 10 years simulation	41
Figure 41: The coastline deformation of improved layout after 1 year, 3 years, 5years and 10 years simulation.....	42
Figure 42: The coastline deformation and erosion rate after 1 year (upper left), 3 years (upper right), 5years (lower left) and 10 years (lower right) simulation of improved layout.....	43
Figure 43: The coastline deformation of original layout and improved layout after 10 years simulation	44
Figure 44: Sediment balance of the original layout after 1 years simulation.....	45
Figure 45: Sediment balance of the improved layout after 1 years simulation.....	45
Figure 46: Model grids for Maasvlakte 2 model	48
Figure 47: Delft3D model of DELTA 21 project in case of original layout.....	49
Figure 48: Delft3D model of DELTA 21 project in case of improved layout (IJntema, 2020).....	49
Figure 49: Open boundaries for Delft3D model.....	50
Figure 50: Locations of three cross-sections	52
Figure 51: 10 days bed-level difference between simulation Morfac=1 and Morfac=10.....	52
Figure 52: Bed level changes along the cross-sections for simulation morfac=1 and 10 at (a) the northern side of Maasvlakte 2, (b) the shipping channel and (c) the dredging point.	53
Figure 53 : 140 days bed-level change difference	54
Figure 54: Bed level changes along the cross-sections at for simulation morfac=10 ,20, 70 and 140 (a) the northern side of Maasvlakte 2, (b) the shipping channel and (c) the dredging point.	55
Figure 55: Flow pattern over a tidal cycle of Maasvlakte 2 model.....	57
Figure 56: Water level at observation points over two tidal cycle of Maasvlakte 2 model	58
Figure 57: Depth average flow velocities at observation points over two tidal cycle of Maasvlakte 2 model	58
Figure 58: Flow pattern over a tidal cycle in case of original DELTA 21 layout.....	59
Figure 59: Water level at observation points over two tidal cycle in case of original DELTA 21 layout.....	59
Figure 60: Depth average velocity at observation points over two tidal cycle in case of original DELTA 21 layout	60
Figure 61Flow pattern over a tidal cycle in case of improved DELTA 21 layout.....	60
Figure 62: Water level at observation points over two tidal cycle in case of improved DELTA 21 layout	61
Figure 63: Depth average velocity at observation points over two tidal cycle in case of improved DELTA 21 layout	61
Figure 64: Residual current over first tidal cycle	63
Figure 65: Bed level change in Maasvlakte 2 model after 5, 10 ,15 and 10 years simulation of Maasvlakte 2 model.....	64

Figure 66: Cumulative bed level change in every five years simulation of Maasvlakte 2 model.....	64
Figure 67: Bed level along two cross sections of Maasvlakte 2 model	65
Figure 68: Mean total sediment transport pattern in 0-5 years simulation of Maasvlakte 2 model	66
Figure 69: Bed level change in Maasvlakte 2 model after 5, 10 ,15 and 10 years simulation in case of original DELTA 21 layout	67
Figure 70: Cumulative bed level change in every five years simulation in case of original DELTA 21 layout	68
Figure 71: Bed level along different cross sections in case of original DELTA 21 layout	70
Figure 72: Magnitude over a tidal cycle in case of original DELTA 21 layout in 15-20 years simulation	71
Figure 73: Residual currents in 0-5 years and 15-20 years simulation in case of original DELTA 21 layout	71
Figure 74: Mean total sediment transport in 0-5 years and 15-20 years simulation in case of original DELTA 21 layout	72
Figure 75: Residual sediment transport at the large scale deposition in case of original DELTA 21 layout	72
Figure 76: Bed level change in Maasvlakte 2 model after 5, 10 ,15 and 10 years simulation in case of improved DELTA 21 layout.....	73
Figure 77: Cumulative bed level change in every five years simulation in case of improved DELTA 21 layout	74
Figure 78: Bed level along different cross sections in case of improved DELTA 21 layout.....	76
Figure 79: Magnitude over a tidal cycle in case of improved DELTA 21 layout in 15-20 years simulation.....	77
Figure 80: Residual currents in 0-5 years and 15-20 years simulation in case of improved DELTA 21 layout	77
Figure 81: Mean total sediment transport in 0-5 years and 15-20 years simulation in case of improved DELTA 21 layout	77
Figure 82: Residual sediment transport at the large scale deposition in case of improved DELTA 21 layout	78
Figure 83: Bed level of three model after 20 simulation at two sections.....	79
Figure 84: Coastline deformation after 10 years in case of original layout	82
Figure 85: Coastline deformation after 10 years in case of improved layout	82

List of table

Table 1: Geological borehole research information form DINOluket	18
Table 2: The coast orientation and wave climate applied in LT-model.....	24
Table 3: Cross-shore depth profile in LT-model	24
Table 4: The calculation of closure depth.....	26
Table 5: Closure depth and active height in LT-model	26
Table 6: Sediment transport rate along original layout.....	32
Table 7: Sediment transport rate along improved layout	32
Table 8: Average erosion rate at maximum retreat location of original layout	39
Table 9: Average erosion rate at maximum retreat location of original layout	42
Table 10: Sediment balance of the original layout after 1 years simulation	44
Table 11: Sediment balance of the improved layout after 1 years simulation	45
Table 12: Magnitude of vertical tide and horizontal tide.....	62



Wave climate in UNIBEST-LT

This appendix elaborate on the wave climate setting in the UNIBEST LT-model. The wave climate used for the design of Maasvlakte 2 is measured at the toe of the sea defense, and reduced to numbers of wave conditions, as shown in Table A.2 and Table A.3. In the wave climate file of the UNIBEST LT-model, the tide information is also included. The two wave climates have same tide data at a water depth of 16.7 m listed in Table A.1.

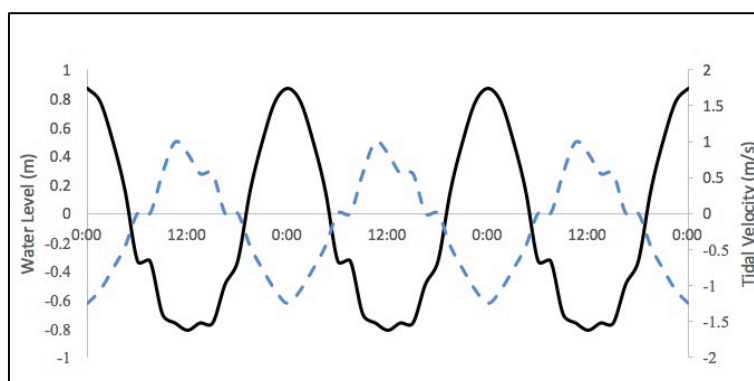


Figure A.1: Tidal signal and velocity in UNIBEST LT-model

Table A.1: Tide information in UNIBEST LT-model

	Water level h [m+NAP]	Tidal velocity V [m/s]	Reference Depth [m]	Percentage of occurrence [%]
1	0.87	-1.25	16.7	8.333
2	0.78	-1.07	16.7	8.333
3	0.51	-0.78	16.7	8.333
4	0.16	-0.46	16.7	8.333
5	-0.33	0	16.7	8.333
6	-0.33	0	16.7	8.333
7	-0.7	0.56	16.7	8.333
8	-0.76	0.99	16.7	8.333
9	-0.81	0.83	16.7	8.333
10	-0.76	0.55	16.7	8.333
11	-0.76	0.55	16.7	8.333
12	-0.49	0	16.7	8.333

Table A.2: Wave climate measure at northwest coast

	Hs (m)	Tp (s)	Direction (°N)	Duration (Days)
1	0.25	2.25	180	2.268
2	0.5	3.18	180	0.224
3	0.25	2.25	210	0.644
4	0.5	3.18	210	3.439
5	1	4.5	210	1.507
6	1.5	5.51	210	0.19
7	0.25	2.25	240	2.81
8	0.5	3.18	240	21.005
9	1	4.5	240	21.019
10	1.5	5.51	240	8.41
11	2	6.36	240	1.385
12	2.5	7.12	240	0.102
13	0.25	2.25	270	9.234
14	0.5	3.18	270	27.068
15	1	4.5	270	18.2
16	1.5	5.51	270	13.907
17	2	6.36	270	7.722
18	2.5	7.12	270	2.819
19	3	7.79	270	0.878
20	3.75	8.71	270	0.361
21	4.75	9.81	270	0.02
22	0.25	2.25	300	6.834
23	0.5	3.18	300	19.873
24	1	4.5	300	12.371
25	1.5	5.51	300	7.449
26	2	6.36	300	3.873
27	2.5	7.12	300	2.029
28	3	7.79	300	1.078
29	3.75	8.71	300	0.688
30	4.75	9.81	300	0.098
31	0.25	2.25	330	16.658
32	0.5	3.18	330	57.907
33	1	4.5	330	22.434
34	1.5	5.51	330	8.605
35	2	6.36	330	3.463
36	2.5	7.12	330	1.312
37	3	7.79	330	0.483
38	3.75	8.71	330	0.263
39	4.75	9.81	330	0.024

Table A.3: Wave climate measure at southwest coast

	Hs (m)	Tp (s)	Direction (°N)	Duration (days)
1	0.25	2.25	360	4.429
2	0.5	3.18	360	22.653
3	1	4.5	360	12.19
4	1.5	5.51	360	4.673
5	2	6.36	360	1.605
6	2.5	7.12	360	0.561
7	3	7.79	360	0.161
8	3.75	8.71	360	0.068
9	0.25	2.25	390	3.644
10	0.5	3.18	390	7.761
11	1	4.5	390	4.098
12	1.5	5.51	390	1.473
13	2	6.36	390	0.38
14	2.5	7.12	390	0.054
15	0.25	2.25	240	2.561
16	0.5	3.18	240	25.166
17	1	4.5	240	25.629
18	1.5	5.51	240	14.39
19	2	6.36	240	5.415
20	2.5	7.12	240	1.054
21	3	7.79	240	0.117
22	3.75	8.71	240	0.024
23	0.25	2.25	270	8.356
24	0.5	3.18	270	24.99
25	1	4.5	270	15.014
26	1.5	5.51	270	10.814
27	2	6.36	270	7.502
28	2.5	7.12	270	4.21
29	3	7.79	270	1.659
30	3.75	8.71	270	0.927
31	4.75	9.81	270	0.107
32	0.25	2.25	300	4.132
33	0.5	3.18	300	13.297
34	1	4.5	300	8.985
35	1.5	5.51	300	5.434
36	2	6.36	300	3.073
37	2.5	7.12	300	1.639
38	3	7.79	300	0.79
39	3.75	8.71	300	0.58
40	4.75	9.81	300	0.093
41	0.25	2.25	330	8.288
42	0.5	3.18	330	35.804

Appendix

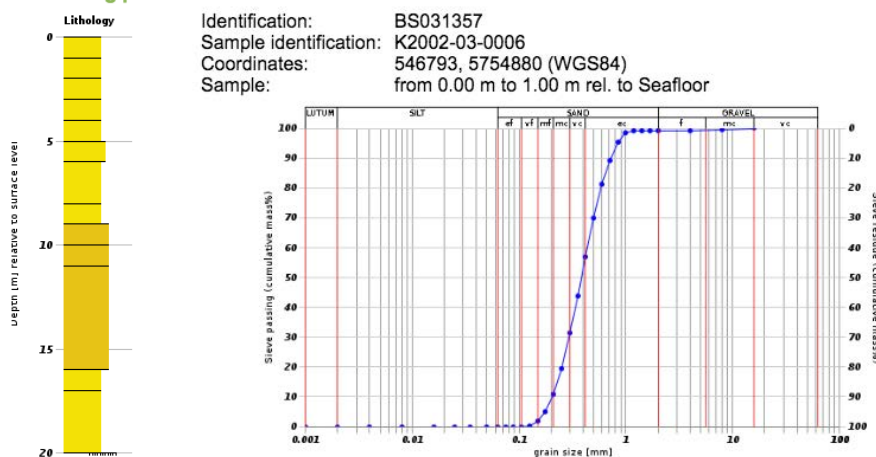
43	1	4.5	330	17.961
44	1.5	5.51	330	9.424
45	2	6.36	330	4.878
46	2.5	7.12	330	2.259
47	3	7.79	330	0.976
48	3.75	8.71	330	0.61
49	4.75	9.81	330	0.088

B

Geological borehole research

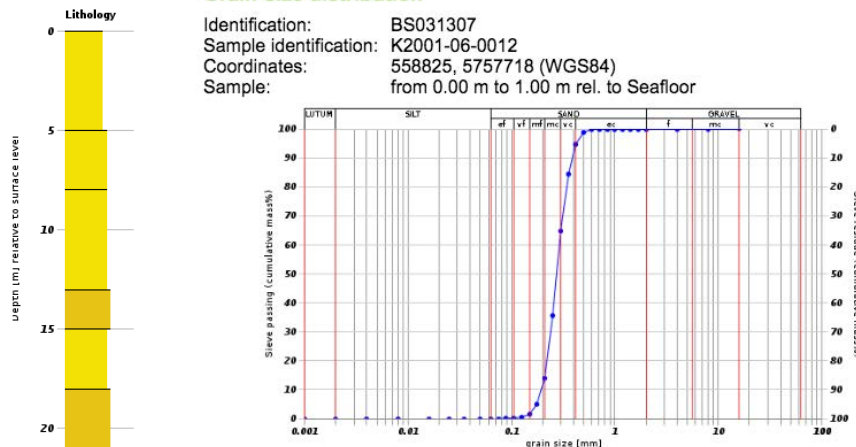
This appendix gives the borehole log profiles and grain size distributions from DINOloket.nl at several geological borehole research locations. The research data is given in Figure B.1.

Borehole log profile Grain-size distribution



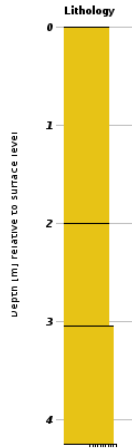
(1) Borehole log profiles and grain size distributions of research BS031357

Borehole log profile Grain-size distribution



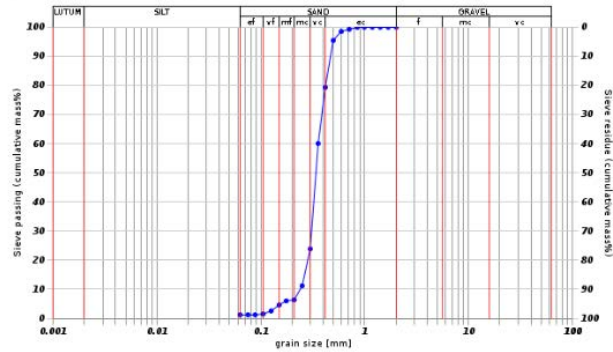
(2) Borehole log profiles and grain size distributions of research BS031307

Borehole log profile



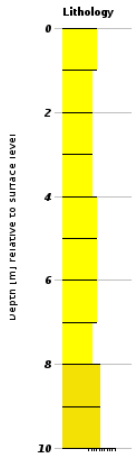
Grain-size distribution

Identification: BS031056
 Sample identification: K1993-02-0039
 Coordinates: 551191, 5746951 (WGS84)
 Sample: from 0.00 m to 1.00 m rel. to Seafloor



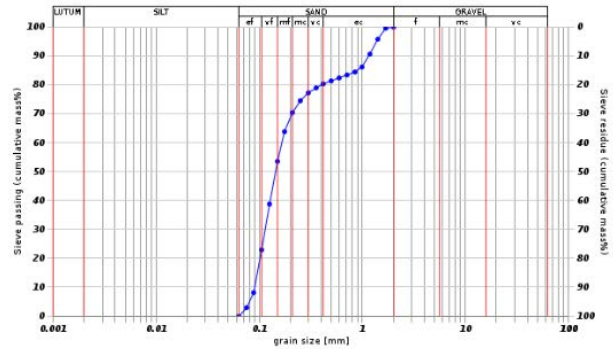
(3) Borehole log profiles and grain size distributions of research BS031056

Borehole log profile



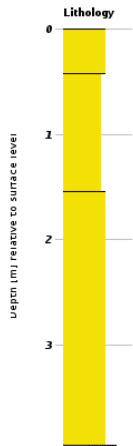
Grain-size distribution

Identification: BS031020
 Sample identification: K1993-07-0002
 Coordinates: 563754, 5752175 (WGS84)
 Sample: from 2.00 m to 3.00 m rel. to Seafloor



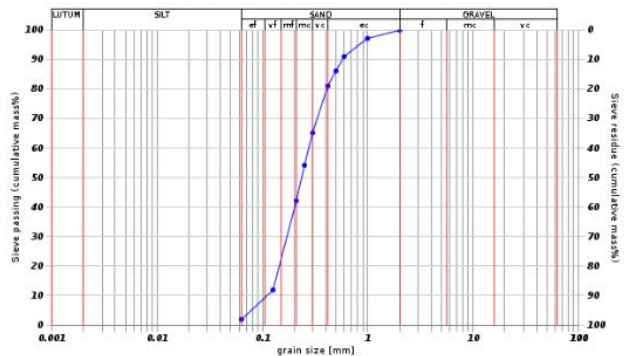
(4) Borehole profiles and grain size distributions of research BS031020

Borehole log profile



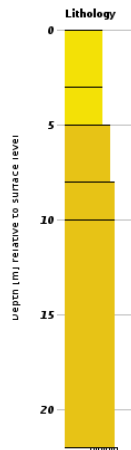
Grain-size distribution

Identification: BQ160622
 Sample identification: K1995-08-0051
 Coordinates: 569399, 5764231 (WGS84)
 Sample: from 0.00 m to 1.00 m rel. to Seafloor

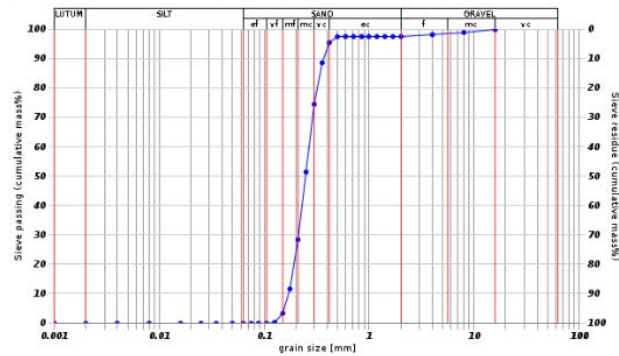


(5) Borehole log profiles and grain size distributions of research BQ160622

Borehole log profile Grain-size distribution

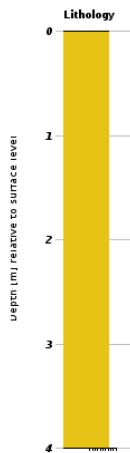


Identification: BP180532
 Sample identification: K2001-05-0034
 Coordinates: 562475, 5763046 (WGS84)
 Sample: from 0.00 m to 1.00 m rel. to Seafloor

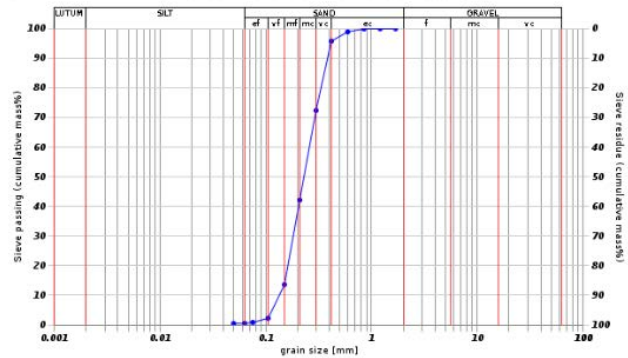


(6) Borehole log profiles and grain size distributions of research BP180532

Borehole log profile Grain-size distribution



Identification: BP180020
 Sample identification: K1972-00-0294
 Coordinates: 549165, 5763024 (WGS84)
 Sample: from 0.00 m to 0.20 m rel. to Surface level



(7) Borehole log profiles and grain size distributions of research BP180020

Figure B.1: Borehole log profiles and grain size from DINOlaket

C

Additional simulation results

This appendix gives additional simulation result of Delft3D morphodynamic model that can support analysis in Chapter 7. The cumulative bed level change after 5 years, 10 years, 15 years and 20 years simulation of three models is demonstrated. Figure C.1, Figure C.2 and Figure C.3 sequentially gives the result of Maasvlakte 2 model, DELTA 21 model in case of original layout and improved layout.

The location of large scour hole at the head of Valmeer can be discovered. Expansion and migration of the large scale deposition at northern side of Valmeer is clearly demonstrated in Figure C.2 and Figure C.3. A strong eroded area between the large scale deposition and sea defense is developed in case of original layout. This feature can also be found in case of improved layout after 20 years, as shown in Figure C.3(d).

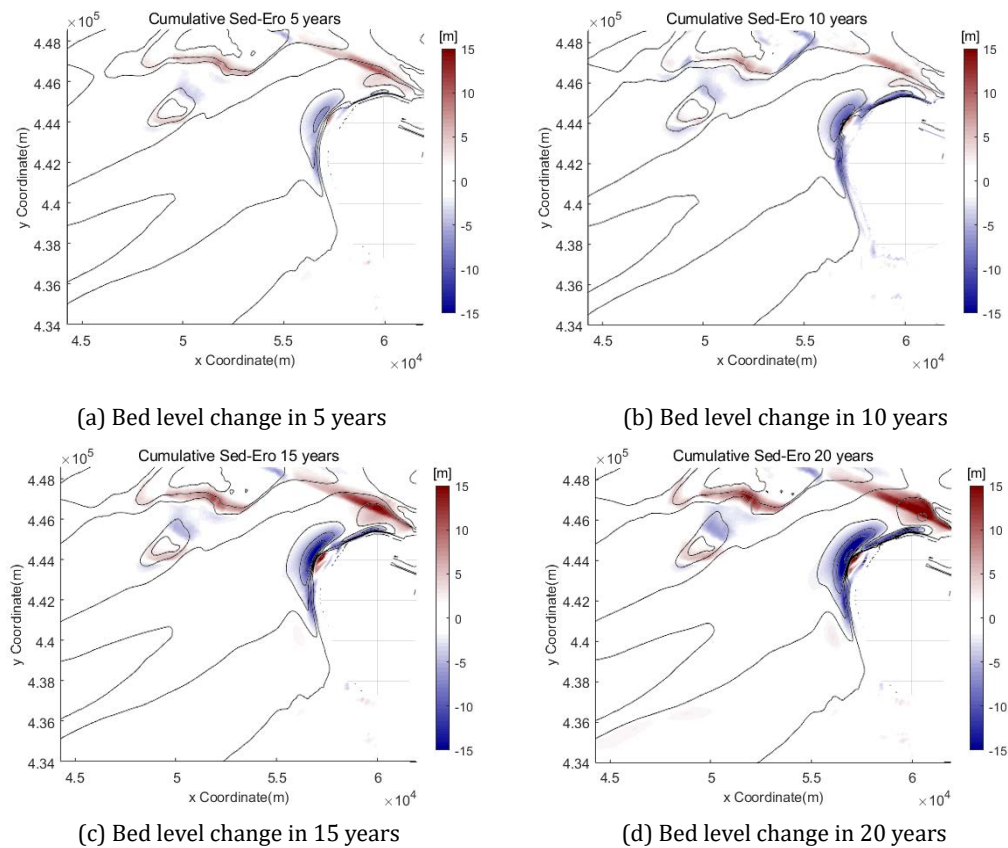


Figure C.1: Cumulative bed level change of Maasvlakte 2 model

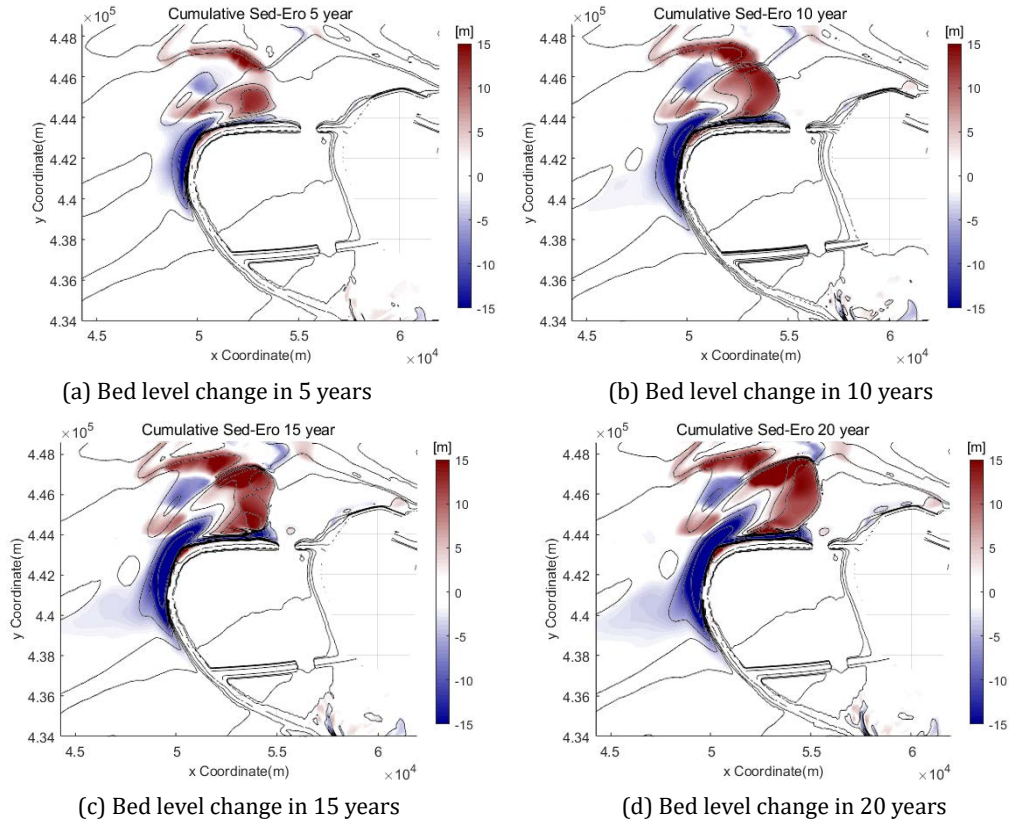
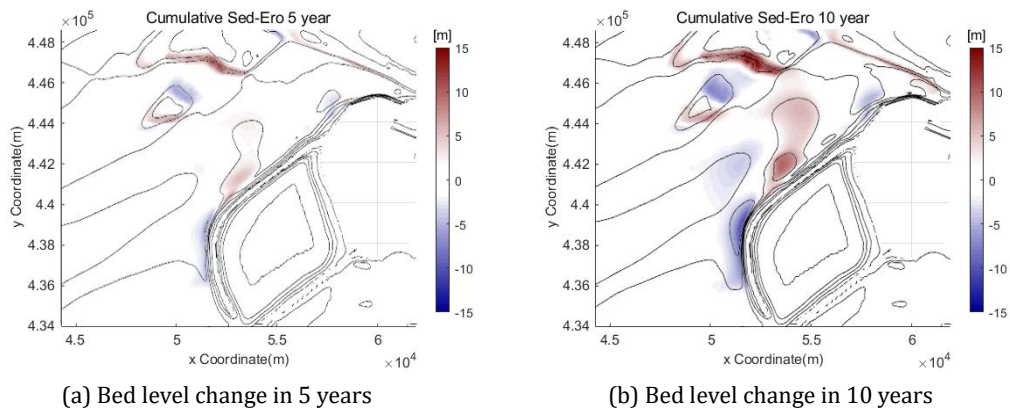
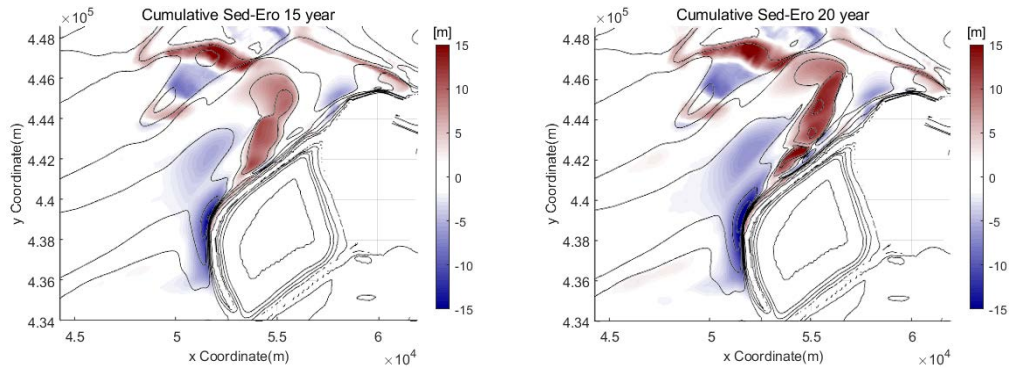


Figure C.2: Cumulative bed level change of DELTA 21 model in case of original layout





(c) Bed level change in 15 years

(d) Bed level change in 20 years

Figure C.3: Cumulative bed level change of DELTA 21 model in case of improved layout